



HAL
open science

New approaches for the rapid diagnosis of organic acidemias

Chiraz El Saddik

► **To cite this version:**

Chiraz El Saddik. New approaches for the rapid diagnosis of organic acidemias. Analytical chemistry. Université Paris-Saclay; Université Libanaise, 2022. English. NNT : 2022UPASF024 . tel-03676543

HAL Id: tel-03676543

<https://theses.hal.science/tel-03676543>

Submitted on 24 May 2022

HAL is a multi-disciplinary open access archive for the deposit and dissemination of scientific research documents, whether they are published or not. The documents may come from teaching and research institutions in France or abroad, or from public or private research centers.

L'archive ouverte pluridisciplinaire **HAL**, est destinée au dépôt et à la diffusion de documents scientifiques de niveau recherche, publiés ou non, émanant des établissements d'enseignement et de recherche français ou étrangers, des laboratoires publics ou privés.

New approaches for the rapid diagnosis of organic acidemias

Nouvelles approches pour le diagnostic rapide des acidémies organiques

Thèse de doctorat de l'université Paris-Saclay et de l'Université Libanaise

École doctorale n° 571,
Sciences chimiques : molécules, matériaux, instrumentation et biosystèmes, 2MIB
Spécialité de doctorat : Chimie
Graduate School : Chimie. Référent : Faculté des sciences d'Orsay

Thèse préparée dans l'**Institut de Chimie Physique** (Université Paris-Saclay, CNRS)
sous la direction de **Philippe MAITRE**, Directeur de Recherche CNRS,
la co-direction de **Fawaz EL OMAR**, Professeur des Universités,
le co-encadrement de **Fathi MOUSSA**, Professeur des Universités Emérite,
et le co-encadrement d'**Abdel Karim EL OMAR**, Maître de conférences

Thèse soutenue à Paris-Saclay, le 23 mars 2022, par

Chiraz EL SADDIK

Composition du Jury

David TOUBOUL DR, Université Paris-Saclay	Président
Nathalie DELAUNAY CR (HDR), Université Paris Sciences & Lettres	Rapporteuse et Examinatrice
Luke MACALEESE CR (HDR), Université Claude Bernard Lyon 1	Rapporteur et Examinateur
Hélène LAVANANT MCF, Université de Rouen Normandie	Examinatrice
Philippe MAITRE DR, Université Paris-Saclay	Directeur de thèse

Titre : Nouvelles approches pour le diagnostic rapide des acidémies organiques

Mots clés : Métabolomique ciblée, mobilité ionique différentielle, acidémies organiques, biomarqueurs isomères

Résumé : Un diagnostic précis des maladies métaboliques repose sur la séparation des isomères pour la quantification des métabolites biomarqueurs. Cette thèse se concentre sur le diagnostic des acidémies organiques, notamment l'acidémie méthylmalonique. L'analyse vise à cibler le biomarqueur spécifique de cette maladie, l'acide méthylmalonique. Les acidémies organiques sont couramment diagnostiquées par chromatographie en phase gazeuse couplée à la spectrométrie de masse qui est considérée comme technique de référence dans le domaine clinique. Néanmoins, le protocole est généralement fastidieux et long. Des méthodes basées sur la chromatographie liquide couplée à la spectrométrie de masse ont été développées pour répondre aux besoins d'un diagnostic rapide. Cependant, le principal défi est la séparation des isomères qui sont abondants dans les biofluides, ce qui rend l'identification du biomarqueur ambiguë.

La spectrométrie de mobilité différentielle couplée à la spectrométrie de masse (DMS-MS) pourrait être une approche alternative. Une méthode basée sur la DMS-MS est développée pour une séparation efficace des métabolites isomères permettant une identification et une quantification fiables des biomarqueurs dans le plasma. Le protocole proposé est simple et rapide. La performance analytique de cette méthode est évaluée en termes de la robustesse de la mesure de DMS, la linéarité, la répétabilité, la limite de détection et l'effet de matrice sur la concentration des analytes. Une analyse simultanée de différentes classes de métabolites d'intérêt biologique présents dans le plasma est également démontrée dans la perspective d'un diagnostic d'urgence. Cette étude constitue une preuve de concept en vue de l'intégration de la DMS-MS dans le répertoire des méthodes analytiques standardisées.

Title: New approaches for a rapid diagnosis of organic acidemias

Keywords: Targeted metabolomics, differential mobility spectrometry, organic acidemias, isomeric biomarkers

Abstract: Accurate diagnosis of metabolic diseases relies on separation of isomers for quantification of biomarkers. This thesis focuses on diagnosis of organic acidemias, particularly methylmalonic acidemia. Diagnosis is based on analysis of its specific biomarker, methylmalonic acid. Methylmalonic acidemia is routinely diagnosed using gas chromatography hyphenated to mass spectrometry, which is considered as reference technique in clinical settings. Nevertheless, analytical workflow of gas chromatography-based methods is generally tedious and time-consuming. Liquid chromatography-based methods have been developed in order to answer the need for fast diagnosis. Sample preparation and analysis time are particularly improved. The key challenge, however, remains separation of isomers that are abundant biofluids. Isomers can interfere with biomarker, which can lead to ambiguous identification.

Differential mobility spectrometry hyphenated to mass spectrometry (DMS-MS) could be an alternative approach. A DMS-MS based method is developed for a powerful separation of isomeric metabolites, allowing for reliable identification and quantification of biomarkers found in plasma. Our proposed protocol is simpler and faster than conventional methods. Analytical performance of DMS-MS method is evaluated in terms of robustness of DMS measurement, linearity, intra- and inter- day precision, limit of detection and matrix effect on analyte concentration. Simultaneous analysis of different classes of clinically relevant metabolites in plasma is also demonstrated in the perspective of emergency diagnosis. This proof of concept study aims towards integration of DMS into current standardized analytical methods in clinical field.

Thesis supervisors at Université Paris-Saclay

- Philippe MAITRE, DR
- Fathi MOUSSA, PU

Thesis supervisors at Lebanese University

- Fawaz EL OMAR, PU
- Abdel Karim EL OMAR, MCF

Collaborator at Necker Hospital

- Jean-François BENOIST, PU-PH

Remerciements

Cette thèse cotutelle entre l'Université Paris-Saclay et l'Université Libanaise a été réalisée à l'Institut de Chimie Physique (ICP). Il est temps de remercier l'ensemble des personnes qui ont contribué, de près ou de loin, à l'élaboration de ce travail.

Cette thèse n'aurait pas été possible sans le soutien de l'Université Paris-Saclay, qui m'a permis, grâce aux diverses aides financières, de me consacrer sereinement à mon projet de recherche lors de mon séjour en France.

Je tiens à exprimer ma sincère gratitude particulièrement à Dr. Philippe MAITRE, mon directeur de thèse. Je lui remercie pour la confiance qu'il m'a témoigné et les discussions fructueuses m'ont poussée au-delà de mes limites. Son expertise et son sens de communication et pédagogie m'ont permis d'acquérir de connaissances en chimie physique qui m'étaient inconnues. Je lui remercie également pour les ondes positives qu'il m'a transmises afin de 'garder le moral' tout au long de ces années. Je lui en suis extrêmement reconnaissante.

Je souhaite remercier vivement Pr. Fathi MOUSSA, mon co-encadrant de thèse, pour son aide, son suivi et toutes ses interprétations et remarques constructives. Son contact a d'ailleurs été très enrichissant tant au niveau humain qu'au niveau professionnel.

J'adresse mes remerciements au Pr. Jean-François BENOIST, notre collaborateur à l'Hôpital Necker impliqué dans l'ANR DMIRGNOSIS, qui s'est engagé dans la réussite de ce projet. Je lui remercie pour toutes ses informations complémentaires afin de comprendre et cerner clairement le contexte du sujet. Ses suggestions valorisantes ont énormément amélioré la qualité de ce manuscrit. Je tiens à lui exprimer ma reconnaissance pour l'honneur qu'il me fait en participant au jury.

Mes remerciements s'adressent également à Dr. Eskander ALHAJJI, chercheur invité à l'ICP, pour sa précieuse contribution pour toutes les manipulations de mobilité. Je lui remercie aussi pour son investissement et surtout pour les heures passées dans la

bonne humeur à optimiser les conditions expérimentales. Un grand merci pour tous les moments passés ensemble, sa bienveillance et son intérêt qu'il a fait preuve à mon égard.

J'adresse ma profonde gratitude à Dr. Nathalie DELAUNAY, chargée de recherche CNRS à l'Université Paris Sciences & Lettres, et Dr. Luke MACALEESE, chargé de recherche CNRS à l'Université Claude Bernard Lyon 1, d'avoir accepté d'évaluer ce travail en qualité de rapporteurs. Je présente également mes sincères remerciements à Dr. Hélène LAVANANT, Maître de conférences à l'Université de Rouen Normandie, d'avoir accepté le rôle d'examinatrice de cette thèse.

J'aimerais aussi remercier sincèrement Dr. David TOUBOUL, Chargé de recherche CNRS, pour son attention et son suivi, ainsi que ses suggestions et interprétations pertinentes quant aux résultats. Je lui remercie notamment de me faire l'honneur de participer au jury à titre d'examineur.

Je tiens à remercier du côté de l'Université Libanaise Pr. Fawaz EL OMAR et Dr. Abdel Karim EL OMAR, mes co-encadrant, pour avoir accepté de diriger cette thèse.

Je remercie chaleureusement tous les membres de l'ICP qui ont participé d'une manière ou d'une autre à la réalisation de ce travail. J'adresse mes remerciements aux différents membres à CLIO, en particulier, Estelle LOIRE qui m'a aidé à utiliser les spectromètres de masse, et Bernard RIEUL pour l'aide qu'il a pu m'apporter et son assistance pour notre « cher » module de mobilité.

Je ne souhaite pas oublier Dr. Francis BERTHIAS, qui était en post-doc dans notre équipe, dont les explications rigoureuses et l'esprit d'analyse m'ont permis de me familiariser avec notre technique de mobilité.

Je désire remercier Dr. Pascal PERNOT, Chargé de recherche CNRS, pour avoir partagé son savoir-faire pour l'élaboration du programme d'analyse de données. J'apprécie sa réactivité et son implication pour développer le calcul des paramètres de quantification.

Je tiens à dire merci également à Sarah, Ninette, Yining et Yali, pour leur compagnie sympathique et leur générosité. Je garde de très beaux souvenirs des moments et conversations ensemble.

Je tiens à remercier aussi Sara et Choayb dont j'ai fait connaissance en France, pour leur présence agréable et leur gentillesse. Les rapports humains dont j'ai profité à leur côté ont fait naître de réels liens d'amitiés.

Un merci spécial va à mes amies de grande date au Liban, Nahla, Kamar, et Souad pour leur encouragement et leur aide apportée à leur façon. Une mention particulière pour Nahla pour son soutien inestimable.

Je remercie du fond du cœur mes parents et mes frères sans lesquels je n'aurais jamais pu atteindre mes objectifs. Qu'ils soient assurés de ma profonde gratitude. C'est aussi à mes chères tantes, Ghada et Ibtissam, que je m'adresse pour manifester ma reconnaissance. Enfin, je remercie infiniment mon fiancé, Teseer, d'être à mes côtés depuis mon arrivée en France, et d'être à mon écoute à tous les moments.

Contents

Synthèse en Français	1
General introduction - DMS-MS: Towards a fast and accurate diagnosis tool for metabolic disorders	1
1. A typical metabolic disorder: methylmalonic acidemia	1
2. Conventional analytical approaches for diagnosis of organic acidemias	4
2.1. Methods based on gas chromatography-mass spectrometry	4
2.2. Methods based on liquid chromatography-mass spectrometry	5
3. Alternative approach: differential mobility spectrometry-mass spectrometry	7
3.1. Ion mobility spectrometry-based techniques	7
3.2. Differential mobility spectrometry-mass spectrometry	9
4. Identification of metabolites using DMS	11
References	14
Chapitre I - Differential Mobility Spectrometry: History, Separation Principle and State of the Art	23
I.1. Origins and evolutions of DMS	23
I.2. Principle of operation of DMS	24
I.2.1. Principle of separation	25
I.2.2. Ion mobility coefficient <i>versus</i> electric field	27
I.3. Three types of ions	29
I.4. DMS separation: influence of modifiers	31
I.4.1. Evidence of ion-modifier clustering	31
I.4.2. Effect of charge accessibility on ion-molecule clustering	33

I.5. Proton-bound dimer: analytical issues	36
I.6. Summary.....	38
References.....	39
Chapitre II : Material and methods.....	43
II.1. DMS-MS instrument.....	43
II.1.1. MS instruments	43
II.1.2. Our home-built DMS device	45
II.1.3. Control of transport gas flow and composition.....	47
II.2. Protocol based on DMS-MS method	48
II.3. Chemicals, reagents and biological samples.....	51
II.3.1. Standards, internal standards and chemicals.....	51
II.3.2. Plasma samples	52
II.4. Sample preparation	52
II.4.1. Precipitation of plasma	52
II.4.2. Standard solutions	52
II.4.2.1. Stock solutions	52
II.4.2.2. Working solutions for optimization of DMS parameters	53
II.4.2.3. Working standard solutions for calibration	53
II.4.3. Control solutions	54
II.4.4. Calibration of organic acids.....	54
II.4.5. Multi-class calibration.....	55
II.4.6. Plasma samples without standards of organic acids.....	57
II.5. Quantitative analysis	57
II.6. Experimental conditions	57
II.7. Data analysis using RStudio	58

II.7.1. Fitting procedure of DMS spectra.....	60
II.7.2. Evaluation of results	61
II.7.3. Calibration curve plot.....	61
II.8. Method validation	62
II.8.1. Stability of CV position.....	63
II.8.2. Linearity, LOD and LOQ.....	63
II.8.3. Intra-assay and inter-assay precision	64
II.8.4. Matrix effect on analyte concentration.....	64
II.9. Summary.....	65
References.....	66
Chapitre III - Lessons learned from DMS-MS analysis of organic acids.....	68
III.1. Ionization <i>via</i> metal cationization	68
III.2. In-source fragmentation of cation-bound dimer.....	71
III.3. Effect of dispersion voltage on DMS separation.....	75
III.4. Effect of polar modifiers on DMS separation.....	77
III.4.1. Modifier effect on DMS separation of organic acids.....	77
III.4.2. Practical limitations.....	80
III.5. Lessons from unwanted modifiers.....	83
III.6. Cationization of organic acids in plasma	87
III.7. Summary.....	89
References.....	90
Chapitre IV - Separation, identification and quantification of organic acids in plasma.....	93
IV.1. Lessons learned from DMS behavior of isomeric organic acids.....	93

IV.1.1. Organic acids isomers as sodium complexes	93
IV.1.2. Effect of structural properties on DMS behavior.....	94
IV.2. DMS separation: attempts for improvement	97
IV.2.1. Effect of dispersion voltage	97
IV.2.2. Effect of polar modifier.....	100
IV.3. Fast identification of organic acids in plasma	101
IV.3.1. Determination of CV values in plasma	101
IV.3.2. Robustness of CV measurement.....	102
IV.4. Quantification of MMA in plasma samples	103
IV.4.1. Determination of linear range, LOD and LOQ.....	104
IV.4.2. Assessment of intra- and inter-day precision.....	107
IV.4.3. Assessment of matrix effect on analyte concentration.....	108
IV.4.4. Added value of DMS-MS for MMA quantification	110
IV.5. Multi-class calibration in plasma samples	114
IV.5.1. Influence of amino acids on organic acids ionization and calibration	114
IV.5.2. Quantification of endogenous concentration of amino acids	117
IV.5.3. DMS-MS: towards a multi-class metabolites analysis method.....	119
IV.6. Summary	120
References.....	123
Annex	128
Chapitre V - Conclusions and perspectives.....	132
References.....	137

List of Figures

<i>Figure 1: Biochemical pathway of propionate. In the case of methylmalonyl-CoA mutase (MCM) deficiency, metabolites upstream the blockage are accumulated leading to an increase in methylmalonic acid (MMA) in biological fluids.</i>	<i>3</i>
<i>Figure 2: Illustration of sample treatment prior to GC-MS analysis.</i>	<i>5</i>
<i>Figure 3: DMS selection of isomeric metabolites at specific values of compensation voltage (CV).</i>	<i>10</i>
<i>Figure 4: Illustration of identification of two isomeric metabolites using conventional techniques based on LC or GC-MS/MS and DMS-MS/MS.</i>	<i>11</i>
<i>Figure I.1: Important milestones associated with the evolution of differential mobility spectrometry (DMS) technology.</i>	<i>24</i>
<i>Figure I.2: Illustration of DMS separation. a) Ion separation occurs under an asymmetric radiofrequency (RF) electric field. Colored dots and lines represent ions and their trajectories between the DMS electrodes, respectively. A compensation voltage (CV) applied to one electrode to compensate the deviation and allows for specific ion transmission. b) A DMS spectrum represents the ion signal intensity plotted against CV value.</i>	<i>26</i>
<i>Figure I.3: Representation of ion mobility coefficient (K) evolution as a function of electric field (E).</i>	<i>28</i>
<i>Figure I.4: Three dispersion plots are illustrated for Type A, B and C ions. Dispersion plot defined as variation of compensation voltage (CV) as a function of dispersion voltage (DV).</i>	<i>30</i>
<i>Figure I.5: Schematic representation of dispersion pots of isomeric 2-methylquinoline derivatives. a) Structures of 6- and 8-substituted derivatives. b) Dispersion plots with only N₂ carrier gas. c) Dispersion plot with water added to N₂ carrier gas.³¹</i>	<i>32</i>
<i>Figure I.6: Schematic representation of dispersion plots tetraalkylammonium cations. a) Structure of tetraalkylammonium cations. b) General shapes of dispersion plots using different modifiers added to N₂ carrier gas.³⁰</i>	<i>34</i>

<i>Figure I.7: Illustration of a typical DMS spectrum displaying monomer and proton-bound dimer peaks.</i>	<i>37</i>
<i>Figure II.1: Scheme of different sections our mass spectrometers QIT and FT-ICR. From left to right: ionization source (ESI), accumulation, transfer region, selection and fragmentation regions to ion detector. Abbreviation: Cap (Capillary).</i>	<i>44</i>
<i>Figure II.2: DMS assemblies. a) Photo of DMS device mounted in ESI source of the FT-ICR (top), without the spray shield (bottom). b) Design of DMS assembly for the FT-ICR instrument and operation principle.</i>	<i>46</i>
<i>Figure II.3: Illustration of N₂ gas flow redirected towards between DMS electrodes as a result of pumping (drag flow), and the other part is used for desolvation (dry gas flow).</i>	<i>47</i>
<i>Figure II.4: Photo of pumping system (CETONI) used for modifier introduction in the heated dry gas line.</i>	<i>48</i>
<i>Figure II.5: Three pairs of isomeric organic acids. Biomarkers are labeled with (*).</i>	<i>49</i>
<i>Figure II.6: DMS-MS workflow organized in 4 steps for separation, identification and quantification of organic acids (OAs) in plasma samples.</i>	<i>50</i>
<i>Figure II.7: Ion chromatogram (XIC) converted to DMS spectra using RStudio software.</i>	<i>58</i>
<i>Figure II.8: Illustration of input files (taskTable, tagTable and quantTable) required for R scripts.</i>	<i>59</i>
<i>Figure II.9: Example of an output figure from analysis.R script showing the 2D location of DMS peak and its profile in CV dimension.</i>	<i>60</i>
<i>Figure II.10: Example of calibration curves generated by using Quantify.R to estimate limit of detection (LOD).</i>	<i>62</i>
<i>Figure II.11: Illustration of validation parameters used for our method. a) Linearity. b) Precision of intra- and inter-assay. c) Matrix effect on concentration. Abbreviation: RSD (relative standard deviation).</i>	<i>64</i>

Figure III.1: Mass spectrum recorded under DMS transparent mode for methylmalonic (MMA), glutaric and adipic acids ionized as lithiated complexes.....70

Figure III.2: Illustration of processes that can occur after DMS selection of dimer and monomer species. a) Post-DMS fragmentation of hydrated dimers of occurring in the transfer region of the mass spectrometer. b) Equilibrium between hydration of ions and fragmentation of monohydrated ions in the quadrupole ion trap due to traces of water in the helium line.....72

Figure III.3: DMS spectra of monomer $[M+Li]^+$ (blue) and the hydrated dimer $[M+Li+H_2O]^+$ (red) of adipic acid (M). Data are fitted and smoothed using a rolling average over two points. Peak intensity of dimer is 20-fold scaled relative to monomer peak at CVdimer.73

Figure III.4: DMS spectrum recorded for adipic acid complexes with lithium after optimizing post-DMS fragmentation settings in transfer region. Data are fitted and smoothed using a rolling average over two points.....74

Figure III.5: Dispersion plots of isomeric organic acids complexed with lithium cation: methylmalonic acid (MMA, dark green diamonds), succinic acid (light green diamonds), glutaric acid (orange squares), methylsuccinic acid (yellow squares), adipic acid (dark blue circles) and methylglutaric acid (light blue circles). N_2 dry gas flow is fixed at $6.5 L \cdot min^{-1}$ and its temperature is set at $220 \text{ }^\circ C$76

Figure III.6: Dispersion plot of isomeric lithiated organic acids for m/z 139 and m/z 153 recorded using only N_2 carrier gas (solid line) and isopropanol added as modifier at $2 \mu L \cdot min^{-1}$ (dotted line). Organic acids are glutaric acid (orange squares), methylsuccinic acid (yellow squares), adipic acid (dark blue circles) and methylglutaric acid (light blue circles). Dry gas flow and temperature are set at $5 L \cdot min^{-1}$ and $200 \text{ }^\circ C$, respectively.....78

Figure III.7: DMS spectra of isomeric lithiated organic acids for m/z 139 and m/z 153 recorded upon addition of modifiers added at $2 \mu L \cdot min^{-1}$ in N_2 carrier gas. a) With isopropanol. b) With methanol. Dry gas flow and temperature are set at $5 L \cdot min^{-1}$ and $200 \text{ }^\circ C$, respectively. Organic acids are glutaric acid (orange squares), methylsuccinic acid (yellow squares), adipic acid (dark blue circles) and methylglutaric acid (light blue circles). Data are fitted and smoothed using a rolling average over two points. All individual spectra are normalized to the maximum.....79

Figure III.8: Effect of isopropanol flow added in N₂ carrier gas on CV position of isomeric lithiated organic acids for m/z 139 and m/z 153: glutaric (orange squares), methylsuccinic (yellow squares), adipic (dark blue circles) and methylglutaric (light blue circles). Dry gas flow and temperature were set at 5 L.min⁻¹ and 200 °C, respectively. .81

Figure III.9: Mass spectra recorded for a mixture of organic acids complexed with sodium cation upon addition of modifiers at 2 μL.min⁻¹ in N₂ carrier gas fixed at 5 L.min⁻¹. a) With acetone. b) With ethylacetate.82

Figure III.10: Illustration of ion desolvation effect on DMS behavior based on Hopkins paper.²⁰ Abbreviation: iPro (isopropanol).....84

Figure III.11: DMS spectra recorded for methylmalonic acid (MMA, dark green diamonds) and adipic acid (dark blue circles) using different carrier composition. a) With only N₂ at 5 L.min⁻¹. b) With only N₂ at 2.4 L.min⁻¹. c) With 2 μL.min⁻¹ of methanol seeded in 5 L.min⁻¹ of N₂ carrier gas. Data are fitted and smoothed using a rolling average over two points. All individual spectra are normalized to the maximum.87

Figure III.12: Mass spectrum recorded for lithiated methylmalonic (MMA), glutaric and adipic acids in plasma diluted by: a) 1/50 and b) 1/100 dilution factor.88

Figure IV.1: DMS spectra recorded for sodiated organic acids (OAs) using N₂ as carrier gas. a) m/z 141 isomers of succinic and methylmalonic (MMA) acids. b) m/z 155 isomers of glutaric and methylsuccinic acids. c) m/z 169 isomers of adipic and methylglutaric acids. Carbon chain structure of OAs (linear or branched) and number of atoms in sodiated ring are noted in brackets. Experiments were performed using methanol:water solution and dispersion voltage value of 1800 V. To facilitate visualization, all individual spectra are fitted and normalized to the maximum. Abbreviations: L (linear), B (branched).95

Figure IV.2: Dispersion plot recorded for sodiated organic acids using N₂ carrier gas: m/z 141 isomers of succinic and methylmalonic (MMA) acids (green diamonds), m/z 155 isomers of glutaric and methylsuccinic acids (orange squares), m/z 169 isomers of adipic and methylglutaric acids (blue circles). Experiments were performed using methanol:water solution. Dry gas flow and temperature were set at 6.5 L.min⁻¹ and 220 °C98

Figure IV.3: Calibration curves of MMA, glutaric and adipic acids spiked in healthy plasma samples. Area ratio organic acid (OA)/internal standard is plotted against OA concentration after dilution. Calibration curves were obtained from experiments performed in duplicate over 6 independent experiments..... 105

Figure IV.4: DMS spectra illustrating simultaneous detection of organic acids and amino acids spiked in plasma. Organic acids are detected as sodiated ions: methylmalonic (MMA), glutaric and adipic acids. Amino acids are detected as protonated ions: alanine (Ala), valine (Val), leucine (Leu), methionine (Met), phenylalanine (Phe) and arginine (Arg). Data are recorded using a DV value of 1800 V, and dry N₂ flow set at 6.5 L.min⁻¹. All individual spectra are normalized to the maximum and smoothed using a rolling average over two points. 115

Figure IV.5: MS spectra recorded for MMA, glutaric and adipic spiked in plasma. a) without HCOOH. b) with HCOOH..... 116

Figure IV.6: Calibration curves of amino acids (AAs) derived from multi-class calibration: alanine (Ala), valine (Val), leucine (Leu), methionine (Met), phenylalanine (Phe) and arginine (Arg). 118

List of Tables

<i>Table II.1: Working standard solutions of organic acids used for calibration of organic acids.</i>	54
<i>Table II.2: Sample preparation for calibration of organic acids.</i>	55
<i>Table II.3: Sample preparation for multi-class calibration.</i>	56
<i>Table II.4: List of 6 amino acid standards and isotopically labeled compounds, as well as their final concentration (μM) used in multi-class calibration samples.</i>	56
<i>Table III.1: CV and FWHM values observed for organic acids as lithiated complexes. Data were recorded using a mixture of N_2/He gases (92:8) and N_2 only as carrier gas (100:0) fixed at $2.4 \text{ L}\cdot\text{min}^{-1}$.</i>	85
<i>Table IV.1: Structural properties related of organic acids complexed with sodium cation.</i>	94
<i>Table IV.2: CV values obtained from DMS spectra recorded with and without methanol used as modifier gas in N_2 dry gas. N_2 dry gas flow was set at $6.5 \text{ L}\cdot\text{min}^{-1}$ and methanol flow was fixed at $2 \mu\text{L}\cdot\text{min}^{-1}$ which corresponds to $\sim 0.02\%$ molar percentage.</i>	100
<i>Table IV.3: Comparison between DMS data recorded in methanol:water and plasma solutions for sodiated organic acids.</i>	101
<i>Table IV.4: CV values recorded for organic acid added to methanol:water solution and plasma sample over a period of 4 months.</i>	102
<i>Table IV.5: Slope, intercept and R^2 values associated with linear regression equation for MMA, glutaric and adipic acids averaged for experiments performed over 6 independent experiments.</i>	105
<i>Table IV.6: Mean values of limit of detection (LOD) and quantification (LOQ) in μM derived using linear regression method for analytes.¹⁸</i>	106
<i>Table IV.7: Intra-day precision data associated with concentration measurement of MMA, glutaric and adipic acids. Control samples are prepared from one plasma sample (P1) by spiking a mixture of three OAs at 20 and 50 μM after dilution. Mean concentration,</i>	

standard deviation (SD) and relative SD (RSD) are calculated for each concentration using 6 replicates (n = 6) analyzed on one day..... 107

Table IV.8: Inter-day precision of concentration measurement of MMA, glutaric and adipic acids spiked at 20 or 50 μ M into two different plasma, P6 and P1, after dilution. Control sample in P6 and P1 are analyzed over 4 days (n = 4), and 11 days (n = 11), respectively. Mean concentration, standard deviation (SD) and relative SD (RSD) are calculated for each concentration. 108

Table IV.9: Matrix effect on MMA, glutaric and adipic acid concentration. Analytes are spiked at 20 and 50 μ M in calibration sample in six different plasma samples (P1-P6). Corresponding recovery and relative standard deviation (RSD) are calculated for each concentration. 109

Table IV.10: Linearity parameters derived from measurements on organic acids (OAs) and multi-class calibration. 117

Table IV.11: Slope, intercept and R^2 values associated with linear regression equation of amino acids..... 118

Table IV.12: Endogenous concentration measured for amino acids in plasma compared to typical reference concentration range. 119

List of Abbreviations

α	Differential mobility function
μ	reduced mass of ions and carrier gas molecules
AA	Amino acid
ACE	Acetone
Bu	Butyl
CCS	Collision cross section
CV	Compensation voltage
DC	Direct current
DMS	Differential mobility spectrometry
Do	Dodecyl
DT-IMS	Drift tube ion mobility spectrometry
DV	Dispersion voltage
E	Electric field
E/N	Reduced Electric field
EIC (or XIC)	Extracted ion chromatogram
ESI	ElectroSpray
EtAc	Ethyl acetate
FAIMS	Field asymmetric waveform ion mobility spectrometry
FT-ICR	Fourier Transform ion cyclotron resonance
FWHM	Full-width at half maximum
GC	Gas chromatography

HCOOH	Formic acid
He	Helium
Hx	Hexyl
IEM	Inborn errors of metabolism
IMD	Inherited metabolic disorder
IMS	Ion mobility spectrometry
iPro	Isopropanol
IS	Internal standard
K	Ion mobility coefficient
LC	Liquid chromatography
Lc	Critical limit
LOD	Limit of detection
LOQ	Limit of quantification
<i>m/z</i>	mass-to-charge ratio
Me	Methyl
MCM	Methylmalonyl-CoA mutase
MMA	Methylmalonic acid
MS	Mass spectrometry
MS/MS	Tandem mass spectrometry
N	Gas number density
N ₂	Dinitrogen
OA	Organic acid

PC	Peak capacity
PDB	Proton-bound dimer
QIT	Quadrupole ion trap
R	Alkyl chain
R ₄ N ⁺	Tetraalkylammonium ion
RF	Radiofrequency
R _{pp}	Resolution peak to peak
RSD	Relative standard deviation
RT	Retention time
SA	Succinic acid
SD	Standard deviation
td	Drift time
TWIMS	Travelling wave ion mobility spectrometry

Synthèse en Français

Les erreurs innées du métabolisme (EIMs) représentent une collection diverse et hétérogène d'environ 500 maladies génétiques. Ces maladies regroupent tous les troubles dont les voies métaboliques sont altérées avec des caractéristiques biochimiques, cliniques et/ou physiopathologiques spécifiques. Dans la plupart des cas, l'altération de la voie biochimique induit des changements dans la concentration de métabolites endogènes critiques. Ceux-ci sont appelés biomarqueurs car ils constituent la signature biochimique spécifique d'une maladie.

L'acidémie méthylmalonique est une classe importante des erreurs innées du métabolisme. L'acidémie méthylmalonique est un exemple typique d'acidémie organique et qui sera discuté tout au long de ce manuscrit. L'acidémie méthylmalonique est l'un des troubles les plus fréquents et peut entraîner des conséquences graves. Cette maladie est due à une mutation du gène codant pour l'enzyme méthylmalonyl-CoA mutase impliquée dans la voie du catabolisme des acides aminés. L'enzyme est rendue inactive, ce qui entraîne le blocage de la voie métabolique, et par suite l'accumulation de l'acide méthylmalonique dans les fluides biologiques comme le plasma et l'urine. L'acide méthylmalonique est considéré comme le biomarqueur primaire et spécifique de cette maladie.

La détection et la quantification du biomarqueur sont essentiels pour un diagnostic précoce de l'acidémie méthylmalonique. Les techniques métabolomiques basées sur la spectrométrie de masse (MS) sont généralement employées pour le diagnostic des acidémies organiques. La spectrométrie de masse est généralement couplée à une méthode de pré-séparation, telle que la chromatographie en phase gazeuse ou liquide.

L'état de l'art du diagnostic de l'acidémie organique repose sur la chromatographie en phase gazeuse couplée à la spectrométrie de masse (GC-MS). Cette méthode est utilisée comme méthode de référence pour le diagnostic. Des centaines d'acides organiques endogènes et exogènes, excrétés dans l'urine, peuvent être séparés, identifiés et quantifiés par GC-MS. Une fois le diagnostic effectué, le suivi biologique des acidémies organiques repose sur la quantification d'un ou de quelques biomarqueurs seulement.

La GC-MS offre également plusieurs avantages pour une analyse ciblée et non ciblée des acides organiques. L'ionisation standard par impact d'électrons utilisée avec la GC-MS conduit à une sensibilité élevée, une efficacité d'ionisation élevée, ainsi qu'à une fragmentation étendue des acides organiques dérivés. Ces modèles de fragmentation fournissent des informations structurales qui sont pertinentes pour l'identification des métabolites. Les spectres de masse de référence peuvent être trouvés dans des bibliothèques spectrales universelles. Il est important de noter que le pouvoir de séparation de la GC-MS permet une séparation efficace des acides organiques isomères qui sont abondants dans les fluides biologiques, comme le MMA et son isomère, l'acide succinique.

La GC-MS n'est pas sans inconvénients. En particulier, les acides organiques ne sont pas volatils et doivent être estérifiés pour être transférés en phase gazeuse. Le traitement de l'échantillon nécessite une extraction suivie d'une réaction de dérivation pour améliorer la séparation et la détection des acides organiques. Cette procédure pré-analytique est fastidieuse et prend beaucoup de temps, aussi que la séparation par GC qui prend typiquement 30-60 minutes.

La chromatographie liquide (LC) couplée à la spectrométrie de masse en tandem (MS/MS) s'est avérée être un outil extrêmement puissant pour l'analyse ciblée des métabolites dans les échantillons biologiques. Cette technique a été progressivement

intégrée dans les laboratoires cliniques pour le diagnostic et le suivi thérapeutique des patients. La LC-MS/MS est en particulier appliquée dans le cas de l'acidémie méthylmalonique, car les patients peuvent souffrir d'une insuffisance rénale entraînant une accumulation du MMA dans le plasma. Différentes méthodes ont été développées sans dérivation avec un temps d'analyse plus rapide que celui de la GC-MS. Malgré l'amélioration en termes de préparation des échantillons et la résolution des isobares et isomères, le développement d'une méthode plus rapide, plus simple et sélective est nécessaire.

La spectrométrie de mobilité différentielle couplée à la spectrométrie de masse (DMS-MS) est proposée par notre projet comme une approche alternative ou complémentaire aux méthodes chromatographiques appliquée pour le diagnostic des acides organiques.

La technologie de DMS a été appliquée avec succès pour la séparation en phase gazeuse de petites molécules, comme les métabolites. Ceci lui permet de fournir une grande utilité dans le domaine de la métabolomique. La DMS est connue pour son pouvoir de séparation des isomères et isobares. La DMS peut aussi agir comme un filtre d'ions en amont du spectromètre de masse sans ajouter un temps supplémentaire à celui de l'analyse en MS. Un autre avantage est basé sur la mesure de DMS appelé voltage de compensation (CV) peut servir comme un paramètre d'identification des métabolites. En d'autres termes, le biomarqueur ciblé peut être sélectionné à une valeur de CV distincte de celle des autres métabolites isomères présents dans un mélange complexe comme les milieux biologiques. Cette idée est au cœur de notre travail pour identifier les acides organiques dans le plasma.

Cette thèse porte sur le développement d'une méthode simple et rapide basée sur la DMS-MS pour le diagnostic des acides organiques pertinents, en particulier l'acide méthylmalonique, biomarqueur de l'acidémie méthylmalonique. Notre objectif ultime

|Synthèse en Français

est d'évaluer les performances analytiques du DMS-MS pour la séparation, l'identification et la quantification des biomarqueurs dans des échantillons de plasma.

Dans un premier temps, une phase d'optimisation des conditions expérimentales sera abordée. Des paramètres ont été optimisés pour améliorer l'ionisation des acides organiques en mode positif. Le control du flux et de la composition du gaz de mobilité a été effectuée. C'est une étape clé pour obtenir une séparation et une identification en DMS stables. Ensuite, la robustesse des valeurs de CV des acides organiques sous différentes conditions est évaluée. La dernière partie de ce projet est la quantification des biomarqueurs dans le plasma. La linéarité de la méthode, la répétabilité de la mesure de concentration, la limite de détection et l'effet de matrice sur la concentration des analytes sont présentés. Une analyse simultanée des acides organiques et des acides aminés présents dans le plasma est également démontrée dans la perspective d'un diagnostic d'urgence. Cette étude constitue une preuve de concept en vue de l'intégration de la DMS-MS dans le domaine d'applications liées à l'analyse des métabolites.

General introduction - DMS-MS: Towards a fast and accurate diagnosis tool for metabolic disorders

1. A typical metabolic disorder: methylmalonic acidemia

Inherited metabolic disorders (IMDs), or inborn error of metabolism (IEMs), represent a vast, diverse and heterogeneous collection of around 500 genetic diseases caused by rare mutations affecting the function of individual proteins.¹ IMDs encompass all conditions in which metabolic pathways are altered with specific biochemical, clinical, and/or pathophysiological features. IMDs are life-threatening defects that irretrievably lead to significant organ dysfunctions (*i.e.* brain, liver, cardiac, kidney, muscle...). In most cases, alteration in biochemical pathway induces changes in concentration of critical endogenous metabolites. These are called biomarkers because they constitute the specific biochemical signature of a disease.^{2, 3} In other words, metabolic disorders can be early diagnosed based on the variation of concentration of biomarkers.

In the last four decades, IMDs have gained notable interest in medical field to improve diagnosis, treatment and prevention. Organic acidemias or acidurias consist of an important class of metabolic disorders for which considerable progress has been made for the management of patient.⁴ They are caused by defects in amino acids breakdown which results in accumulation of organic acids in biological fluids and tissues. Organic acidemias were converted from lethal acute to chronic diseases, so that most of patients can reach adulthood with social prospects.

Classical clinical onset of organic acidemias occurs at neonatal period.⁴ Biochemical features generally present with hyperammonaemia and high anion gap metabolic acidosis. Severity of diseases varies depending on genotype. Patients have considerable variability in symptoms including coma, failure to thrive, vomiting,

|General Introduction

hypotonia, mental retardation and chronic neurological disease. Treatment consists of life-long low-protein diet to reduce toxic precursors. In some cases, organ transplantation (liver or combined liver/kidney) is directed towards correction of enzymatic defect. Due to acute and recurrent episodes of life-threatening coma, diagnosis and appropriate treatment are indeed essential to help children to reach their full potential.

Methylmalonic acidemia is a typical example of organic acidemia that is discussed throughout this manuscript. Methylmalonic acidemia is one of the most frequent disorder and could lead to severe consequences. It was first described in 1967.⁵ This disorder is inherited in an autosomal recessive fashion affecting at least 1 out of 50 000 individuals.⁶ It is a heterogeneous condition caused by mutation in genes encoding methylmalonyl-CoA mutase (MCM) enzyme or involved in the biosynthesis of its specific cofactor, adenosyl cobalamin, produced from vitamin B₁₂ (also called cobalamin). MCM is involved in the mitochondrial catabolic pathway of some amino acids. According to its pathophysiology, it belongs to the group of toxic inborn errors of metabolism. From a biochemical point of view, methylmalonic acidemia is associated to organic acidemia group, since a defect in enzyme activity leads to a build-up of toxic organic acids, notably methylmalonic acid (MMA), in biological fluids. MMA is thus a primary and specific biomarker of methylmalonic acidemia.⁷

Crucial steps of MMA metabolic pathway are depicted in Figure 1. MMA is an intermediate metabolite in the breakdown of valine, isoleucine, methionine and threonine, and also in the oxidation of odd chain carbon fatty acids. This mitochondrial pathway starts with production of propionyl-CoA that is successively converted to D- and L-methylmalonyl-CoA, through enzymatic reactions. MMA is produced from D-methylmalonyl-CoA by removing the coenzyme A moiety. Methylmalonyl-CoA mutase catalyzes cobalamin-dependent conversion of L-methylmalonyl-CoA to succinyl-CoA

|General Introduction

that enters into the tricarboxylic acid cycle (TCA cycle). MMA and metabolites, which are generated upstream this enzyme blockage, are thus accumulated, particularly in plasma and urine.

Increased MMA concentration in biological fluids reflects defect of either of MCM itself or defect of transformation of vitamin B₁₂ into adenosylcobalamin, its active form.⁸ Physiological concentration of MMA is found <0.4 μM in plasma or <4.0 mmol/mol of creatinine in urine. Vitamin B₁₂ deficiency, due to insufficient intake or absorption defects, leads to slight increase of MMA levels. In the case of MCM deficiency, a massive increase of MMA levels, however, occurs in plasma and urine. MMA concentration is thus 100-fold higher than physiological concentration. Since metabolic changes can appear before clinical symptoms, early detection and quantification of MMA are the cornerstone of an early diagnosis.

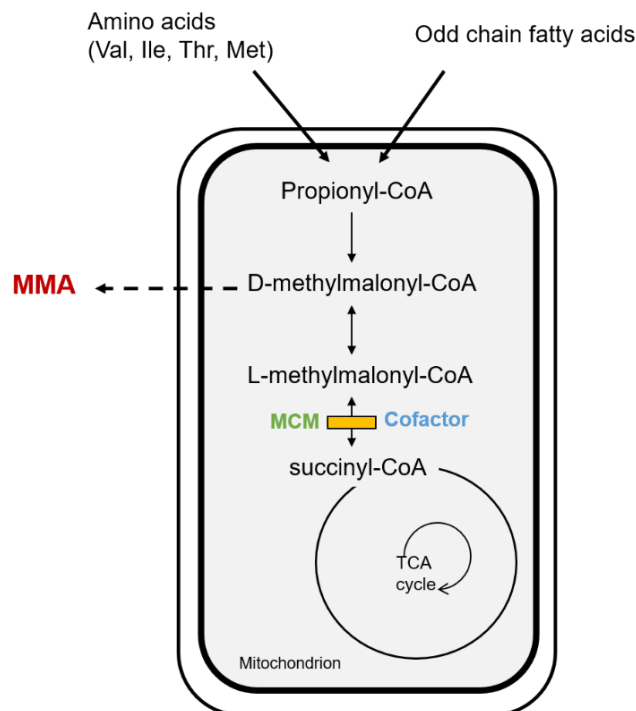


Figure 1: Biochemical pathway of propionate. In the case of methylmalonyl-CoA mutase (MCM) deficiency, metabolites upstream the blockage are accumulated leading to an increase in methylmalonic acid (MMA) in biological fluids.

2. Conventional analytical approaches for diagnosis of organic acidemias

Most IMDs are diagnosed using metabolomics based strategies.⁹ Metabolomics is defined as the systematic study of metabolites found within a biological system.^{10, 11} Metabolomics holds promises for better understanding of disease mechanism and biomarker discovery.¹² Two types of approaches can be distinguished. Untargeted metabolomics (or fingerprinting) consists of an exhaustive analysis of all metabolites present in a given sample, and targeted metabolomics (or metabolic profiling) aims to identify and quantify a selected set of known metabolites related to specific diseases or metabolic pathways. Both approaches were applied for methylmalonic acidemia.^{13,}

14

Mass spectrometry (MS)-based metabolomics techniques are typically employed in routine settings. Nuclear magnetic resonance is also an important tool, but MS is less expensive and more sensitive which is desired for quantification of metabolites in complex mixtures.¹⁵ Mass spectrometry is usually coupled to a pre-separation method, such as gas or liquid chromatography, for routine diagnosis. This technique is used at our partner laboratory at Necker Hospital.

2.1. Methods based on gas chromatography-mass spectrometry

The state of the art of organic acidemia diagnosis relies on gas chromatography hyphenated to mass spectrometry (GC-MS). In the 1970s, GC-MS was developed for untargeted analysis of organic acids in urine.¹⁶⁻¹⁸ This method is still used nowadays as reference method for diagnosis purposes. Hundreds of endogenous and exogenous organic acids excreted in urine can be separated, identified and quantified by GC-MS. Once diagnosed, biological monitoring of organic acidemias is based on quantification of only one or few biomarkers.

|General Introduction

GC-MS offers also several advantages for untargeted and targeted organic acids analysis. The standard electron impact ionization used with GC-MS leads to high sensitivity, high ionization efficiency, as well as an extensive fragmentation of derivatized organic acids.¹⁹⁻²¹ These fragmentation patterns provide structural information that are relevant for metabolites identification. Reference mass spectra can be found in universal spectral libraries for a broad range of metabolites.²² Importantly, separation power of GC-MS allows efficient separation of isomeric organic acids that are abundant in biological fluids, such as MMA and its isomer, succinic acid (SA).²³

GC-MS is not without drawbacks. In particular, organic acids are non-volatile and must be esterified to be transferred to gas phase. Sample treatment requires solvent or solid phase extraction followed by derivatization reaction,²³⁻²⁶ to improve separation and detection of organic acids (Figure 2). This pre-analytical procedure is tedious and time-consuming (~ 2h) besides GC separation that typically takes 30-60 min. Therefore, efforts were directed towards developing a rapid, simple and selective method based on liquid chromatography.

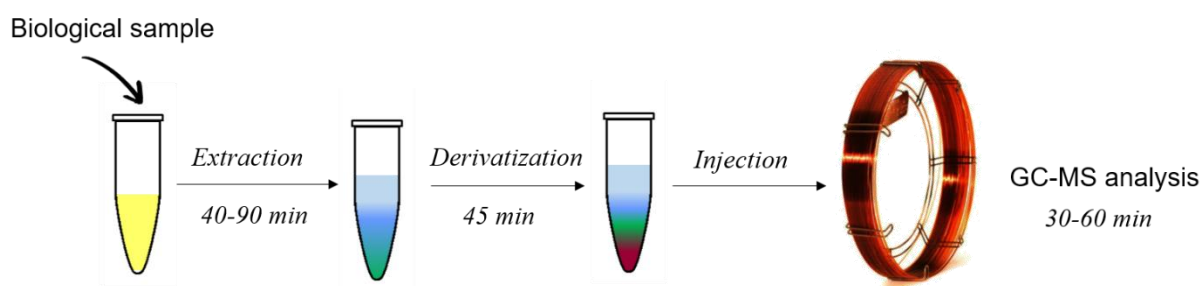


Figure 2: Illustration of sample treatment prior to GC-MS analysis.

2.2. Methods based on liquid chromatography-mass spectrometry

Liquid chromatography (LC) coupled with tandem mass spectrometry (MS/MS) was found to be an extremely powerful tool for qualitative and quantitative analysis of

|General Introduction

metabolites in biological samples.²⁷ In 2000, the greatest breakthrough has come from emergence of atmospheric-pressure ionization techniques such as electrospray. This led to development of targeted LC-MS/MS methods.²⁸⁻³⁰ This technology has progressively been integrated in clinical laboratories for routine diagnosis and patient's follow-up. In particular, LC-MS/MS is applied in the case of methylmalonic acidemia since patients can suffer from renal failure leading to MMA accumulation in plasma.

First applications using high-performance liquid chromatography (HPLC) hyphenated to MS/MS required solvent extraction and derivatization for sample treatment. Derivatization is used to improve selectivity and specificity of LC. The advantage is that analysis time was significantly faster than conventional GC-MS methods. LC-MS/MS method has been developed for analysis of MMA and SA derivatives within ~3 min analytical run, in plasma and urine.³¹ MMA and SA derivatives may be distinguished based on differences in their fragmentation patterns. Kushnir *et al.* have published another method for faster (<1 min) and more specific analysis.³² However, the entire analysis, including sample preparation, for a batch of 100 specimens can be performed in ~4 h. In 2006, a simple and automated sample preparation based on solid-phase extraction has been proposed for analysis of MMA in plasma.³³ Protocol of these LC-MS/MS methods was later optimized in terms of biological sample volume and isomer resolution.^{34, 35}

In parallel, different methods have been developed without derivatization for more practical procedure.^{36, 37} Organic acids were analyzed in negative ionization mode using hyphenated to sensitive mass spectrometers. MMA and succinic acid in plasma were separated within 3 min.³⁶ Column washing and reconditioning increased assay time to 10 min per sample.

In 2018, ultra-performance LC has been integrated to high resolution tandem mass spectrometry for diagnosis of inborn errors of metabolism. More precisely, a study has demonstrated the suitability of this method for fast and accurate quantification of a panel of 71 urinary organic acids.³⁸ Despite improvements in terms of sample preparation and isobar resolution, separation of isomeric metabolites remains a difficult task. Interference from endogenous isomers can lead to ambiguous biomarker identification. Different protocols and methodologies are applied to overcome this issue.

3. Alternative approach: differential mobility spectrometry-mass spectrometry

3.1. Ion mobility spectrometry-based techniques

Ion mobility spectrometry (IMS) refers to an attractive separation technique of ions in gaseous phase. Ions are electrically driven through an ion mobility cell filled with an inert gas, for example rare gas or dinitrogen, at ambient pressure and temperature, under the influence of an electric field.^{39, 40} Mobility of an ion relies on its size, shape and mass-to-charge ratio. IMS gained recent interest for separation and identification of molecules.^{41, 42} IMS has been applied in several fields starting from chemical warfare agent, illicit drugs to biological molecules such as metabolites,⁴³ glycans,⁴⁴ proteins,⁴⁵ lipids⁴⁶ and biopharmaceuticals.⁴⁷ In particular, IMS has been recently investigated in clinical field for routine diagnosis.⁴⁸ Breath analysis using IMS technique allows for diagnosis of diseases associated to pulmonary system. New applications emerge in different areas, and the list continues to grow.

Several IMS versions have been developed in the last decades, each having its own principle of operation and design. A detailed description and comparison of the different IMS variants can be found in recent reviews.^{49, 50} Two main categories are

generally distinguished.⁵¹ Time-dispersive methods generate an arrival time spectrum with all ions drifting along a similar path. Ions are separated based on their drift time needed to traverse a pressurized IMS cell, *i.e.* Drift tube IMS (DT-IMS) and travelling wave IMS (TWIMS). Space-dispersive methods allow for separation of ions along different drift paths based on differences in their ion mobility. These methods include differential mobility spectrometry (DMS), also known as field asymmetric waveform ion mobility spectrometry (FAIMS). A DMS spectrum is recorded as a function of a direct current (DC) voltage called compensation voltage (CV), which can be adjusted to specifically transmit ions. A review article by B. Schneider in 2015 covers in depth all aspects of space-dispersive techniques.⁵²

Both time- and space- IMS methods can be hyphenated to mass spectrometry instruments (IMS-MS), with which tandem mass spectrometry can be performed (IMS-MS/MS). They also share the principle added values of IMS to MS^{41, 53} that facilitates their integration into the current clinical repertory of analytical methods, as discussed in the recent literature.⁴⁸ IMS-based techniques offer several advantages in terms of speed, specificity and cost. More precisely, mobility separation typically occurs on the millisecond timescale, thus ~3 orders of magnitude faster than chromatography (~seconds). Analytical merits of IMS, such as increasing selectivity and sensitivity of MS, make IMS strategies suitable for analysis of complex mixtures.^{54, 55} As a result, low-abundance metabolites in biological samples can be easily distinguished and sufficient information can be acquired. For example, profiling of human blood metabolome was performed using IMS-MS, and separation of 300 isomeric metabolites was separated within various classes.⁵⁶

The main advantage of IMS is separation of isomers and isobars unresolved with low MS resolution. In many instances, diverse isomeric species were first separated by IMS-MS which was not reported previously with other methods.^{57, 58} Performance and

applications of methods may, however, vary particularly in terms of ion separation and identification.

3.2. Differential mobility spectrometry-mass spectrometry

Differential mobility spectrometry-mass spectrometry (DMS-MS) is proposed in our project as an alternative or complementary approach to chromatographic methods for diagnosis of organic acids. But, one would ask why choosing DMS rather than DT-IMS for analysis of small molecules?

DMS technology is successfully applied for gas-phase separation of small molecules,⁵³ while DT-IMS is primarily dedicated for characterization of macromolecules. DMS could find a greatest utility in metabolomic workflows,⁵⁹ particularly for its powerful separation of isomeric metabolites,⁶⁰⁻⁶³ endogenous as well as exogenous species. For instance, DMS can distinguish between isomers of lipids,⁶⁴ carbohydrates,^{65, 66} amino acids and derivatives such as sarcosine, α - and β -alanine⁶⁷ and α -, β -, and γ -aminobutyric acids.⁶⁸

DMS has also been shown to be very orthogonal to different mass analyzers, which is an important aspect for improving the resolving power of the analytical method.^{54, 69} DMS can thus act as an ion pre-filter.⁷⁰ Ions can be introduced into DMS device continuously allowing real-time monitoring of samples. An additional advantage is that targeted biomarker can be selected at distinct CV value than other metabolites featuring in complex mixture with isomeric species as illustrated in Figure 3. Finally, it has also been shown that the number of false positive assignments can be reduced using DMS.⁷¹

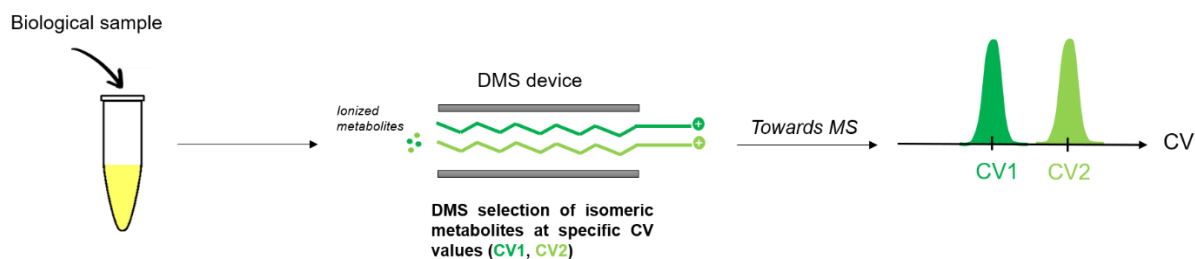


Figure 3: DMS selection of isomeric metabolites at specific values of compensation voltage (CV).

Analytical and diagnosis performance of DMS-MS/MS has been recently evaluated.⁷²⁻⁷⁴ In a recent study,⁷² 800 diverse metabolites were selected using standards dissolved in organic solution. Metabolite coverage achieved with DMS has been shown comparable to that achieved with high-performance liquid chromatography hyphenated to MS. Studies were conducted for separation, identification and quantification of biomarkers in biological fluids, such as amphetamine type stimulants and amino acids and related compounds.^{73, 74}

Both studies^{73, 74} demonstrate that DMS-MS/MS method is adequate for clinical practice. Simple sample pretreatment requires only protein precipitation, and entire analysis time is shortened to less than 1 min. Importantly, concentrations derived from DMS-MS/MS were found in good agreement with the levels obtained with routine LC-MS/MS. Therefore, DMS-MS/MS approach can contribute to potential improvement of clinical applications, allowing for a simple, fast and robust diagnosis.

Interestingly, high orthogonality between DMS and LC has been evidenced based on DMS hyphenated to LC-MS/MS.⁷⁵ Two-dimensional separation using LC-DMS-MS/MS was reported for eight isobaric species in urine.⁷⁶ DMS can distinguish between isobars and isomers co-eluted in chromatographic dimension. Similarly, an approach based on coupling DMS to LC-MS/MS was developed for sensitive and selective quantification of isomeric steroids in plasma samples.⁷⁷ Other advantages gained with

DMS, namely simple preparation of biological samples, fast analysis and high selectivity, are indeed important benefits for routine diagnosis.⁷⁸

4. Identification of metabolites using DMS

Metabolite identification is often an issue using MS-based metabolomics. Identification of metabolites is generally based on three parameters acquired in GC or LC-MS/MS: retention time (RT), m/z values and fragmentation spectra (MS^2).⁷⁹ Many factors complicate metabolite assignment from RT databases such as inter-instrument comparability of RT and lack of stability. In addition, as discussed, isomeric metabolites (same m/z) can be co-eluted at nearly the same RT and may display similar fragmentation spectra using conventional techniques, as shown in Figure 4. Additional robust and confident molecular identifier is thus needed.

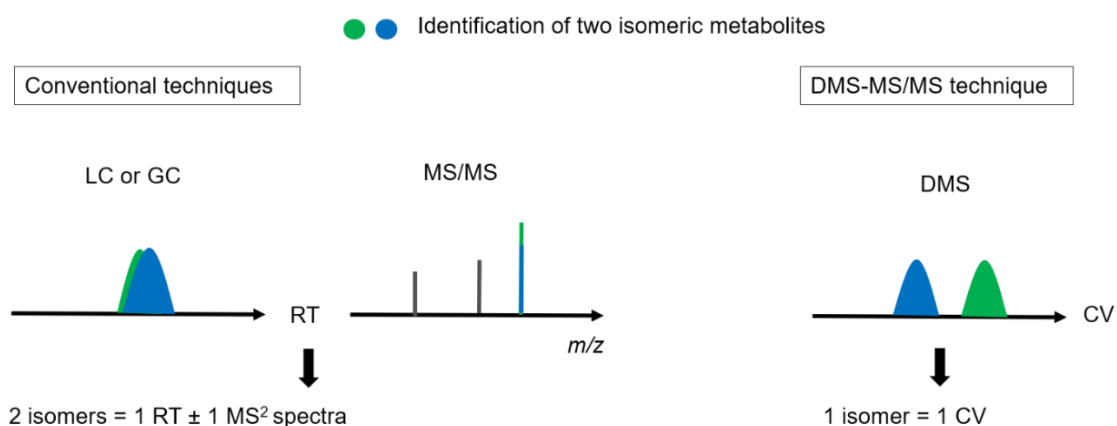


Figure 4: Illustration of identification of two isomeric metabolites using conventional techniques based on LC or GC-MS/MS and DMS-MS/MS.

To address this issue, several studies convey benefits of classical IMS for structural identification of metabolites, especially isomeric species.^{46, 80, 81} IMS-derived cross collision section (CCS) provides complementary information to m/z , as shown for peptides, lipids and carbohydrates.⁸² As a result, more and more CCS libraries have been created to enhance metabolites characterization.^{81, 83}

The idea of using the so-called CV as an identifier was further investigated.⁷⁴ A chromatography-like CV spectrum of analytes of interest provides information about species present in a sample. The characteristic CV can be an identification parameter as retention time obtained with GC/LC methods. In the case of isomers, DMS can allow a selective transmission of one species at a specific CV value, and consequently a reliable identification (Figure 4). CV value could be a valuable criterion for an accurate and specific characterization of metabolites.

This chapter introduces DMS as a promising technique for diagnosis of inherited metabolic disorders. The case of methylmalonic acidemia is discussed. Conventional techniques currently applied in routine are based on GC- and LC- methods. Both techniques achieve analytical goals for analysis of metabolites/biomarkers, but a simple and fast analytical method is still needed. DMS can play an important role for fast separation, reliable identification and quantification of biomarkers in biological fluids. As such, DMS-MS could be an appropriate alternative and complementary method of conventional approaches applied for clinical diagnosis.

This thesis deals with a development of a robust method based on DMS for diagnosis of pertinent metabolites. In this thesis, there is a particular focus on methylmalonic acid, biomarker of methylmalonic acidemia. Our ultimate objective is to evaluate DMS-MS analytical performance for separation of MMA from its isomer succinic acid, its identification and quantification in plasma samples.

Chapter I consists of a literature review of fundamentals that underly DMS separation process. The chapter provides a summary of DMS history, then DMS principle and mechanisms of separation based on evidences provided in recent literature.

Chapter II outlines experimental workflow adapted in this work. This chapter includes, reagents and materials used for sample preparation and calibration. Then, our mass

spectrometers and home-built mobility device used for optimization and organic acids analysis are described. Data analysis and validation method are also reported.

Chapter III begins with a discussion of ionization of organic acids in positive mode. Results about how ion reaction occurring in transfer region can convolute DMS spectra are presented with examples. Optimization of important DMS parameters is detailed, particularly of dry gas flow effect on ion desolvation before DMS entering. The chapter closes with a discussion for the choice of cation for analysis of organic acids in plasma.

Chapter IV presents a proof-of-concept of DMS-MS protocol to be used for analysis of organic acids in plasma. Separation is carried out in our standard DMS conditions. DMS identification of a set of isomeric organic acids in plasma was successful over a large period of time. Additionally, the method was validated for quantification of MMA in plasma. Combined calibration of organic acids and amino acids within the same plasma sample was achieved in the perspective of multi-class metabolites analysis.

Finally, **Chapter V** is dedicated to conclusions and future directions related to this work.

References

1. Ferreira, C. R.; Rahman, S.; Keller, M.; Zschocke, J.; Grp, I. A., An international classification of inherited metabolic disorders (ICIMD). *J. Inherit. Metab. Dis.* **2021**, *44* (1), 164-177.
2. Zhang, A.; Sun, H.; Wu, X.; Wang, X., Urine metabolomics. *Clin. Chim. Acta* **2012**, *414*, 65-69.
3. Zhang, A. H.; Sun, H.; Wang, X. J., Saliva Metabolomics Opens Door to Biomarker Discovery, Disease Diagnosis, and Treatment. *Appl. Biochem. Biotechnol.* **2012**, *168* (6), 1718-1727.
4. Vaidyanathan, K.; Narayanan, M. P.; Vasudevan, D. M., Organic acidurias: an updated review. *Indian J Clin Biochem* **2011**, *26* (4), 319-325.
5. Oberholz.Vg; Levin, B.; Burgess, E. A.; Young, W. F., Methylmalonic aciduria - an inborn error of metabolism leading to chronic metabolic acidosis. *Arch. Dis. Child.* **1967**, *42* (225), 492-&.
6. Matsui, S. M.; Mahoney, M. J.; Rosenberg, L. E., The natural-history of the inherited methylmalonic acidemias. *N. Engl. J. Med.* **1983**, *308* (15), 857-861.
7. Kolker, S.; Schwab, M.; Horster, F.; Sauer, S.; Hinz, A.; Wolf, N. I.; Mayatepek, E.; Hoffmann, G. F.; Smeitink, J. A. M.; Okun, J. G., Methylmalonic acid, a biochemical hallmark of methylmalonic acidurias but no inhibitor of mitochondrial respiratory chain. *J. Biol. Chem.* **2003**, *278* (48), 47388-47393.
8. White, A. M.; Cox, E. V., Methylmalonic acid excretion and vitamin b12 deficiency in the human. *Annals of the New York Academy of Sciences* **1964**, *112* (2), 915-921.
9. Gowda, G. A. N.; Zhang, S. C.; Gu, H. W.; Asiago, V.; Shanaiah, N.; Raftery, D., Metabolomics-based methods for early disease diagnostics. *Expert Rev. Mol. Diagn.* **2008**, *8* (5), 617-633.
10. Nicholson, J. K.; Lindon, J. C.; Holmes, E., 'Metabonomics': understanding the metabolic responses of living systems to pathophysiological stimuli via multivariate statistical analysis of biological NMR spectroscopic data. *Xenobiotica* **1999**, *29* (11), 1181-1189.
11. Oliver, S. G., Systematic functional analysis of the yeast genome (vol 16, pg 373, 1998). *Trends in Biotechnology* **1998**, *16* (10), 447-447.

12. Zhang, A. H.; Sun, H.; Yan, G. L.; Wang, P.; Wang, X. J., Metabolomics for Biomarker Discovery: Moving to the Clinic. *Biomed Res. Int.* **2015**, 2015, 6.
13. Wikoff, W. R.; Gangoiti, J. A.; Barshop, B. A.; Siuzdak, G., Metabolomics identifies perturbations in human disorders of propionate metabolism. *Clinical Chemistry* **2007**, 53 (12), 2169-2176.
14. Tsoukalas, D.; Alegakis, A.; Fragkiadaki, P.; Papakonstantinou, E.; Nikitovic, D.; Karataraki, A.; Nosyrev, A. E.; Papadakis, E. G.; Spandidos, D. A.; Drakoulis, N.; Tsatsakis, A. M., Application of metabolomics: Focus on the quantification of organic acids in healthy adults. *Int. J. Mol. Med.* **2017**, 40 (1), 112-120.
15. Patti, G. J.; Yanes, O.; Siuzdak, G., Metabolomics: the apogee of the omics trilogy. *Nat. Rev. Mol. Cell Biol.* **2012**, 13 (4), 263-269.
16. Chalmers, R. A.; Lawson, A. M.; Watts, R. W., Studies on the urinary acidic metabolites excreted by patients with beta-methylcrotonylglycinuria, propionic acidemia and methylmalonic acidemia, using gas-liquid chromatography and mass spectrometry. *Clin Chim Acta* **1974**, 52 (1), 43-51.
17. Tanaka, K.; Hine, D. G.; West-Dull, A.; Lynn, T. B., Gas-chromatographic method of analysis for urinary organic acids. I. Retention indices of 155 metabolically important compounds. *Clin Chem* **1980**, 26 (13), 1839-46.
18. Tanaka, K.; West-Dull, A.; Hine, D. G.; Lynn, T. B.; Lowe, T., Gas-chromatographic method of analysis for urinary organic acids. II. Description of the procedure, and its application to diagnosis of patients with organic acidurias. *Clin Chem* **1980**, 26 (13), 1847-53.
19. Fu, X. W.; Kimura, M.; Iga, M.; Yamaguchi, S., Gas chromatographic-mass spectrometric screening for organic acidemias using dried urine filter paper: determination of alpha-ketoacids. *J. Chromatogr. B* **2001**, 758 (1), 87-94.
20. Lee, S. H.; Kim, S. O.; Chung, B. C., Gas chromatographic mass spectrometric determination of urinary oxoacids using O-(2,3,4,5,6-pentafluorobenzyl)oxime trimethylsilyl ester derivatization and cation-exchange chromatography. *J. Chromatogr. B* **1998**, 719 (1-2), 1-7.
21. Hagen, T.; Korson, M. S.; Sakamoto, M.; Evans, J. E., A GC/MS/MS screening method for multiple organic acidemias from urine specimens. *Clin Chim Acta* **1999**, 283 (1-2), 77-88.

22. Dagan, S., Comparison of gas chromatography-pulsed flame photometric detection-mass spectrometry, automated mass spectral deconvolution and identification system and gas chromatography-tandem mass spectrometry as tools for trace level detection and identification. *Journal of Chromatography A* **2000**, 868 (2), 229-247.
23. Marcell, P. D.; Stabler, S. P.; Podell, E. R.; Allen, R. H., QUANTITATION OF METHYLMALONIC ACID AND OTHER DICARBOXYLIC-ACIDS IN NORMAL SERUM AND URINE USING CAPILLARY GAS-CHROMATOGRAPHY MASS-SPECTROMETRY. *Anal. Biochem.* **1985**, 150 (1), 58-66.
24. Stabler, S. P.; Marcell, P. D.; Podell, E. R.; Allen, R. H.; Lindenbaum, J., ASSAY OF METHYLMALONIC ACID IN THE SERUM OF PATIENTS WITH COBALAMIN DEFICIENCY USING CAPILLARY GAS-CHROMATOGRAPHY MASS-SPECTROMETRY. *J. Clin. Invest.* **1986**, 77 (5), 1606-1612.
25. Rasmussen, K., Solid-phase sample extraction for rapid determination of methylmalonic acid in serum and urine by a stable-isotope-dilution method. *Clin Chem* **1989**, 35 (2), 260-4.
26. Gibbs, B. F.; Itiaba, K.; Mamer, O. A.; Crawhall, J. C.; Cooper, B. A., A rapid method for the analysis of urinary methylmalonic acid. *Clin. Chim. Acta* **1972**, 38 (2), 447-453.
27. Xiao, J. F.; Zhou, B.; Ransom, H. W., Metabolite identification and quantitation in LC-MS/MS-based metabolomics. *Trends Analyt Chem* **2012**, 32, 1-14.
28. Want, E. J.; Wilson, I. D.; Gika, H.; Theodoridis, G.; Plumb, R. S.; Shockcor, J.; Holmes, E.; Nicholson, J. K., Global metabolic profiling procedures for urine using UPLC-MS. *Nat Protoc* **2010**, 5 (6), 1005-18.
29. Roux, A.; Lison, D.; Junot, C.; Heilier, J. F., Applications of liquid chromatography coupled to mass spectrometry-based metabolomics in clinical chemistry and toxicology: A review. *Clin. Biochem.* **2011**, 44 (1), 119-135.
30. Gamoh, K.; Saitoh, H.; Wada, H., Improved liquid chromatography/mass spectrometric analysis of low molecular weight carboxylic acids by ion exclusion separation with electrospray ionization. *Rapid Communications in Mass Spectrometry* **2003**, 17 (7), 685-689.
31. Magera, M. J.; Helgeson, J. K.; Matern, D.; Rinaldo, P., Methylmalonic acid measured in plasma and urine by stable-isotope dilution and electrospray tandem mass spectrometry. *Clinical Chemistry* **2000**, 46 (11), 1804-1810.

32. Kushnir, M.; Komaromy-Hiller, G.; Shushan, B.; Urry, F. M.; Roberts, W., Analysis of dicarboxylic acids by tandem mass spectrometry. High-throughput quantitative measurement of methylmalonic acid in serum, plasma, and urine. *Clinical chemistry* **2001**, *47* 11, 1993-2002.
33. Schmedes, A.; Brandslund, I., Analysis of Methylmalonic Acid in Plasma by Liquid Chromatography–Tandem Mass Spectrometry. *Clinical Chemistry* **2006**, *52* (4), 754-757.
34. Blom, H. J.; van Rooij, A.; Hogeveen, M., A simple high-throughput method for the determination of plasma methylmalonic acid by liquid chromatography-tandem mass spectrometry. *Clin. Chem. Lab. Med.* **2007**, *45* (5), 645-650.
35. Pedersen, T. L.; Keyes, W. R.; Shahab-Ferdows, S.; Allen, L. H.; Newman, J. W., Methylmalonic acid quantification in low serum volumes by UPLC-MS/MS. *Journal of Chromatography B-Analytical Technologies in the Biomedical and Life Sciences* **2011**, *879* (19), 1502-1506.
36. Lakso, H. A.; Appelblad, P.; Schneede, J., Quantification of Methylmalonic Acid in Human Plasma with Hydrophilic Interaction Liquid Chromatography Separation and Mass Spectrometric Detection. *Clinical Chemistry* **2008**, *54* (12), 2028-2035.
37. Klupczynska, A.; Plewa, S.; Sytek, N.; Sawicki, W.; Dereziński, P.; Matysiak, J.; Kokot, Z. J., A study of low-molecular-weight organic acid urinary profiles in prostate cancer by a new liquid chromatography-tandem mass spectrometry method. *Journal of Pharmaceutical and Biomedical Analysis* **2018**, *159*, 229-236.
38. Körver-Keularts, I.; Wang, P.; Waterval, H.; Kluijtmans, L. A. J.; Wevers, R. A.; Langhans, C. D.; Scott, C.; Habets, D. D. J.; Bierau, J., Fast and accurate quantitative organic acid analysis with LC-QTOF/MS facilitates screening of patients for inborn errors of metabolism. *J Inherit Metab Dis* **2018**, *41* (3), 415-424.
39. Cohen, M. J.; Karasek, F. W., Plasma Chromatography™—A New Dimension for Gas Chromatography and Mass Spectrometry. *Journal of Chromatographic Science* **1970**, *8* (6), 330-337.
40. Hill, H. H.; Siems, W. F.; St. Louis, R. H., Ion mobility spectrometry. *Anal. Chem.* **1990**, *62* (23), 1201A-1209A.
41. D'Atri, V.; Causon, T.; Hernandez-Alba, O.; Mutabazi, A.; Veuthey, J.-L.; Cianferani, S.; Guillarme, D., Adding a new separation dimension to MS and LC–MS: What is the utility of ion mobility spectrometry? *Journal of Separation Science* **2018**, *41* (1), 20-67.

42. Lanucara, F.; Holman, S. W.; Gray, C. J.; Evers, C. E., The power of ion mobility-mass spectrometry for structural characterization and the study of conformational dynamics. *Nature Chemistry* **2014**, *6*, 281.
43. Dwivedi, P.; Wu, P.; Klopsch, S. J.; Puzon, G. J.; Xun, L.; Hill, H. H., Metabolic profiling by ion mobility mass spectrometry (IMMS). *Metabolomics* **2008**, *4* (1), 63-80.
44. Jin, L.; Barran, P. E.; Deakin, J. A.; Lyon, M.; Uhrin, D., Conformation of glycosaminoglycans by ion mobility mass spectrometry and molecular modelling. *Phys. Chem. Chem. Phys.* **2005**, *7* (19), 3464-3471.
45. McLean, J. A.; Ruotolo, B. T.; Gillig, K. J.; Russell, D. H., Ion mobility-mass spectrometry: a new paradigm for proteomics. *International Journal of Mass Spectrometry* **2005**, *240* (3), 301-315.
46. Paglia, G.; Angel, P.; Williams, J. P.; Richardson, K.; Olivos, H. J.; Thompson, J. W.; Menikarachchi, L.; Lai, S.; Walsh, C.; Moseley, A.; Plumb, R. S.; Grant, D. F.; Palsson, B. O.; Langridge, J.; Geromanos, S.; Astarita, G., Ion mobility-derived collision cross section as an additional measure for lipid fingerprinting and identification. *Anal Chem* **2015**, *87* (2), 1137-44.
47. Beck, A.; Terral, G.; Debaene, F.; Wagner-Rousset, E.; Marcoux, J.; Janin-Bussat, M. C.; Colas, O.; Van Dorselaer, A.; Cianféroni, S., Cutting-edge mass spectrometry methods for the multi-level structural characterization of antibody-drug conjugates. *Expert Rev Proteomics* **2016**, *13* (2), 157-83.
48. Chouinard, C. D.; Wei, M. S.; Beekman, C. R.; Kemperman, R. H. J.; Yost, R. A., Ion Mobility in Clinical Analysis: Current Progress and Future Perspectives. *Clinical Chemistry* **2016**, *62* (1), 124-133.
49. Kanu, A. B.; Dwivedi, P.; Tam, M.; Matz, L.; Hill Jr., H. H., Ion mobility-mass spectrometry. *Journal of Mass Spectrometry* **2008**, *43* (1), 1-22.
50. Cumeras, R.; Figueras, E.; Davis, C. E.; Baumbach, J. I.; Gràcia, I., Review on Ion Mobility Spectrometry. Part 1: current instrumentation. *Analyst* **2015**, *140* (5), 1376-1390.
51. May, J. C.; McLean, J. A., Ion Mobility-Mass Spectrometry: Time-Dispersive Instrumentation. *Anal. Chem.* **2015**, *87* (3), 1422-1436.
52. Schneider, B. B.; Nazarov, E. G.; Londry, F.; Vouros, P.; Covey, T. R., Differential mobility spectrometry/mass spectrometry history, theory, design optimization, simulations, and applications. *Mass Spectrometry Reviews* **2016**, *35* (6), 687-737.

53. Laphorn, C.; Pullen, F.; Chowdhry, B. Z., Ion mobility spectrometry-mass spectrometry (IMS-MS) of small molecules: Separating and assigning structures to ions. *Mass Spectrometry Reviews* **2013**, *32* (1), 43-71.
54. Guevremont, R.; Barnett, D. A.; Purves, R. W.; Vandermeij, J., Analysis of a tryptic digest of pig hemoglobin using ESI-FAIMS-MS. *Anal. Chem.* **2000**, *72* (19), 4577-4584.
55. Donohoe, G. C.; Maleki, H.; Arndt, J. R.; Khakinejad, M.; Yi, J. H.; McBride, C.; Nurkiewicz, T. R.; Valentine, S. J., A New Ion Mobility-Linear Ion Trap Instrument for Complex Mixture Analysis. *Anal. Chem.* **2014**, *86* (16), 8121-8128.
56. Dwivedi, P.; Schultz, A. J.; Hill, H. H., *Int. J. Mass Spectrom.* **2010**, *298*, 78.
57. Liu, Y. S.; Clemmer, D. E., Characterizing oligosaccharides using injected-ion mobility mass spectrometry. *Anal. Chem.* **1997**, *69* (13), 2504-2509.
58. Xing, Z.; Chiu, V. M.; Stoica, G.; Gina, L. G.; Schenk, J. O.; Hill, H. H., Metabolic Analysis of Striatal Tissues from Parkinson's Disease-like Rats by Electrospray Ionization Ion Mobility Mass Spectrometry. *Anal. Chem.* **2014**, *86* (6), 3075-3083.
59. Wernisch, S.; Pennathur, S., Application of differential mobility-mass spectrometry for untargeted human plasma metabolomic analysis. *Analytical and Bioanalytical Chemistry* **2019**, *411* (24), 6297-6308.
60. Parson, W. B.; Schneider, B. B.; Kertesz, V.; Corr, J. J.; Covey, T. R.; Van Berkel, G. J., Rapid analysis of isomeric exogenous metabolites by differential mobility spectrometry – mass spectrometry. *Rapid Communications in Mass Spectrometry* **2011**, *25* (22), 3382-3386.
61. Coy, S. L.; Krylov, E. V.; Schneider, B. B.; Covey, T. R.; Brenner, D. J.; Tyburski, J. B.; Patterson, A. D.; Krausz, K. W.; Fornace, A. J.; Nazarova, E. G., Detection of radiation-exposure biomarkers by differential mobility prefiltered mass spectrometry (DMS-MS). *International Journal of Mass Spectrometry* **2010**, *291* (3), 108-117.
62. Maccarone, A. T.; Duldig, J.; Mitchell, T. W.; Blanksby, S. J.; Duchoslav, E.; Campbell, J. L., Characterization of acyl chain position in unsaturated phosphatidylcholines using differential mobility-mass spectrometry. *Journal of lipid research* **2014**, *55* (8), 1668-1677.
63. Purves, R. W.; Guevremont, R., Electrospray Ionization High-Field Asymmetric Waveform Ion Mobility Spectrometry–Mass Spectrometry. *Anal. Chem.* **1999**, *71* (13), 2346-2357.

64. Bowman, A. P.; Abzalimov, R. R.; Shvartsburg, A. A., Broad Separation of Isomeric Lipids by High-Resolution Differential Ion Mobility Spectrometry with Tandem Mass Spectrometry. *J Am Soc Mass Spectrom* **2017**, *28* (8), 1552-1561.
65. Levin, D. S.; Vouros, P.; Miller, R. A.; Nazarov, E. G., Using a nanoelectrospray-differential mobility spectrometer-mass spectrometer system for the analysis of oligosaccharides with solvent selected control over ESI aggregate ion formation. *J Am Soc Mass Spectrom* **2007**, *18* (3), 502-11.
66. Campbell, M. T.; Glish, G. L., Fragmentation in the ion transfer optics after differential ion mobility spectrometry produces multiple artifact monomer peaks. *International Journal of Mass Spectrometry* **2018**, *425*, 47-54.
67. Berthias, F.; Maatoug, B.; Glish, G.; Moussa, F.; Maitre, P., Resolution and Assignment of Differential Ion Mobility Spectra of Sarcosine and Isomers. *J. Am. Soc. Mass Spectrom.* **2018**, *29* (4), 752-760.
68. Wang, Y.; Alhajji, E.; Rieul, B.; Berthias, F.; Maître, P., Infrared isomer-specific fragmentation for the identification of aminobutyric acid isomers separated by differential mobility spectrometry. *International Journal of Mass Spectrometry* **2019**, *443*, 16-21.
69. Baird, M. A.; Shliaha, P. V.; Anderson, G. A.; Moskovets, E.; Laiko, V.; Makarov, A. A.; Jensen, O. N.; Shvartsburg, A. A., High-Resolution Differential Ion Mobility Separations/Orbitrap Mass Spectrometry without Buffer Gas Limitations. *Anal Chem* **2019**, *91* (10), 6918-6925.
70. Shvartsburg, A. A.; Seim, T. A.; Danielson, W. F.; Norheim, R.; Moore, R. J.; Anderson, G. A.; Smith, R. D., High-Definition Differential Ion Mobility Spectrometry with Resolving Power up to 500. *J. Am. Soc. Mass Spectrom.* **2013**, *24* (1), 109-114.
71. Hernandez-Mesa, M.; Le Bizec, B.; Monteau, F.; Garcia-Campana, A. M.; Dervilly-Pinel, G., *Anal. Chem.* **2018**, *90*, 4616.
72. Wernisch, S.; Afshinnia, F.; Rajendiran, T.; Pennathur, S., Probing the application range and selectivity of a differential mobility spectrometry–mass spectrometry platform for metabolomics. *Analytical and Bioanalytical Chemistry* **2018**, *410* (12), 2865-2877.
73. Chen, P.-S.; Chen, S.-H.; Chen, J.-H.; Haung, W.-Y.; Liu, H.-T.; Kong, P.-H.; Yang, O. H.-Y., Modifier-assisted differential mobility–tandem mass spectrometry method for detection and quantification of amphetamine-type stimulants in urine. *Analytica Chimica Acta* **2016**, *946*, 1-8.

74. Berthias, F.; Wang, Y. L.; Alhajji, E.; Rieul, B.; Moussa, F.; Benoist, J. F.; Maitre, P., Identification and quantification of amino acids and related compounds based on Differential Mobility Spectrometry. *Analyst* **2020**, *145* (14), 4889-4900.
75. Campbell, J. L.; Le Blanc, J. C. Y.; Kibbey, R. G., Differential mobility spectrometry: a valuable technology for analyzing challenging biological samples. *Bioanalysis* **2015**, *7* (7), 853-856.
76. Varesio, E.; Le Blanc, J. C. Y.; Hopfgartner, G., Real-time 2D separation by LC × differential ion mobility hyphenated to mass spectrometry. *Analytical and Bioanalytical Chemistry* **2012**, *402* (8), 2555-2564.
77. Jin, W.; Jarvis, M.; Star-Weinstock, M.; Altemus, M., A sensitive and selective LC-differential mobility-mass spectrometric analysis of allopregnanolone and pregnanolone in human plasma. *Analytical and Bioanalytical Chemistry* **2013**, *405* (29), 9497-9508.
78. Ray, J. A.; Kushnir, M. M.; Yost, R. A.; Rockwood, A. L.; Meikle, A. W., Performance enhancement in the measurement of 5 endogenous steroids by LC-MS/MS combined with differential ion mobility spectrometry. *Clin. Chim. Acta* **2015**, *438*, 330-336.
79. Lynn, K. S.; Cheng, M. L.; Chen, Y. R.; Hsu, C.; Chen, A.; Lih, T. M.; Chang, H. Y.; Huang, C. J.; Shiao, M. S.; Pan, W. H.; Sung, T. Y.; Hsu, W. L., Metabolite Identification for Mass Spectrometry-Based Metabolomics Using Multiple Types of Correlated Ion Information. *Anal. Chem.* **2015**, *87* (4), 2143-2151.
80. Sinclair, E.; Hollywood, K. A.; Yan, C.; Blankley, R.; Breitling, R.; Barran, P., Mobilising ion mobility mass spectrometry for metabolomics. *Analyst* **2018**, *143* (19), 4783-4788.
81. Paglia, G.; Williams, J. P.; Menikarachchi, L.; Thompson, J. W.; Tyldesley-Worster, R.; Halldórsson, S.; Rolfsson, O.; Moseley, A.; Grant, D.; Langridge, J.; Palsson, B. O.; Astarita, G., Ion Mobility Derived Collision Cross Sections to Support Metabolomics Applications. *Anal. Chem.* **2014**, *86* (8), 3985-3993.
82. May, J. C.; Goodwin, C. R.; Lareau, N. M.; Leaptrot, K. L.; Morris, C. B.; Kurulugama, R. T.; Mordehai, A.; Klein, C.; Barry, W.; Darland, E.; Overney, G.; Imatani, K.; Stafford, G. C.; Fjeldsted, J. C.; McLean, J. A., Conformational Ordering of Biomolecules in the Gas Phase: Nitrogen Collision Cross Sections Measured on a Prototype High Resolution Drift Tube Ion Mobility-Mass Spectrometer. *Anal. Chem.* **2014**, *86* (4), 2107-2116.

83. Hines, K. M.; May, J. C.; McLean, J. A.; Xu, L., Evaluation of Collision Cross Section Calibrants for Structural Analysis of Lipids by Traveling Wave Ion Mobility-Mass Spectrometry. *Anal. Chem.* **2016**, *88* (14), 7329-7336.

Chapitre I - Differential Mobility Spectrometry: History, Separation Principle and State of the Art

The main characteristics of differential mobility spectrometry instrument and method are described in this chapter. DMS separation of isomers is detailed, and physico-chemical mechanisms that help to understand the separation process are discussed. Literature data are provided to describe the influence of different factors on ions behavior, as well as some important analytical issues found with DMS.

I.1. Origins and evolutions of DMS

Some milestones associated with the evolution of differential mobility spectrometry (DMS) over the years are given in Figure I.1. A more complete general picture can be found in Reference 1.¹ The original concept of DMS device is found in Soviet Union research in the 1980s.² At that time, DMS device equipped with a simple ion source was used for the detection of traces of chemicals such as explosives. The development of this technology continued in different directions. While standalone DMS is still used nowadays, DMS becomes even more powerful in combination with other analytical methods such as tandem mass spectrometry (MS).

When DMS migrated to North America, GC-DMS systems were commercialized by Sionex, Inc. (Bedford, MA) for environmental and toxicological applications.^{3, 4} DMS hyphenated to MS was first published in the literature in 1993.⁵ DMS device was coupled to a quadrupole mass spectrometer with atmospheric ionization source for measurement of atmospheric contaminants. Since that time, DMS has evolved considerably into an inexpensive but powerful analytical tool for the separation and characterization of gas phase ions. More than 45 000 papers have been published in the field of DMS since 1995 (source: SciFinder 2021, date of information gathering: September 2021).

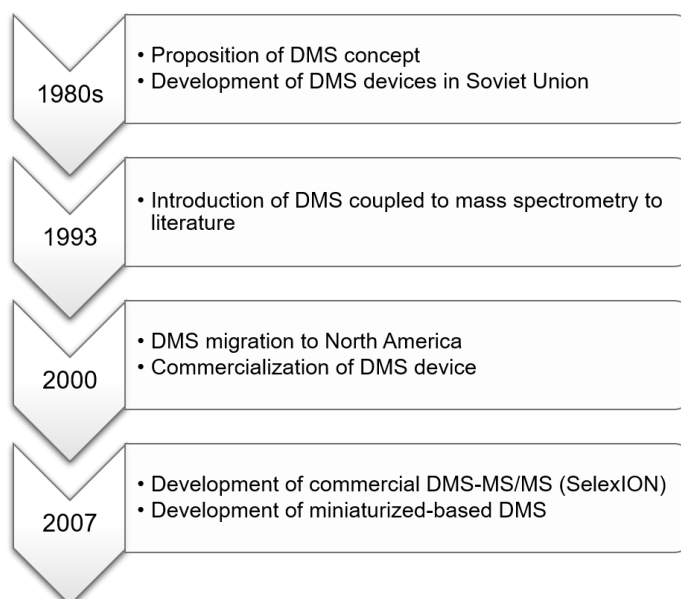


Figure I.1: Important milestones associated with the evolution of differential mobility spectrometry (DMS) technology.

In 2007, AB SCIEX in collaboration with Sionex developed a commercial DMS-MS/MS system with the trade name SelexION,^{6,7} which is still commercialized and coupled to several tandem mass instrument, QTrap (Sciex 5500, 6500 and 6500+ series) and QqTOF (Sciex TripleTOF 5600+ and 6600) (see: <https://sciex.com/>). In parallel, miniaturized-based DMS (μ DMS) has emerged for microscale analysis.^{8,9} Nowadays, μ DMS represents an attractive strategy to achieve fast analysis and high ion transmission efficiency. Micro machine-based DMS is notably applied for the separation of protein and peptide mixture.¹⁰

I.2. Principle of operation of DMS

A DMS cell consists of two parallel planar electrodes, with a defined width and length, spaced by a gap. DMS device is inserted in the electrospray source (ESI), between the needle and the transfer glass capillary to the spectrometer. What happens in the DMS

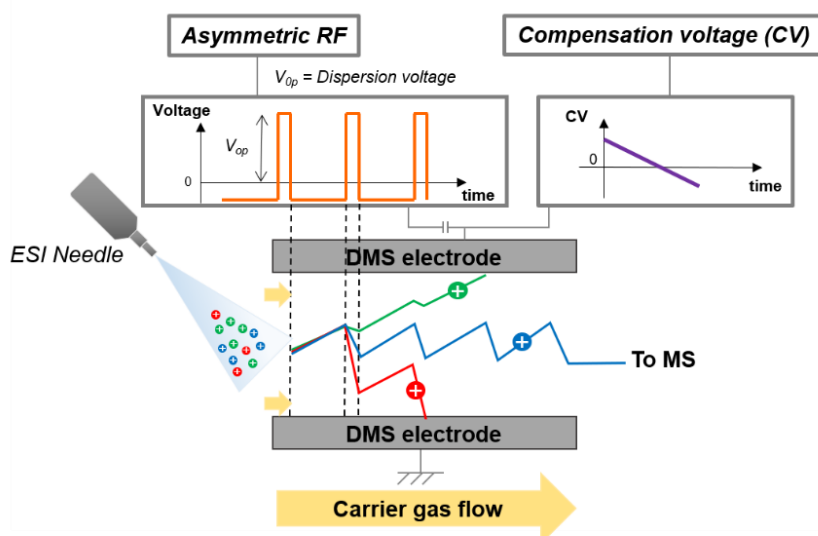
cell? What is the fundamental concept behind the separation process? These questions are detailed in this section.

I.2.1. Principle of separation

DMS separation principle can be illustrated with three isomeric molecules (blue, green and red ions), as in Figure I.2. Once ions are generated by ESI, they are transported by a carrier gas, usually dinitrogen, between the two DMS electrodes, from the atmospheric pressure region towards the low-pressure region of the MS instrument. DMS can be operated in transparent mode (or electric field is turned off), where ions can still pass through the DMS device when DMS electrodes are grounded. Ion signal is found to be decreased by one order of magnitude on recorded mass spectra. A practical advantage of this transparent mode is that a full mass spectrum can be recorded without removing the DMS device. It also allows optimization of ionization and other settings of the MS/MS before starting DMS operation.

DMS separation relies on mobility differences between low and high electric field. In practice, an asymmetric radiofrequency (RF) electric field is applied on the electrodes. As illustrated in Figure I.2a, this RF alternates between high and low electric field, which induces a *zig-zag* ion motion perpendicular to the carrier gas flow in DMS channel. Under the low field portion, ions migrate towards one electrode with very similar mobility (ion trajectories are parallel). Under the high field portion of the waveform, however, ions may have different mobilities when migrating towards the other electrode. The amplitude of the RF (V_{op}) is called dispersion voltage (DV) or separation voltage (SV). Other groups may define DV as peak-to-peak voltage (V_{pp}).¹¹ In general, the higher is the DV or SV value, the better is the peak capacity and the resolution.¹

a) Ion separation



b) DMS spectrum

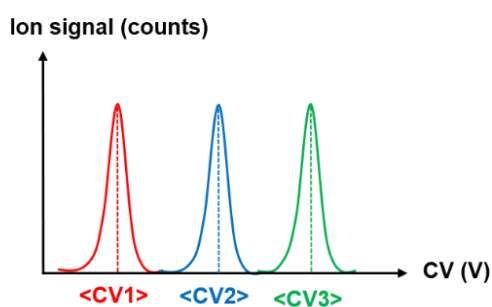


Figure 1.2: Illustration of DMS separation. a) Ion separation occurs under an asymmetric radiofrequency (RF) electric field. Colored dots and lines represent ions and their trajectories between the DMS electrodes, respectively. A compensation voltage (CV) applied to one electrode to compensate the deviation and allows for specific ion transmission. b) A DMS spectrum represents the ion signal intensity plotted against CV value.

Based on literature data, ions exhibit different mobility coefficients under high electric field.¹² As a result, the three ions may have different transverse displacements under the RF electric field, as shown in Figure 1.2a. The resulting ion displacement per cycle can be written as: $K_{HF} \times E_{HF} \times t_{HF} - K_{LF} \times E_{LF} \times t_{LF}$ where K, E and t are the ion mobility, electric field and time, respectively, over one period. HF and LF refer to the high and low electric field, respectively. If transverse displacements under high- and

low- field compensate each other (blue ion), ions are transmitted to the MS instrument. Alternatively, green and red ions are neutralized to either one of the two electrodes.

A compensation voltage (CV) is applied to one electrode compensate transverse displacements under RF. This CV is a constant and adjustable DC voltage, superimposed onto the asymmetric RF. Its purpose is to steer ions to the center axis of the gap, *i.e.* to compensate transverse displacement, and insure their transmission to MS.

A typical CV scan mode is represented in Figure I.2: at a fixed DV value, CV is scanned typically in a range of few 10-volts to sequentially allow ions to pass through the DMS device towards the mass spectrometer. CV value for maximum ion transmission defines the peak position. A DMS spectrum, which can be also called ionogram or extracted ion chromatogram (EIC or XIC),¹³ corresponds to the ion signal intensity at a given mass-to-charge ratio as a function of CV value as represented in Figure I.2b.

I.2.2. Ion mobility coefficient *versus* electric field

This section focuses on the theoretical basis of ion mobility spectrometry, and more precisely DMS operation. It should be noted that mobility equations are usually expressed using the reduced electric field E/N , where E is the electric field ($V.cm^{-1}$), and N is the gas number density (cm^{-3}). E/N is conventionally expressed in Townsend units (Td, $1Td = 10^{-17} V.cm^2$). For a sake of implication, however, electric field will be only used in the following equations.

Ion mobility separation is based on ion acceleration in a transport gas or carrier gas, at atmospheric pressure, by an electric field (E). The average ion velocity is proportional to the electric field through K factor defined as the ion mobility coefficient. This velocity is constant under the effect of a low and uniform electric field, because the kinetic energy gained by the field is transferred to gas during collision. Based on

measurements of ion mobility coefficient made for different types of molecules,^{12, 14} mobility K usually remains constant under low electric field, as illustrated in Figure I.3 for three (isomeric) ions.

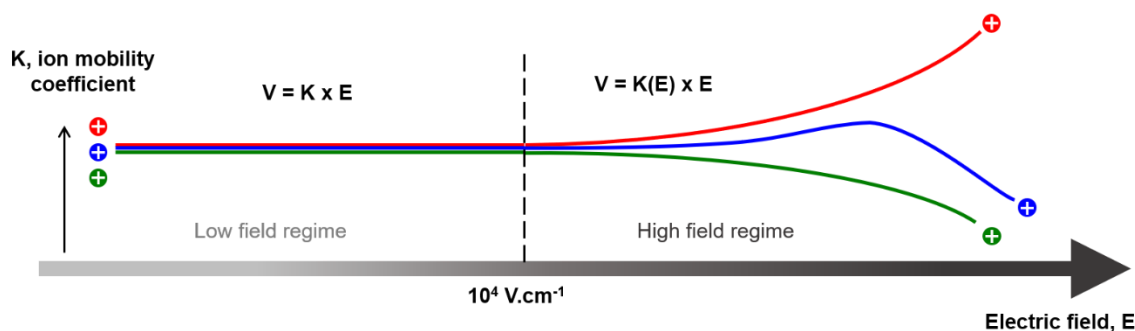


Figure I.3: Representation of ion mobility coefficient (K) evolution as a function of electric field (E).

Low-field mobility forms the basis for ion separation in drift tube ion mobility (DT-IMS) devices. A short pulse length of ions is introduced into the DT-IMS device which defines the time phase. Ions are then time-separated based on their drift time under a relatively low and uniform electric field (typically $<10^4 \text{ V.cm}^{-1}$, $< 30 \text{ Td}$) in a gas at atmospheric pressure. Measured drift time (t_d) is related to K coefficient as in Equation (1), where L , is the length of the drift tube, typically $\sim 1 \text{ m}$, and E , is the electric field.

$$t_d = \frac{L}{K \times E} \quad (1)$$

The mobility coefficient is given by Mason-Schamp equation.¹⁵ The mobility K is related to reduced mass of ions and carrier gas molecules (μ), ion charge (z) and structure (Ω) (Equation (2)). Collision cross section (Ω or CCS) with the given carrier gas is used for identification.^{16, 17} Different groups are involved in this field, and CCS databases are available for a variety of compounds.¹⁸⁻²¹

$$K \propto \frac{z}{\sqrt{\mu\Omega}} \quad (2)$$

As represented in Figure I.3, mobility coefficient K may itself be a function of E when high electric field is applied ($>10^4 \text{ V cm}^{-1}$, $>30 \text{ Td}$).²² Ions may have different mobilities under the effect of high electric field, displaying various behaviors as a function of E , as illustrated in Figure I.3. The dependence of the mobility coefficient on electric field is mathematically translated as in Equation (3):

$$K(E) = K(0)[1 + \alpha(E)] \quad (3)$$

where $K(0)$ is the reduced mobility coefficient, *i.e.* low-field mobility coefficient, and $\alpha(E)$ is the differential mobility alpha function of the ion of interest. Alpha function is a characteristic property of an ion that describes the field dependence of ion mobility, as expressed in the following Equation.

$$\alpha(E) = \frac{K(E) - K(0)}{K(0)} \quad (4)$$

I.3. Three types of ions

Three distinct ion types (A, B and C) can be distinguished using DMS.²²⁻²⁴ These ion behaviors have been observed for different molecules and interpretations have been proposed based on the interactions between ions with carrier gas molecules.^{25, 26} Dependence of alpha function on reduced electric field (E/N) was derived using dispersion plots.¹⁴ Dispersion plots can also represent evolution of CV value as a function of E/N or DV value, as illustrated in Figure I.4., since CV is inversely related to ion mobility coefficient.¹

Type A behavior (red ion) corresponds to a mobility increase as a function of the electric field. As a result, negative CV shift is observed as DV increases. Type A behavior is generally interpreted as resulting from repetitive cycles of clustering/declustering processes between ion and the transport gas atoms or molecules under the asymmetric waveform. Clusters are ion-molecule complexes formed under the low-

field portion of the waveform. Declusterisation occurs under high electric field portion where naked ions are released from clusters through energetic collisions with the gas.

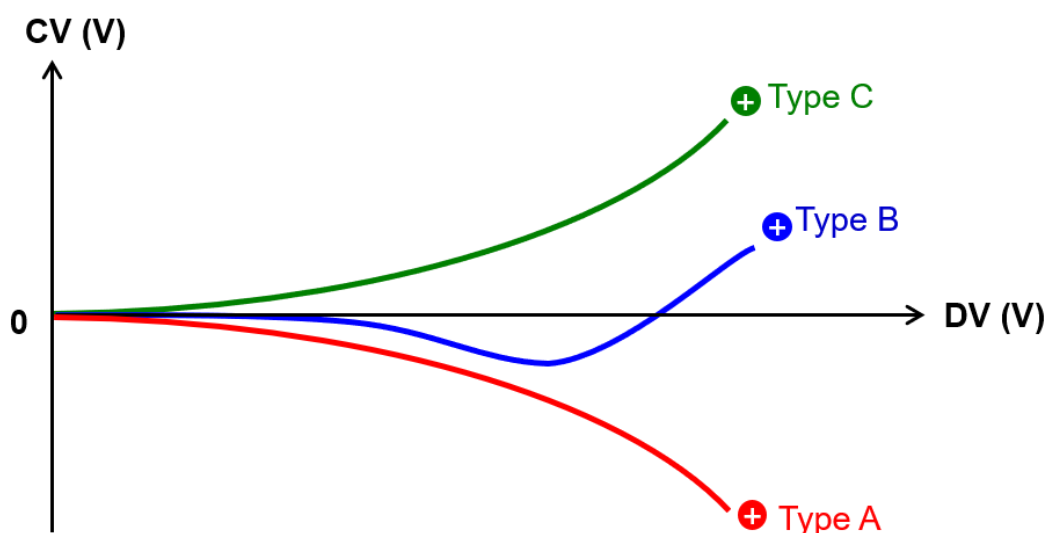


Figure 1.4: Three dispersion plots are illustrated for Type A, B and C ions. Dispersion plot defined as variation of compensation voltage (CV) as a function of dispersion voltage (DV).

This mechanism accounts for the non-linear electric field dependence of the ion differential mobility which is the basis of the DMS separation. DMS separation is also related to the unique ion-molecule interactions. Ion-molecule clustering can occur with N_2 but gets more pronounced in the presence of polar organic molecules, as evidenced by larger negative CV shifts.²⁸⁻³¹

Type C behavior (green ion) corresponds to a decrease of mobility as a function of DV. As a result, CV shifts towards more positive values when increasing DV. This is interpreted as being due to elastic collisions with gas molecules. Type C occurs typically with proton bound dimer which can be considered as hard sphere since charge is embedded, thus preventing strong interactions with gas molecules. Hard sphere collision regime typically dominates the separation with an inert carrier gas such as helium which does not bind strongly with ions.²⁶

Type B behavior (blue ion) illustrates a combination of type A and type C. CV value initially decreases with DV (Type A), reaches a minimum, then increases at higher DV (Type C). In a way, this behavior should be observed with any Type A ion when increasing sufficiently the DV value.

I.4. DMS separation: influence of modifiers

I.4.1. Evidence of ion-modifier clustering

One way to improve DMS separation is the addition of polar molecules called modifiers to the carrier gas. Modifier effect was first described based on experiments performed in presence of moisture in the transport gas.^{5, 27} The observed CV shifts were related to the dynamic clustering-declustering model.^{28, 29} The relationship between an ion DMS behavior and ion-molecule clustering has been examined in several studies.^{25, 26, 30, 31} While the degree of CV shift is traditionally employed to assess ion-molecule clustering in a DMS environment, dispersion plot can also provide experimental evidence of equal importance. Different examples reported in the literature are discussed below.

Hopkins and coworkers have studied DMS behavior of five 2-methylquinolinium isomer pairs using dispersion pots recorded with different carrier gas composition.³¹ Each pair of isomers differs by the position of a substituent (NH₂, CH₃, NO₂, Cl, ...) which is either in the 6-position (red) or 8-position (blue) (Figure I.5a). All isomeric pairs exhibit identical Type C behavior using only N₂ as a carrier gas (Figure I.5b). However, upon addition of water to the carrier gas, DMS behavior changes to Type B and isomers become separated (Figure I.5c). The observed dispersion plots of isomers were found to be distinct, except for amino- and nitro-substituted derivatives. As represented in Figure I.5c, CV shift was more negative for 6- than for 8-substituted ions. Thus, it was

hypothesized that water binds more strongly with 6-substituted ions than with 8-substituted ions.

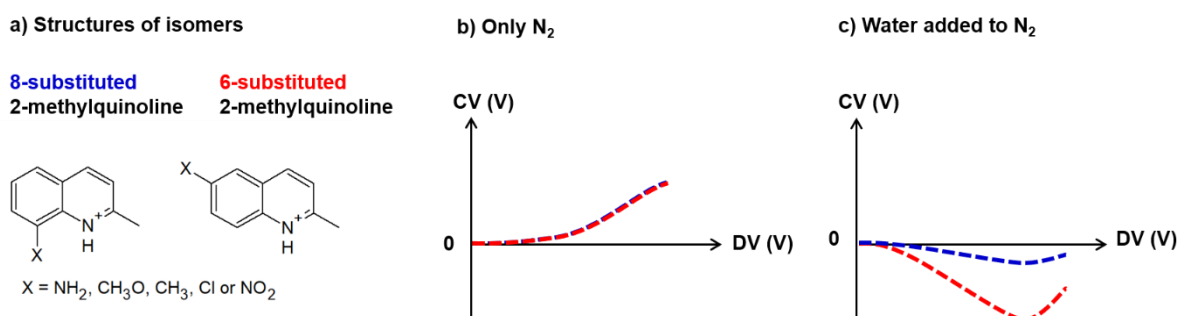


Figure 1.5: Schematic representation of dispersion pots of isomeric 2-methylquinoline derivatives. a) Structures of 6- and 8-substituted derivatives. b) Dispersion plots with only N₂ carrier gas. c) Dispersion plot with water added to N₂ carrier gas.³¹

The weak water clustering with 8-substituted derivatives can be rationalized using steric consideration. Indeed, ion-water cluster results from hydrogen bonding between water and charge site -NH⁺, and steric interaction with proximal substituent on position 8 may makes ion-water interaction weaker. If amino- or nitro- derivatives are considered, however, substitution on 8-position can greatly influence H-bond network.

In the case of 8-amino substituted quinoline, it has been demonstrated that two N-H \cdots O hydrogen bonds were formed.³¹ One between water and -NH⁺ charge, and the other between water and one amino NH in the vicinity (8-position) of the charge site. As a result, the ion-cluster is strongly bound, which explains the large negative CV shift for the 8- similar to the 6-amino substituted isomer.

In the case of the nitro group in the 8-position, the reverse is true. An intramolecular hydrogen bond is formed between -NH⁺ and nitro group in the 8-position of the naked ion. Hence, formation of hydrogen bond between water and -NH⁺ requires distortion and/or disruption of this intramolecular hydrogen bond. As a result, water-ion interaction is not much stronger in the 8- than in the 6-nitro substituted isomer.

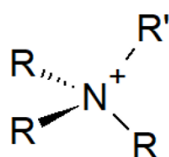
Among factors that may impact ion-modifier clustering, charge delocalization was identified in another related study of protonated substituted quinoline.³² Electronic donating or withdrawing substituents, in particular on 5- and 7-positions, were found to greatly influence DMS behavior of quinoline derivatives. The charge is thus delocalized via resonance, which results in weak interaction between -NH^+ group and methanol used as modifier. Hence, ion-molecule clustering can be modulated by different steric and/or electronic effects, which in turn impact the DMS behavior of ions.

I.4.2. Effect of charge accessibility on ion-molecule clustering

Effect of charge accessibility on ion-modifier clustering was also characterized based on DMS behaviors of a series of tetraalkylammonium cations (R_4N^+).³⁰ For these ions, it can be assumed that the positive charge is localized on N, and is surrounded by four alkyl chains of increasing size as shown in Figure I.6a. Cations with symmetric and asymmetric structure have been studied. The former corresponds to identical alkyl chain (R_4N^+ , R and R' = methyl to decyl), and the latter corresponds to three methyl groups and one alkyl chain ($(\text{R}'\text{-Me}_3\text{N}^+)$).

Dispersion plots have been recorded using a variety of modifiers added to the carrier N_2 gas, and general trends are provided in Figure I.6b. Using N_2 only as a carrier gas, CV of cations is found to increase as a function of DV. Such trend is associated to hard-sphere behavior with weak ion- N_2 interaction (Type C). This DMS behavior is not surprising since ion- N_2 interaction is intrinsically weak and the positive charge is not easily accessible. With this respect, it is interesting to stress that for a given DV value, the smallest CV value corresponds to the smallest alkyl chain ammonium (Me_4N^+).

a) Structure of tetraalkylammonium cation



R, R' = methyl to decyl

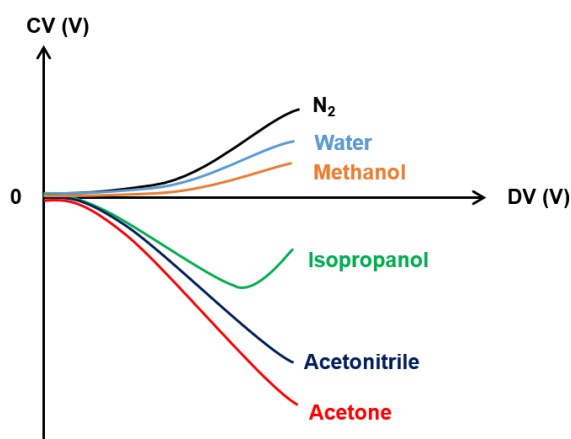
b) Dispersion plots using modifiers in N₂ carrier gas

Figure I.6: Schematic representation of dispersion plots tetraalkylammonium cations. a) Structure of tetraalkylammonium cations. b) General shapes of dispersion plots using different modifiers added to N₂ carrier gas.³⁰

Upon addition of modifiers to the N₂ carrier gas, B- and even A-type behaviors are observed.³⁰ CV values are only slightly shifted with water (light blue curve) and methanol (orange curve). This indicates that weak clusters are formed with R₄N⁺ ions. A more negative CV shift is induced with addition of isopropanol (green curve). Thus, ions more strongly cluster with isopropanol than with methanol and water. CV negative shift increases with addition of acetonitrile, which suggests that clustering is even more pronounced (dark blue curve) than with isopropanol. Ultimately, the most negative CV shift was systematically found to be induced by acetone (red curve). To summarize, one can keep in mind the trend of ion-modifier binding clustering strength: N₂ < water < methanol < isopropanol < acetonitrile < acetone.

The results discussed above illustrate that charge accessibility can greatly control ion-molecule clustering. This conclusion is further reinforced *via* the separation of a series of four isomeric tetraalkylammonium cations: tetrapropylammonium (Pr₄N⁺), protonated tributylamine (Bu₃-HN⁺), protonated dihexylamine (Hx₂- H₂N⁺) and protonated dodecylamine (Do- H₃N⁺). Isomers have the same molecular formula

$C_{12}H_{28}N^+$, but different number of potential H-bonds between charge site and modifiers seeded in the carrier gas.

Clustering is prevented between modifiers and Pr_4N^+ , due to steric hindrance associated with the four alkyl groups surrounding the N^+ charged site. As expected, only acetone and acetonitrile used as modifiers lead to significant negative CV shift (~ -20 V). However, in the case of isomers with one or two H-bonds (Bu_3-HN^+ and $Hx_2-H_2N^+$), the charge site is more accessible. CV shifts observed with acetone, acetonitrile and methanol are nearly the same. In fact, the largest CV shift is found upon addition of isopropanol. This is due to the formation of two H-bonds between $-NH^+$ and isopropanol, leading to strong clustering. Modifiers can more efficiently cluster with $Do-H_3N^+$ ions, when the number of H-bond was increased. Even with water, negative CV shifts are observed. These behaviors arise from the accessibility of charge to modifier molecules.³⁰

To conclude, this systematic study illustrates significant CV shift induced upon modifier addition into N_2 carrier gas strongly depends on charge accessibility.^{30, 31} In the perspective of isomer separation, it should be kept in mind that charge accessibility and delocalization have been found to play a key role in DMS behavior. Hydrogen bonding plays a very special role, which is due to the fact that these hydrogen bonds have ionic character. Ionic hydrogen bonds have been studied thoroughly, and found to be especially strongly bond in proton bond dimers,³³ for example. Hence, isopropanol which allows for the formation of hydrogen bond seems to be an efficient modifier in the sense that different DMS response can be observed for structural isomers.

I.5. Proton-bound dimer: analytical issues

Proton-bound dimer (PBD) are formed under positive ionization conditions, when protonated monomers $[M+H]^+$ are targeted.³⁴ Both homo- and hetero-PBD can be formed, as in the present study. Homo-PBD corresponds to a symmetric shared proton between two monomers $[2M+H]^+$, while hetero-PBD corresponds to a protonated monomer $[M+H]^+$ weakly bound to solvent molecules, *i.e.* $[M+H+H_2O]^+$ or $[M+H+CH_3OH]^+$. From an analytical point of view, formation of PBD is at the expense of $[M+H]^+$ signal.

Identification of DMS peaks corresponding to protonated monomer and its corresponding various PBD has been discussed, for example, for a series of protonated ketones and organophosphorus ions using DMS.^{14, 28} The general DMS spectrum is illustrated in Figure I.7a. Typically, $[M+H]^+$ monomers are observed at negative CV values, while dimers are systematically found at positive CV value. Interestingly, PBD of different organophosphorus compounds were observed at nearly the same CV value leading to a broad peak in the positive CV region. These different PBD correspond to homo-PBD or hetero-PBD formed between two different organophosphorus compounds.

The fact that all these PBD have nearly the same positive CV value can simply be rationalized considering charge (H^+) accessibility. Dinitrogen molecules of carrier gas weakly bind to dimers, especially when PBD are formed with bulky groups. It is important to mention that monomers could also be found at positive CV values. As discussed in the previous section, charge delocalization or intramolecular H-bonding could occur, which prevents clustering between monomer ions and dinitrogen.

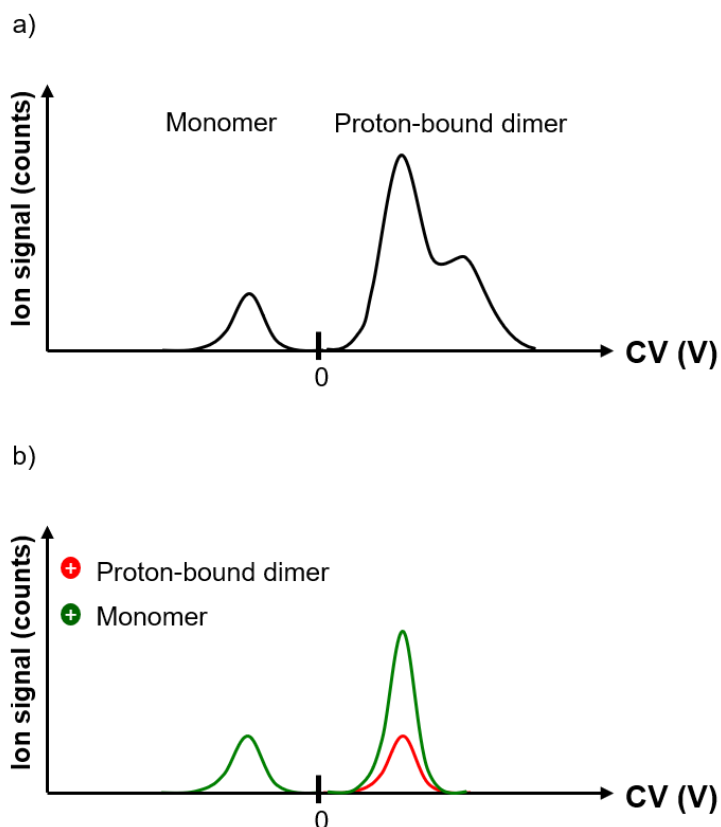


Figure 1.7: Illustration of a typical DMS spectrum displaying monomer and proton-bound dimer peaks.

Furthermore, fragmentation of PBD into $[M+H]^+$ should also be considered, which may lead to a high $[M+H]^+$ signal at positive CV value, characteristic of corresponding PBD. Indeed, DMS-selected PBD can be dissociated into $[M+H]^+$ fragments, in the interface between ambient pressure and high vacuum regions. Additional monomer peaks can thus be found at positive CV values (Figure 1.7b). Assignment of DMS peaks corresponding to potential $[M+H]^+$ monomer should thus be made carefully.

In order to maximize $[M+H]^+$ signal, tandem DMS systems have been proposed.³⁵ The idea is to transmit ions through two successive DMS systems. Both ultraFAIMS and DMS prototype instruments have been used.³⁶ By setting the CV value of the first one to a positive CV value, DMS-selected PBD are activated and fragmented into the

various $[M+H]^+$ of analytical interest. Generated $[M+H]^+$ ions are subsequently characterized using the second DMS stage.

I.6. Summary

This chapter focuses on fundamental and analytical aspects of DMS separation method. Development of DMS, its hyphenation to mass spectrometry and separation principle are discussed. DMS separates ions under the influence of a radiofrequency waveform applied between two parallel electrodes. As discussed, ions can exhibit different behaviors (Type A, B and C) based on ion-molecule interaction. Particular focus is placed on modifier addition to dinitrogen carrier gas to improve ion separation. Systematic studies are reported for understanding and rationalizing modifier effects on clustering. The last section provide evidence on interference of proton-bound dimer species with targeted monomers. From an analytical point of view, dimer formation and post-DMS fragmentation should be taken into consideration when using DMS for correct interpretation of spectra.

References

1. Schneider, B. B.; Nazarov, E. G.; Londry, F.; Vouros, P.; Covey, T. R., Differential mobility spectrometry/mass spectrometry history, theory, design optimization, simulations, and applications. *Mass Spectrometry Reviews* **2016**, *35* (6), 687-737.
2. Gorshkov, M., Inventor's certificate of USSR No. 966583. *G01N27/62* **1982**.
3. Miller, R. A.; Nazarov, E. G.; Eiceman, G. A.; King, A. T., A MEMS radio-frequency ion mobility spectrometer for chemical vapor detection. *Sens. Actuator A-Phys.* **2001**, *91* (3), 301-312.
4. James, J.; Limero, T.; Beck, S.; Cheng, P.; DeVera, V.; Hand, J.; Macatangay, A., International Space Station Air Quality Assessed According to Toxicologically-Grouped Compounds. In *40th International Conference on Environmental Systems*.
5. Buryakov, I. A.; Krylov, E. V.; Nazarov, E. G.; Rasulev, U. K., A new method of separation of multi-atomic ions by mobility at atmospheric pressure using a high-frequency amplitude-asymmetric strong electric field. *International Journal of Mass Spectrometry and Ion Processes* **1993**, *128* (3), 143-148.
6. Schneider, B. B.; Covey, T. R.; Coy, S. L.; Krylov, E. V.; Nazarov, E. G., Planar differential mobility spectrometer as a pre-filter for atmospheric pressure ionization mass spectrometry. *International journal of mass spectrometry* **2010**, *298* (1-3), 45-54.
7. Covey, T. R.; Schneider, B. B.; LeBlanc, Y.; Nazarov, E. G., Polar vapor enhanced separations with planar differential mobility spectrometry–Mass spectrometry. *Current Trends Mass Spectrom* **2012**, 42-48.
8. Wilks, A.; Hart, M.; Koehl, A.; Somerville, J.; Boyle, B.; Ruiz-Alonso, D., Characterization of a miniature, ultra-high-field, ion mobility spectrometer. *International Journal for Ion Mobility Spectrometry* **2012**, 15.
9. Shvartsburg, A. A.; Smith, R. D.; Wilks, A.; Koehl, A.; Ruiz-Alonso, D.; Boyle, B., Ultrafast differential ion mobility spectrometry at extreme electric fields in multichannel microchips. *Anal Chem* **2009**, *81* (15), 6489-95.

10. Winter, D. L.; Wilkins, M. R.; Donald, W. A., Differential Ion Mobility–Mass Spectrometry for Detailed Analysis of the Proteome. *Trends in Biotechnology* **2019**, *37* (2), 198-213.
11. Shvartsburg, A. A.; Danielson, W. F.; Smith, R. D., High-Resolution Differential Ion Mobility Separations Using Helium-Rich Gases. *Anal. Chem.* **2010**, *82* (6), 2456-2462.
12. Krylov, E. V.; Nazarov, E. G.; Miller, R. A., Differential mobility spectrometer: Model of operation. *International Journal of Mass Spectrometry* **2007**, *266* (1), 76-85.
13. Guevremont, R., High-field asymmetric waveform ion mobility spectrometry: A new tool for mass spectrometry. *Journal of Chromatography A* **2004**, *1058* (1), 3-19.
14. Krylov, E.; Nazarov, E. G.; Miller, R. A.; Tadjikov, B.; Eiceman, G. A., Field Dependence of Mobilities for Gas-Phase-Protonated Monomers and Proton-Bound Dimers of Ketones by Planar Field Asymmetric Waveform Ion Mobility Spectrometer (PFAIMS). *The Journal of Physical Chemistry A* **2002**, *106* (22), 5437-5444.
15. Revercomb, H. E.; Mason, E. A., Theory of plasma chromatography/gaseous electrophoresis. Review. *Anal. Chem.* **1975**, *47* (7), 970-983.
16. Ross, D. H.; Cho, J. H.; Xu, L., Breaking Down Structural Diversity for Comprehensive Prediction of Ion-Neutral Collision Cross Sections. *Anal. Chem.* **2020**, *92* (6), 4548-4557.
17. Paglia, G.; Williams, J. P.; Menikarachchi, L.; Thompson, J. W.; Tyldesley-Worster, R.; Halldórsson, S.; Rolfsson, O.; Moseley, A.; Grant, D.; Langridge, J.; Palsson, B. O.; Astarita, G., Ion Mobility Derived Collision Cross Sections to Support Metabolomics Applications. *Anal. Chem.* **2014**, *86* (8), 3985-3993.
18. Dilger, J. M.; Glover, M. S.; Clemmer, D. E., A Database of Transition-Metal-Coordinated Peptide Cross-Sections: Selective Interaction with Specific Amino Acid Residues. *J. Am. Soc. Mass Spectrom.* **2017**, *28* (7), 1293-1303.
19. Hines, K. M.; May, J. C.; McLean, J. A.; Xu, L., Evaluation of Collision Cross Section Calibrants for Structural Analysis of Lipids by Traveling Wave Ion Mobility-Mass Spectrometry. *Anal. Chem.* **2016**, *88* (14), 7329-7336.

20. Goscinny, S.; Joly, L.; De Pauw, E.; Hanot, V.; Eppe, G., Travelling-wave ion mobility time-of-flight mass spectrometry as an alternative strategy for screening of multi-class pesticides in fruits and vegetables. *J Chromatogr A* **2015**, *1405*, 85-93.
21. Zhou, Z.; Shen, X.; Tu, J.; Zhu, Z. J., *Anal. Chem.* **2016**, *88*, 11084.
22. Shvartsburg, A. A., *Differential ion mobility spectrometry: nonlinear ion transport and fundamentals of FAIMS*. CRC Press: 2008.
23. Purves, R. W.; Guevremont, R., Electrospray Ionization High-Field Asymmetric Waveform Ion Mobility Spectrometry–Mass Spectrometry. *Anal. Chem.* **1999**, *71* (13), 2346-2357.
24. Nazarov, E. G.; Coy, S. L.; Krylov, E. V.; Miller, R. A.; Eiceman, G. A., Pressure effects in differential mobility spectrometry. *Anal Chem* **2006**, *78* (22), 7697-706.
25. Schneider, B. B.; Covey, T. R.; Coy, S. L.; Krylov, E. V.; Nazarov, E. G., Control of chemical effects in the separation process of a differential mobility mass spectrometer system. *Eur. J. Mass Spectrom.* **2010**, *16* (1), 57-71.
26. Schneider, B. B.; Covey, T. R.; Coy, S. L.; Krylov, E. V.; Nazarov, E. G., Chemical effects in the separation process of a differential mobility/mass spectrometer system. *Anal. Chem.* **2010**, *82* (5), 1867-1880.
27. Buryakov, I.; Krylov, E.; Makas, A.; Nazarov, E.; Pervukhin, V., Drift spectrometer for the control of amine traces in the atmosphere. *Journal of analytical chemistry (New York, NY)* **1993**, *48* (1), 114-121.
28. Krylova, N.; Krylov, E.; Eiceman, G. A.; Stone, J. A., Effect of moisture on the field dependence of mobility for gas-phase ions of organophosphorus compounds at atmospheric pressure with field asymmetric ion mobility spectrometry. *J Phys Chem A* **2003**, *107* (19), 3648-54.
29. Eiceman, G. A.; Krylov, E. V.; Krylova, N. S.; Nazarov, E. G.; Miller, R. A., Separation of Ions from Explosives in Differential Mobility Spectrometry by Vapor-Modified Drift Gas. *Anal. Chem.* **2004**, *76* (17), 4937-4944.
30. Campbell, J. L.; Zhu, M.; Hopkins, W. S., Ion-molecule clustering in differential mobility spectrometry: lessons learned from tetraalkylammonium cations and their isomers. *J Am Soc Mass Spectrom* **2014**, *25* (9), 1583-91.

31. Liu, C.; Le Blanc, J. C. Y.; Shields, J.; Janiszewski, J. S.; Ieritano, C.; Ye, G. F.; Hawes, G. F.; Hopkins, W. S.; Campbell, J. L., Using differential mobility spectrometry to measure ion solvation: an examination of the roles of solvents and ionic structures in separating quinoline-based drugs. *Analyst* **2015**, *140* (20), 6897-6903.
32. Liu, C.; Le Blanc, J. C. Y.; Schneider, B. B.; Shields, J.; Iii, J. J. F.; Zhang, H.; Stroh, J. G.; Kauffman, G. W.; Kung, D. W.; Shapiro, M.; Ieritano, C.; Shepherdson, E.; Verbuyst, M.; Melo, L.; Hasan, M.; Naser, D.; Janiszewski, J. S.; Hopkins, W. S.; Campbell, J. L., Assessing Physicochemical Properties of Drug Molecules via Microsolvation Measurements with Differential Mobility Spectrometry (vol 3, pg 101, 2017). *ACS Central Sci.* **2017**, *3* (4), 359-359.
33. Roscioli, J. R.; McCunn, L. R.; Johnson, M. A., Quantum structure of the intermolecular proton bond. *Science* **2007**, *316* (5822), 249-254.
34. Safaei, Z.; Eiceman, G. A.; Puton, J.; Stone, J. A.; Nasirikheirabadi, M.; Anttalainen, O.; Sillanpää, M., Differential Mobility Spectrometry of Ketones in Air at Extreme Levels of Moisture. *Scientific Reports* **2019**, *9* (1), 5593.
35. Menlyadiev, M. R.; Tarassov, A.; Kielnecker, A. M.; Eiceman, G. A., Tandem differential mobility spectrometry with ion dissociation in air at ambient pressure and temperature. *Analyst* **2015**, *140* (9), 2995-3002.
36. Brown, L. J.; Smith, R. W.; Toutoungi, D. E.; Reynolds, J. C.; Bristow, A. W. T.; Ray, A.; Sage, A.; Wilson, I. D.; Weston, D. J.; Boyle, B.; Creaser, C. S., Enhanced analyte detection using in-source fragmentation of field asymmetric waveform ion mobility spectrometry-selected ions in combination with time-of-flight mass spectrometry. *Anal. Chem.* **2012**, *84* (9), 4095-4103.

Chapitre II : Material and methods

II.1. DMS-MS instrument

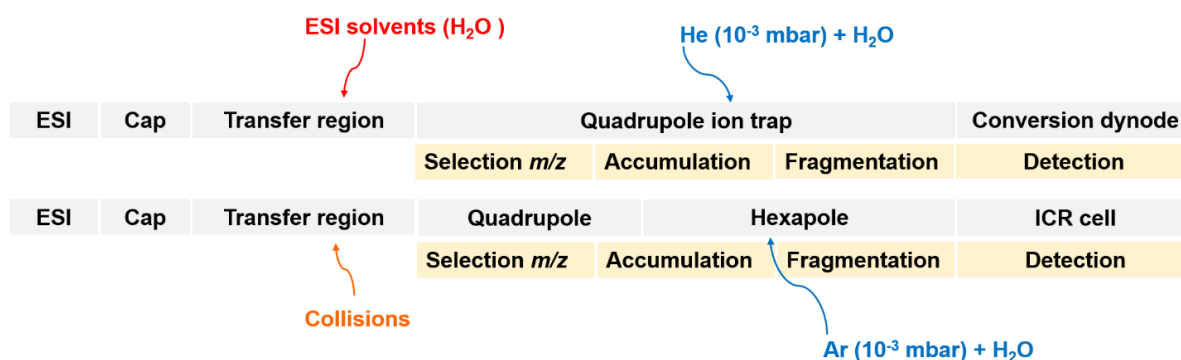
II.1.1. MS instruments

Two commercial (Bruker daltonics) tandem mass spectrometers were used to perform DMS-MS/MS experiments: a 3D quadrupole ion trap mass spectrometer (QIT, ESQUIRE 3000+), which is a relatively low-resolution instrument, and a 7 T APEX-Qe hybrid Fourier Transform ion cyclotron resonance mass spectrometer (FT-ICR), which provides a high mass resolution that allows for the resolution of isobars. Both are used for optimization of experimental conditions. QIT was then used for quantification of organic acids.

The different sections of both QIT and FT-ICR are schematized in Figure II.1. One finds going from left to right the ionization source up to the ion detector. Our FT-ICR instrument is a hybrid instrument featuring a so-called quadrupole-hexapole interface allowing for tandem mass spectrometry operations. Note that mass-selection and fragmentation can also be performed in the ICR cell, but these features were not used in the frame of this thesis.

The two tandem mass spectrometers are equipped with an ElectroSpray ionization (ESI) source, and these two ESI sources are quite similar. Ions formed in these atmospheric pressure conditions are then transmitted towards a lower pressure region of the instrument through a glass transfer capillary (noted Cap in Figure II.1). This capillary is of high importance for the DMS operation because the flow rate as well as the nature of the gas (N₂, ESI solvent, ...) going through are important parameters for DMS.

QIT and FTICR regions



Reaction

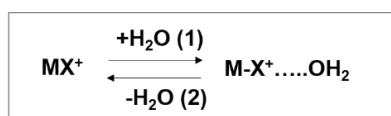


Figure II.1: Scheme of different sections our mass spectrometers QIT and FT-ICR. From left to right: ionization source (ESI), accumulation, transfer region, selection and fragmentation regions to ion detector. Abbreviation: Cap (Capillary).

Using the QIT, ion accumulation and subsequent mass-selection, and collision induced dissociation (CID) are performed successively within the ion-trap, pressurized with He at $\sim 10^{-3}$ mbar, prior to ion extraction for their detection based on a conversion dynode. Using the FT-ICR, ions can be first mass-selected in a linear quadrupole before being accumulated and fragmented in a linear hexapole pressurized with Ar at $\sim 10^{-3}$ mbar. They are then pulse extracted towards the low-pressure region ($\sim 10^{-10}$ mbar) of the ICR cell for detection.

Two phenomena can occur after ionization of organic acids as complexes with alkali cation. As discussed in Chapter 1, corresponding cation-bound dimer could also be observed. As illustrated in Figure II.1, at the exit of transfer capillary, ions are transferred through the ion optics in transfer region, from atmospheric pressure region to a lower pressure region. At the interface, monomers can bind water molecules coming from residual ESI solvent. Dimer can thus be formed (see forward reaction noted (1)). This reaction is reversible. Dimers may experience collisions with gas leading to their fragmentation (see Reaction (2)). This is the so-called in-source fragmentation,

also known as in-source collision induced dissociation.^{1, 2} Conversely, hydration of monomers may also occur during the accumulation and/or trapping periods (10-100 ms), due to residual water always present in He and Ar, using the QIT or FT-ICR, respectively. The issue of formation of hydrated complexes is discussed in the next chapter.

II.1.2. Our home-built DMS device

Our home-built differential mobility spectrometry (DMS) device has been successfully coupled to our QIT^{3, 4} and FT-ICR⁵ mass spectrometers. The mechanical conception of the setup is based on the model developed by Glish and co-workers.⁶ ESI housing is modified in order to integrate the mobility device, which requires a translation of the ESI needle in particular. For this purpose, a spacer has been added in order to fit the DMS housing. The door holding the ESI needle has been also modified so as to allow for adjustment of the position of the ESI needle relative to the DMS entrance. This parameter is critical not only for the optimization of ion signal, but also to prevent ESI solvent to mix into the DMS carrier gas.

DMS assemblies are illustrated in Figure II.2. The DMS cell is integrated between the ESI emitter and the glass transfer capillary. As can be seen in this Figure, it is composed of two parallel electrodes ($0.7 \times 6 \times 25$ mm for gap height, width, and length, respectively), between which ions are transported from atmospheric pressure region to the mass spectrometer through the glass transfer capillary. DMS housing is mounted so as to fit the inlet of this capillary. Both were electrically grounded, and the high voltage required for ionization is thus applied to the ESI needle. As such, the DMS is transparent (DMS off, RF = 0 and CV = 0) and all ions are transmitted to the MS/MS instrument.

DMS allows space separation of ions, and working principles can be found in a book

by A. Shvartsburg textbook⁷ or a review by B. Schneider.⁸ In practice, an asymmetric bisinusoidal radiofrequency (RF) is applied between the electrodes (see Figure II.2). This RF creates an alternating electric field perpendicular to the direction of the carrier gas flow. This asymmetric RF is obtained by adding two sinusoidal waveforms: one at 1.7 MHz, the other at 3.4 MHz and at 50% of the amplitude of the first sinusoidal waveform. Dispersion voltage or separation voltage (DV or SV) is defined by the zero-to-peak voltage (V_{op}) of the waveform throughout this thesis.

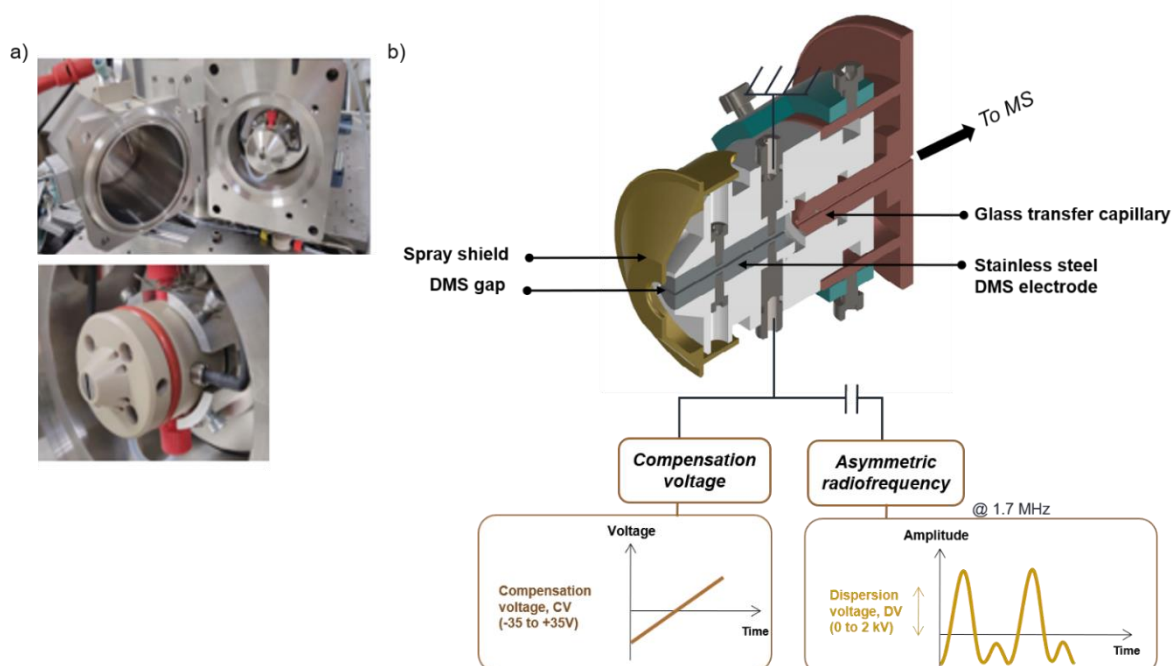


Figure II.2: DMS assemblies. a) Photo of DMS device mounted in ESI source of the FT-ICR (top), without the spray shield (bottom). b) Design of DMS assembly for the FT-ICR instrument and operation principle.

Ions are transmitted through DMS only if their transverse displacements under the RF compensate each other. Alternatively, a DC compensation voltage (CV) is applied to one electrode, allowing transmission of targeted ions.

If the same DMS electrodes are used, spaced by the same gap, and the same electronics is used for driving the electric field, DMS spectra are found to be very similar when recorded on the two instruments. In particular, peaks are found at the

same CV position. One difference is that acquisition time on FT-ICR is longer than on QIT, due in particular to the long time acquired for accurate mass measurements.

II.1.3. Control of transport gas flow and composition

Default DMS transport gas is dinitrogen (N_2). An NIGen LCMS 40-1 (Claind, Tremezzina, Italy) N_2 generator was used to produce N_2 gas with a purity up to 99.99%. N_2 gas flow and temperature are controlled using Bruker software. As shown in Figure II.3, part of the N_2 desolvation or dry gas of the ESI source (red arrows) is redirected through the DMS electrodes as a result of the pumping through the glass capillary transfer. Corresponding drag flow value depends on the glass capillary features (diameter in particular). It has been measured to be $15.1 \text{ cm}^3 \cdot \text{s}^{-1}$ on QIT and $24.7 \text{ cm}^3 \cdot \text{s}^{-1}$ on FT-ICR. As a result, the residence time of ions is longer using the QIT (7.5 ms) than the FT-ICR (4.6 ms), which results in narrower DMS peaks, in the former than in the latter case.

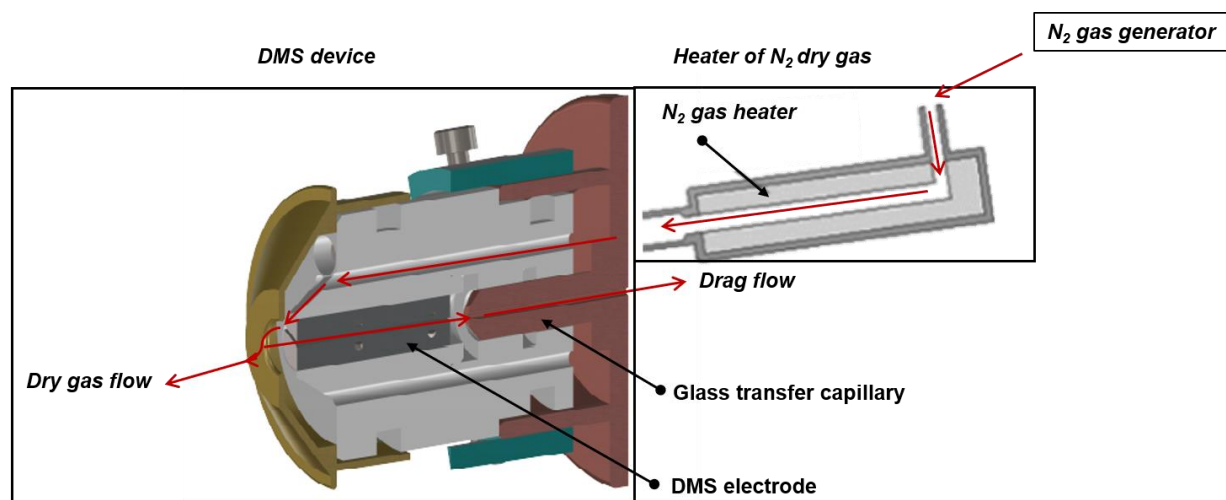


Figure II.3: Illustration of N_2 gas flow redirected towards between DMS electrodes as a result of pumping (drag flow), and the other part is used for desolvation (dry gas flow).

Addition of polar modifiers to N_2 carrier gas was attempted as modifiers can induce significant CV changes. Since the induced shifts of CV value are significant and very sensitive to the modifier flow, a very stable and reproducible system had to be set-up. Initial experiments were performed using an LC system, but the flow range was not

sufficiently large for our purpose. A specific syringe pump system (CETONI GmbH, Automatisierung und Microsysteme, GERMANY) was thus used for introducing modifier molecules in the heated dry gas line (Figure II.4). The gas line was heated to ensure homogenous distribution of the small liquid amount in the N₂ gas before reaching the region where both desolvation gas flow and temperature can be controlled using the Bruker software. A liquid flow rate of modifiers ranging from 0.5 to 10 $\mu\text{L}\cdot\text{min}^{-1}$ was controlled using the Bruker software. A liquid flow rate of modifiers ranging from 0.5 to 10 $\mu\text{L}\cdot\text{min}^{-1}$ was controlled using neMESYS software. It should be noted that the molar percentage of modifier vapor added in dinitrogen carrier gas (flow fixed at 5 or 6.5 $\text{L}\cdot\text{min}^{-1}$) is extremely low. The value varies between 0.005% and 0.3%, which is one or two orders of magnitude lower than percentages reported in the literature.⁹ These low percentages are found sufficient since full resolution of isomers can be obtained.

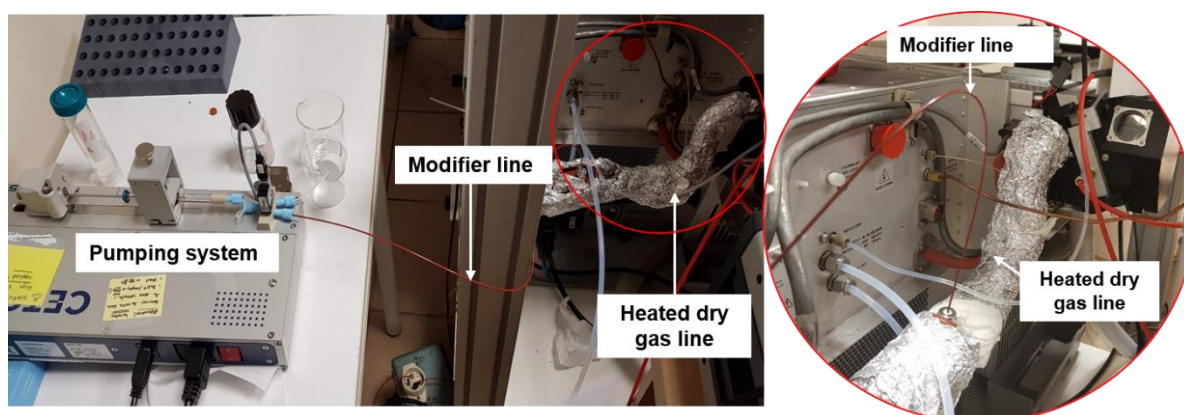


Figure II.4: Photo of pumping system (CETONI) used for modifier introduction in the heated dry gas line.

II.2. Protocol based on DMS-MS method

Our protocol based on differential mobility spectrometry hyphenated to mass spectrometry (DMS-MS) is developed for analysis of organic acids (OAs) in plasma. Analytical performance of DMS-MS is evaluated using a panel of biomarkers for which isomers are naturally occurring in biological fluids (Figure II.5). Separation of isomeric

species is indeed essential allowing for a reliable identification and quantification of biomarkers.

We are interested in analysis of methylmalonic acid (MMA) as a biomarker of methylmalonic acidemia, in presence of its isomer, succinic acid. MMA and succinic acid can be found in plasma.¹⁰ When developing an assay for MMA, the lack of interference from succinic acid should be demonstrated. Two biomarkers of relevant metabolic defects labeled with (*) symbol in Figure II.5 are also selected. Glutaric acid is a biomarker of glutaric acidemia type I, and adipic acid is a biomarker of mitochondrial fatty acid beta-oxidation deficiency.¹¹ As shown in Figure II.5, corresponding isomers of glutaric and adipic acids are methylsuccinic and methylglutaric acids, respectively, and are included in our method development. Analysis of the three isomer pairs would provide more evidence of DMS capability for isomer separation leading to an accurate identification and quantification of biomarkers.

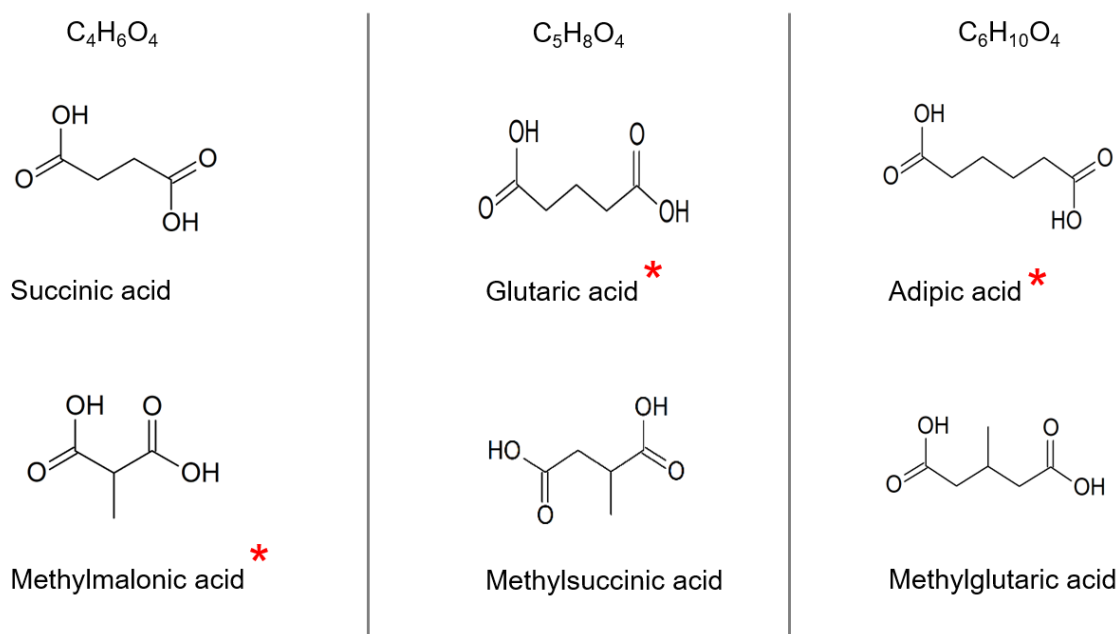


Figure II.5: Three pairs of isomeric organic acids. Biomarkers are labeled with (*).

Since amino acids can also be found in plasma, organic acids and amino acids can be analyzed together.¹² Therefore, a set of 6 amino acids (AAs) is selected including

alanine, valine, leucine, methionine, phenylalanine and arginine. Experiments were performed in the perspective of using DMS-MS as multiclass-metabolites method. Multi-class calibration allows combined measurement of pathophysiological concentrations of organic acids and amino acids in plasma sample.

Our workflow is proposed for validation of DMS-MS method used for quantification of OAs biomarkers. It is organized in four steps, as represented in Figure II.6. Each step is described in details in this chapter. Briefly, the workflow starts with protein precipitation of plasma samples by adding sulfosalicylic acid (1). Deproteinized plasma is diluted with solvents and spiked with standards of organic acids for calibration as schematized in step (2) in Figure II.6. To demonstrate the feasibility of a multi-class metabolites analysis, standards of organic acids and amino acids are combined for preparation of multi-class calibration samples. Through the addition of isotopically enriched internal standard (IS), analysis can be undertaken in a precise manner.¹³

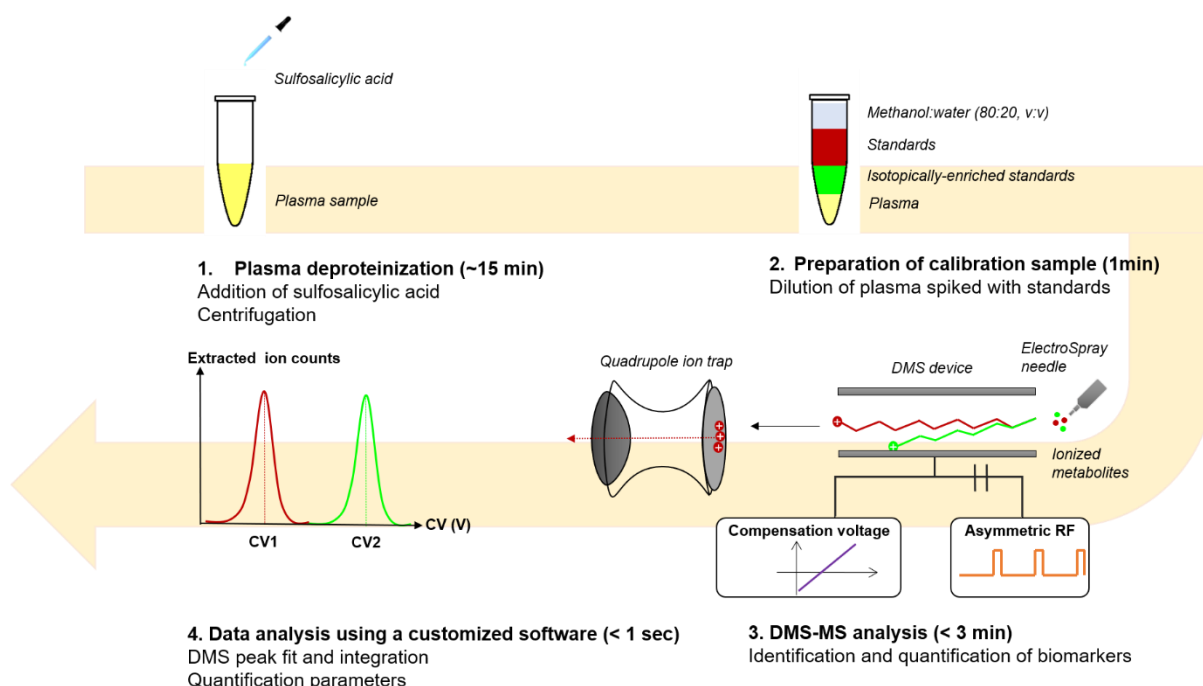


Figure II.6: DMS-MS workflow organized in 4 steps for separation, identification and quantification of organic acids (OAs) in plasma samples.

Upon electrospray ionization, separation of isomers is achieved with DMS (3) coupled to a 3D quadrupole ion trap (QIT). Optimization of experimental conditions is carried out for a stable and robust DMS-measurement. Targeted biomarkers are selected and identified based on their compensation voltage (CV) values. Ultimately, data analysis and treatment are achieved using a customized software (4). Peak shape of DMS spectra (CV, peak width and area) is determined as well as calibration curves and quantification parameters.

II.3. Chemicals, reagents and biological samples

II.3.1. Standards, internal standards and chemicals

Standards and internal standards were used for calibration and quantification protocols. Commercial OA standards and stable internal standard (MMA-d₃) were provided by Sigma-Aldrich (St. Louis, MO, USA) and Sticing VUmc (Amsterdam, The Netherlands), respectively. Commercial standard solution of mixture of AAs (Type B, AN-II purchased from FUJIFILM Wako Pure Chemical Industries, Osaka, Japan). Corresponding stable isotope compounds were obtained from Eurisotop (Saint Aubin, France).

Solvents, lithium chloride and sodium chloride were purchased from Merck KGaA (Darmstadt, Germany) and formic acid from Fisher Scientific (Hampton, New Hampshire, USA). Methanol and water were used as solvents, isopropanol, acetone and ethyl acetate as modifiers added to dinitrogen as carrier gas. Deionized water is obtained using Millipore Direct-Q 3 UV (Lilipore corporation, Burlington, Massachussetes, USA). All reagents were of analytical-reagent grade. Certified graduated pipettes were used throughout for sample preparation.

II.3.2. Plasma samples

Plasma samples used in this study were collected for diagnosis purpose as part of patient routine care at the Metabolic Biochemistry Department at Necker Hospital (Paris). Samples containing MMA at normal levels ($<0.4 \mu\text{M}$) were selected and analyzed anonymously. Informed consent was obtained from control patients for the use of leftover samples for analytical development. All procedures followed were in accordance with the ethical standards of French public health regulations (Code de la Santé Publique - Article L1121-3, amended by Law n ° 2011-2012, 29 Décembre 2011 - article 5).

II.4. Sample preparation

II.4.1. Precipitation of plasma

Protein precipitation is only required for pretreatment of plasma before analysis. Plasma was deproteinized by adding sulfosalicylic acid 30 % (10:1, v:v). Protein precipitate was removed by centrifugation, and supernatant was collected and stored at $-20 \text{ }^{\circ}\text{C}$. Just before analysis, frozen plasma was thawed and diluted at a final 1/50 dilution factor in methanol:water (80:20 v:v) solution.

II.4.2. Standard solutions

II.4.2.1. Stock solutions

Two stock solutions of standard organic acids were prepared. Mixture 1 includes biomarkers of interest, methylmalonic, glutaric and adipic acids. Mixture 2 contains their isomers, succinic, methylsuccinic and methylglutaric acids. Stock solution mixtures were prepared by dissolution of OAs in methanol:water (80:20, v:v) solvent, at initial concentration of 10 mM, and stored at $-20 \text{ }^{\circ}\text{C}$ until analysis. Amino acids

mixture is based on commercial solution where concentration of all components was 2.5 mM.

Stock solutions of internal standards were prepared in a water MilliQ. MMA-d₃ solution was prepared at 1 mM. Internal standards of amino acids were mixed at concentrations within the range of 66.7-200 µM. This solution is noted IS mixture throughout this chapter. All stock solutions were stored at -20 °C until analysis.

II.4.2.2. Working solutions for optimization of DMS parameters

Stock solution mixtures were diluted up to a final concentration of 0.1 mM in methanol:water (80:20, v:v) or in plasma samples. In methanol:water solution, lithium and sodium cations were added to form complexes with OAs. For lithium complexes, lithium chloride was added so as to achieve a concentration ratio of 1:10 (OA:Li⁺), as often found in the literature.⁴ For sodium complexes, sodium chloride was added at 140 mM similar to endogenic concentration of sodium cation in plasma. Therefore, sodium chloride was not added to plasma samples, because sodium concentration is physiologically maintained around 142 mM in plasma.

Working solution of both mixture 1 and mixture 2 was used for optimization of DMS-MS parameters, and subsequently for assessment of DMS performance for separation and identification of organic acids.

II.4.2.3. Working standard solutions for calibration

Working standard solutions of OAs were freshly prepared at 5 different concentrations from stock solution of mixture 1. Stock solution was diluted at 50, 100, 200, 500 and 1000 µM using methanol:water (80:20) solvent mixture, as given in Table II.1. These solutions were used for preparation of calibration sample.

Table II.1: Working standard solutions of organic acids used for calibration of organic acids.

Working solution	S1	S2	S3	S4	S5
Concentration of organic acids (μM)	50	100	200	500	1000

Working solution of amino acids was used for multi-class calibration. Commercial standard solution at initial concentration of 2500 μM is 30-fold diluted in methanol:water (50:50 v:v). AAs were found at 83.4 μM in working solution.

II.4.3. Control solutions

Two control solutions were used to assess intra- and inter- assay precision. Control solutions were prepared with two different plasma samples (P1 and P6) at a 1/50 final dilution factor. Samples were prepared as follows: 11 μL of deproteinized plasma was added to 50 μL of working standard solution S3 and S4, in order to obtain a final concentration of 20 μM and 50 μM , respectively. 429 μL of methanol:water solution was added to complete volume to 500 μL . 10 μL of MMA-d₃ was added to achieve a final concentration of 20 μM in sample.

In parallel, solutions were prepared with six different plasma samples (P1–P6). These solutions were used to evaluate matrix effect on OA concentration. Protocol of preparation was similar to that described above. Two samples were prepared with each plasma spiked with working standard mixtures. Final concentration of OAs in each sample was 20 and 50 μM . MMA-d₃ was diluted at 20 μM .

II.4.4. Calibration of organic acids

Calibration of organic acids was performed in a pool of plasma (P0) using working standard solutions of mixture 1 and stock solution of MMA-d₃ (Table II.2). Calibration samples were prepared with the following components as given in Table II.2:

- 11 μL of deproteinized plasma (P0),
- 50 μL of each working standard solutions (S1-S5),
- 429 μL of methanol:water solvent solution,
- 10 μL of MMA-d₃ stock solution.

Plasma was thus 50-fold diluted. Final concentrations of OAs ranged from 5 to 50 μM in diluted plasma, and MMA-d₃ had a final concentration of 20 μM .

Table II.2: Sample preparation for calibration of organic acids.

Calibration samples of organic acids	
Volume (μL)	Calibrator
Composition	
Deproteinized plasma (P0)	11
Working standard solution (S2-S4)	50
Methanol:water solution (80:20, v:v)	429
Stock solution of MMA-d₃	10

II.4.5. Multi-class calibration

Preparation of multi-calibration samples was identical to the aforementioned method for calibration of OAs (Table II.3). Three tubes were prepared using 11 μL of deproteinized plasma and 50 μL of working standard solutions of OAs (S2, S3 and S4). Then, dilution factors of working standard solution of AAs were chosen in order to obtain final concentrations of AAs: 1.7, 3.3, 6.7 μM . A volume of 10 μL of stock solutions of both MMA-d₃ and IS mixture was added. Methanol:water (80:20 v:v) with formic acid (0.5 %). A volume of this solvent mixture was added in each tube to reach 500 μL , as described in Table II.3.

Table II.3: Sample preparation for multi-class calibration.

Sample preparation for multi-class calibration			
Volume (μL)	Tube 1	Tube 2	Tube 3
Composition			
Deproteinized plasma (P6)		11	
Working standard OA solution (S2, S3 and S4)		50	
Working standard AA solution	40	20	10
Acidified methanol:water solution (80:20, v:v)	379	399	409
IS mixture		10	
Stock solution of MMA-d₃		10	

Organic acids were diluted at three concentrations, 10, 20 and 50 μM in calibration samples. AAs concentration range allows to measure endogenous concentration of AAs at physiological levels. MMA-d₃ final concentration remains at 20 μM . Final concentration of IS of each amino acid is given in Table II.4.

Table II.4: List of 6 amino acid standards and isotopically labeled compounds, as well as their final concentration (μM) used in multi-class calibration samples.

Amino acids				
Standards		Isotopically stable internal standards		
Compounds	$[\text{M}+\text{H}]^+$ (m/z)	Compounds	$[\text{M}+\text{H}]^+$ (m/z)	Concentration (μM)
Alanine	90	Alanine- ¹³ C ₂	92	4.0
Valine	118	Valine-d ₈	126	4.0
Leucine	133	Leucine-d ₃	135	2.7
Methionine	150	Methionine-d ₃	153	1.6
Phenylalanine	166	Phenylalanine-d ₅	171	1.3
Arginine	175	Arginine- ¹⁵ N ₂	177	1.3

II.4.6. Plasma samples without standards of organic acids

Plasma samples were prepared in a similar manner for both calibrations. In the case of OAs calibration, a volume of 11 μL of plasma and 10 μL of MMA- d_3 stock solution were added without standards. Then, a volume of 479 μL was used for methanol:water (80:20) solvent mixture.

For multi-class calibration, plasma was also diluted by 1/50 dilution factor with 469 μL methanol:water acidified with formic acid. 10 μL of solution of MMA- d_3 and 10 μL of IS mixture of AAs were added to achieve final concentrations as in calibration samples.

II.5. Quantitative analysis

Calibration curves of OAs were generated from calibration samples analyzed in duplicate over 6 independent experiments. Multi-class calibration was performed in duplicate on one day. In order to check for potential carry-over, a blank run was systematically performed between two sample runs.

Linear calibration curve parameters were obtained by plotting peak area ratio of compound/IS *versus* the nominal compound concentration. The CV, FWHM, and DMS peak area values were derived from the fitting procedure described in section II.6. Concentrations of unknown samples can be calculated from their corresponding area ratios using the corresponding calibration curve.

II.6. Experimental conditions

Identical conditions have been used throughout for DMS-MS analysis. Electrospray was operated in positive ionization mode. Organic acids were cationized with lithium or sodium, whereas amino acids were ionized by protonation. The voltage of the ESI emitter was set to +4.5 kV and the entrance glass transfer capillary was grounded.

Samples were infused at $100 \mu\text{L}\cdot\text{h}^{-1}$. N_2 dry gas flow was fixed at $6.5 \text{ L}\cdot\text{min}^{-1}$ and its temperature at $220 \text{ }^\circ\text{C}$. The MS instrument parameters, *i.e.*, ion charge control option, were tuned so as to avoid saturation of the ion trap.

Dispersion voltage was fixed at 1800 V , and CV was scanned in 0.1 V increment. A custom-built labView program (v12.0.1f5, National Instrument) was used to generate and control the applied voltages. MS data acquisition is performed with Bruker software (Bruker Daltonics) under chromatogram mode. Synchronization of the CV step change ($\pm 0.1 \text{ V}$) was achieved using the LabView program. DataAnalysis 3.4 software (Bruker Daltonics) was used to visualize ion chromatograms.

II.7. Data analysis using RStudio

Data analysis was performed using a customized RStudio software. DMS spectra are generated by plotting extracted ion chromatogram (XIC) as function of CV value *via* RStudio (Figure II.7). RStudio is composed of three R scripts (*analysis.R*, *checkRep.R*, *quantify.R*) for analysis, statistics and quantification based on DMS spectra of metabolites. A detailed protocol of using RStudio is described on GitHub site.¹⁴

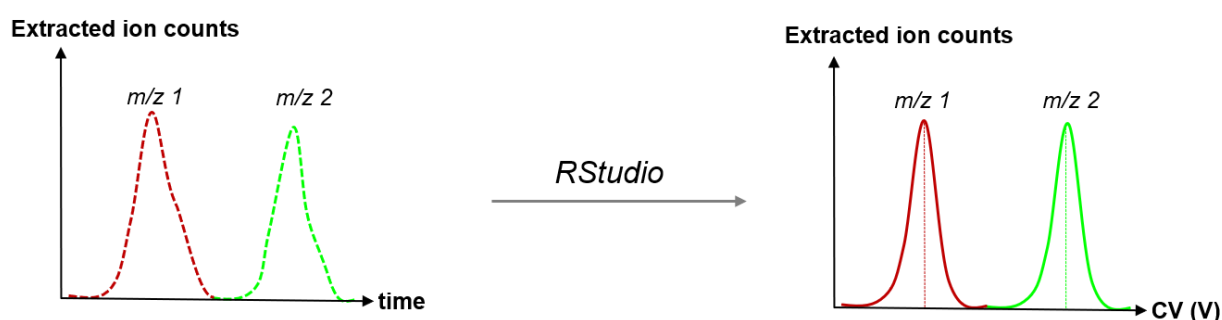


Figure II.7: Ion chromatogram (XIC) converted to DMS spectra using RStudio software.

Three input files, formally named *taskTable*, *tagTable*, *quantTable*, are first created. Structure of each is represented in Figure II.8. These files are used in pair for R scripts.

TagTable and *taskTable* are specified for *analysis.R*. The same *quantTable* and *taskTable* set is used for *checkrep.R* and *quantify.R*.

-*taskTable* includes series of DMS-MS experiments. *MS_file* is an ASCII file format extracted using DataAnalysis Bruker software. Each line of *MS_file* corresponds to a mass spectrum at a specified time. Each line of *DMS_file* contains relevant dispersion voltage and CV voltage values, and in particular, applied and measured CV values. Corresponding *DMS_file* is generated by the LabView program. In addition, values of *t0* and *CV0* allows for conversion of Esquire time to DMS CV values. These values are collected during data acquisition in the lab book. *Dilu* parameter is meant to be the dilution factor of the standard metabolites when spiked into plasma sample.

-*tagTable* is the list of targets, organic acids in the present case, associated to their 'approximate' *m/z* value (*m/z_ref*). Expected CV value, *CV_ref*, can also be added. Both *m/z_ref* and *CV_ref* define approximate peak position, which is then optimized using *analysis.R*.

-*quantTable* defines pairs of metabolites and internal standards added to calibration samples. This file is organized in five columns: target metabolite (Name), its internal standard (IS), endogenous concentration of metabolite (*COA_plasma*) and concentration of standard OA spiked in plasma (*COA_ref*) and that of internal standard (*CIS_ref*).

taskTable

MS_file	DMS_file	t0	CV0	dilu
---------	----------	----	-----	------

tagTable

Name	<i>m/z_ref</i>	<i>CV_ref</i>
------	----------------	---------------

quantTable

Name	IS	<i>COA_plasma</i>	<i>COA_ref</i>	<i>CIS_ref</i>
------	----	-------------------	----------------	----------------

Script	<i>taskTable</i>	<i>tagTable</i>	<i>quantTable</i>
Analysis.R	x	x	
Checkrep.R	x		x
Quantify.R	x		x

Figure II.8: Illustration of input files (*taskTable*, *tagTable* and *quantTable*) required for R scripts.

II.7.1. Fitting procedure of DMS spectra

The `analysis.R` script is used for 2D peak fitting using a product of two Gaussian functions in m/z and CV spaces, respectively. As a result, DMS peak centroid (CV), MS peak centroid (m/z), full width at half-maximum (FWHM) in both dimensions and peak area are extracted for each DMS-MS peak.

Figure II.9 shows an example of `analysis.R` output file of methylmalonic acid ion. It is composed of two plots. On the left panel, a 2D heat map is centered on fitted DMS peak position (dotted lines) resulting from optimization of m/z_{ref} and CV_{ref} values in `tagTable` (solid red lines). Green area corresponds to allowed search window of CV value. Blue "circles" show 2D (m/z , CV) iso-intensity curves. Data are coded in color intensity from pale yellow to red. Corresponding CV peak profile for data integrated over m/z (green curve) is shown on the right panel. Red lines and green area have the same meaning as for 2D heat map. The best fit is presented in blue. Fitted data (CV, FWHM and Area) are provided on the plot.

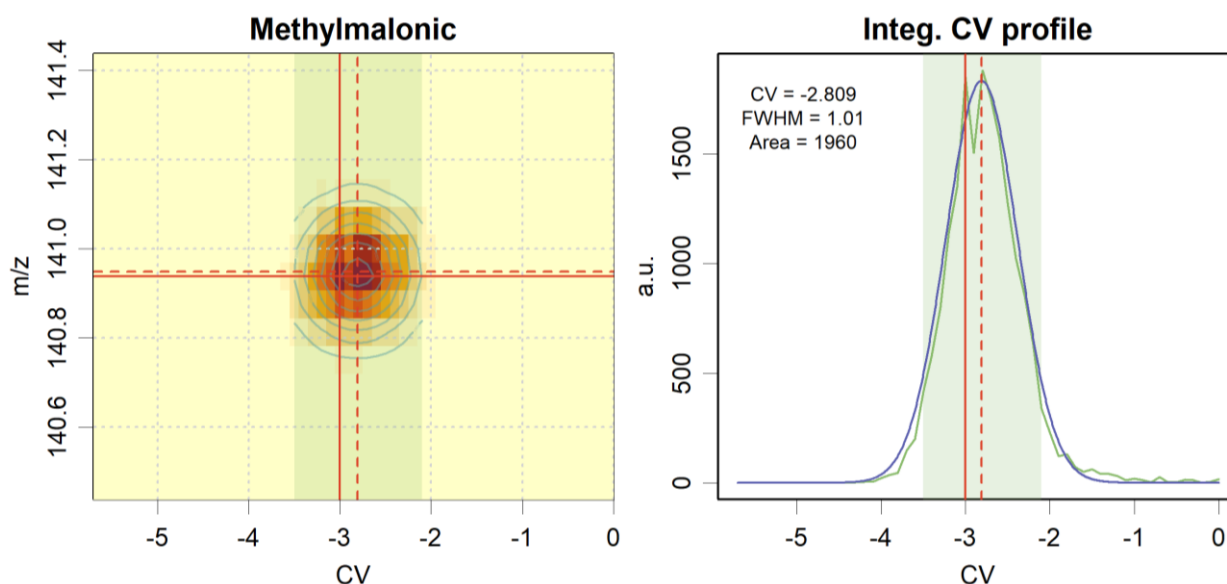


Figure II.9: Example of an output figure from `analysis.R` script showing the 2D location of DMS peak and its profile in CV dimension.

II.7.2. Evaluation of results

The aim of using *checkrep.R* is to assess repeatability and reproducibility performance within a series of data sets. Fitted data and uncertainty of each parameter are collected in a table for all targets and for each experiment. In addition, ratio of areas is calculated for targets and internal standards as specified in *quantTable*. Mean values, uncertainty and variability over a set of experiments are also given, which is useful for quantification plots and method validation.

II.7.3. Calibration curve plot

Quantification parameters are derived using *quantify.R*. A calibration curve is plotted for each target. As shown in Figure II.10, peak area ratio is plotted against concentration ratio. Linear regression provides solid line depicted in red in a model with intercept forced to go through the origin (0,0) and in green with variable intercept unforced through 0. Dashed lines are fitted with 95% confidence level. Limit of detection has been estimated using the model of regression line forced to 0, and concentration of unknown samples was calculated using regression model with variable intercept. LOD calculation is based on linear regression method and is discussed in the following section.

A new version called *repAndQuantify.R* is developed as a combination between *checkrep.R* and *quantify.R* for a fast analysis. A regression equation for area ratio as a function of metabolite concentration is provided, associated with statistics for slope, intercept and quantification parameters.

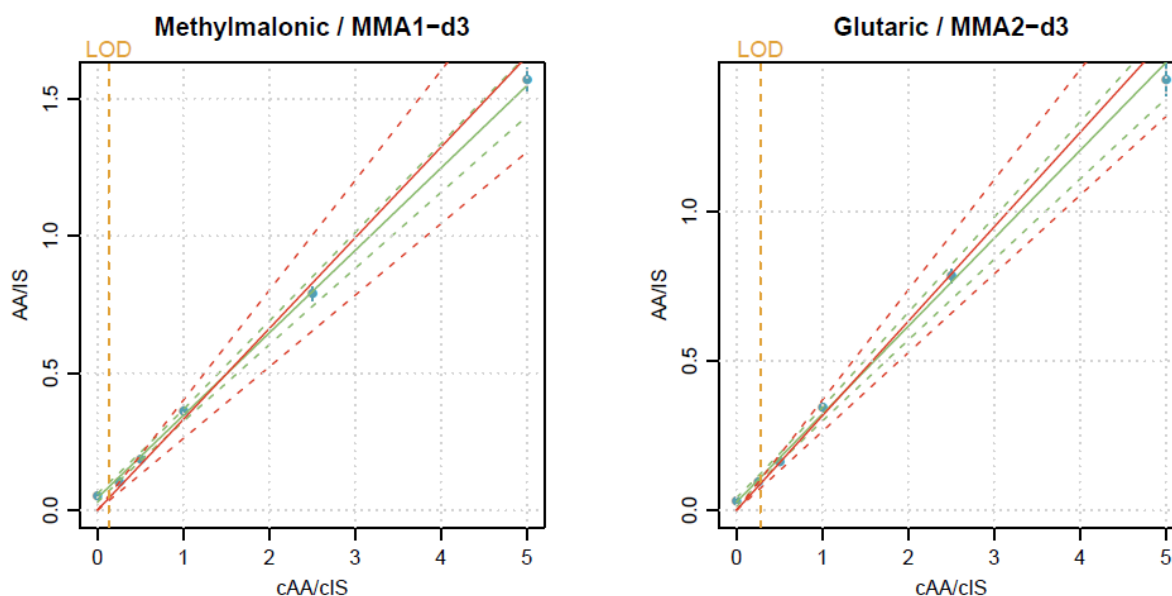


Figure II.10: Example of calibration curves generated by using Quantify.R to estimate limit of detection (LOD).

II.8. Method validation

The objective of validation of our method is to demonstrate that DMS-MS/MS protocol is suitable for accurate identification and quantification of biomarkers. First, robustness of DMS measurement in terms of accuracy on DMS peak position was evaluated in the perspective of using specific CV for metabolite identification. Stability of CV values over time and under different experimental conditions is an interesting probe of DMS robustness. Our second goal is quantification of organic acids in plasma sample. The method was validated for OA biomarkers, *i.e.* methylmalonic, glutaric and adipic acids. Method linearity, intra-assay and inter-assay precision and matrix effect were assessed. More precisely, linearity is assessed at high concentration range of MMA as biomarker organic acidemia, *i.e.*, 100-3000 μM in plasma. Then, precision of the measurement of biomarker concentration with our method is also evaluated. Limit of detection (LOD) and limit of quantification (LOQ) were as well calculated.^{15, 16,17}

II.8.1. Stability of CV position

Stability of CV position was evaluated through the comparison of standard deviation of CV values determined for OAs using working solutions in both methanol:water solution and plasma. A series of DMS experiments were carried out over a period of 4 months, during which DMS device was mounted and unmounted several times. Potential matrix and analyte concentration effects on DMS peak position were expected. Eight different plasma samples were used and plasma dilution factor was changed from 1/100 to 1/50. Concentration of analytes was varied between 5 and 100 μM . CV value should be robust to such experimental changes. Hence, CV measurement is considered reproducible and stable if standard deviation is on the order of CV increment fixed at ± 0.1 V for DMS experiments.

II.8.2. Linearity, LOD and LOQ

Linearity (Figure II.11a) was assessed using calibration curves performed over 6 independent experiments in 5-50 μM concentration range. Calibration curves were plotted as area ratio of OA/IS against OA concentration. Associated characteristics of calibration curve equation, LOD and LOQ were derived using linear regression method implemented in RStudio scripts.⁷⁻¹⁸ Linear regression method can be an alternative to the well-known signal-to-noise method, when MS analysis does not involve background noise.¹⁵ LOD can be defined as $3 \times \text{SD}_b/S$, where SD_b is the standard deviation of the intercepts of the regression lines, and S is the slope. LOQ is 3-fold LOD value.

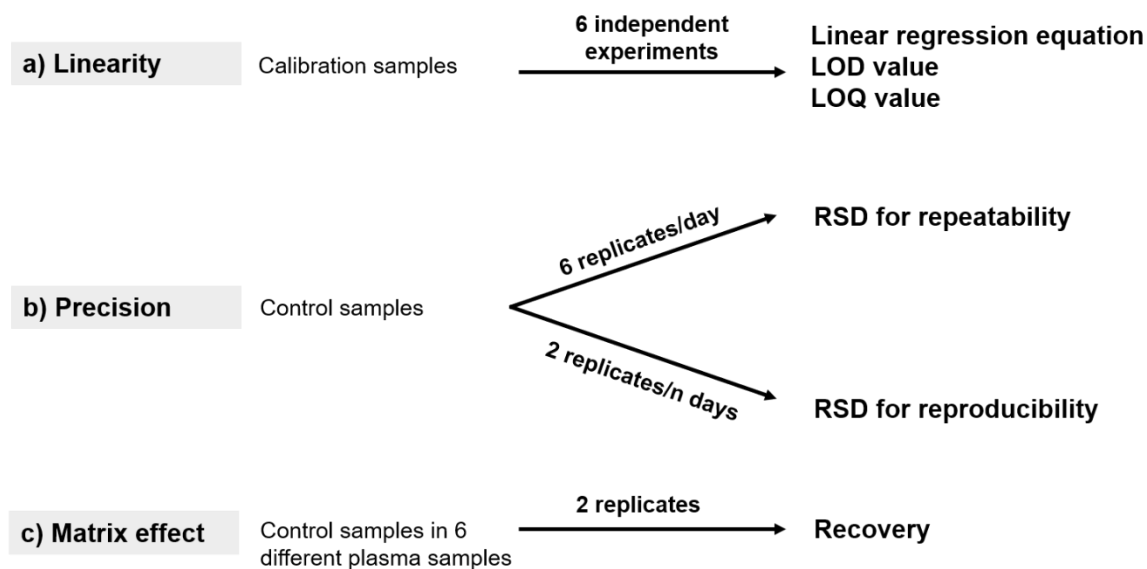


Figure II.11: Illustration of validation parameters used for our method. a) Linearity. b) Precision of intra- and inter-assay. c) Matrix effect on concentration. Abbreviation: RSD (relative standard deviation).

II.8.3. Intra-assay and inter-assay precision

Precision (Figure II.11b) was evaluated using control samples. Intra-assay precision (repeatability) was evaluated by 6 repetitive replicates of each same sample in a single analytical run. In addition, inter-day precision (reproducibility) was determined using two replicates of each control sample within n days. Mean concentration of replicates is calculated using regression equation. Precision was expressed in terms of coefficient of variation or relative standard deviation (RSD) in percent for each mean concentration. RSD value should vary within 3-4% for good repeatability and 5-8% for reproducibility.

II.8.4. Matrix effect on analyte concentration

Matrix effect or influence of biological matrix on concentration of spiked standards in plasma was assessed (Figure II.11c). Matrix effect was determined using samples prepared with 6 different plasma samples from healthy controls (P1-P6). Each sample was analyzed in duplicate, and a mean value of concentration is derived to calculate

recovery. Recovery of spike in each plasma is calculated in percent as measured concentration over the nominal concentration. An acceptable recovery for an individual metabolite was defined between 85-115%.

II.9. Summary

This chapter discusses our proposed DMS-MS workflow for separation of isomers, identification and quantification of biomarkers. Samples were prepared for optimization of experimental conditions. Protocol of sample preparation is used for organic acids and multi-class calibration in plasma. Fitting procedure based on RStudio software is also described. DMS peak shape and calibration curves are derived and statistics on quantification parameters are determined in a simple and fast manner. Method validation is detailed for assessment of robustness of DMS measurement and quantification of organic acids biomarkers. The chapter closes with a description of our DMS-MS experimental setups used for experiments.

References

1. Harrison, A. G., Energy-resolved mass spectrometry: a comparison of quadrupole cell and cone-voltage collision-induced dissociation. *Rapid Communications in Mass Spectrometry* **1999**, *13* (16), 1663-1670.
2. Carl, D. R.; Moision, R. M.; Armentrout, P. B., In-Source Fragmentation Technique for the Production of Thermalized Ions. *J. Am. Soc. Mass Spectrom.* **2009**, *20* (12), 2312-2317.
3. Berthias, F.; Maatoug, B.; Glish, G.; Moussa, F.; Maitre, P., Resolution and Assignment of Differential Ion Mobility Spectra of Sarcosine and Isomers. *J. Am. Soc. Mass Spectrom.* **2018**, *29* (4), 752-760.
4. Hernandez, O.; Isenberg, S.; Steinmetz, V.; Glish, G. L.; Maitre, P., Probing Mobility-Selected Saccharide Isomers: Selective Ion-Molecule Reactions and Wavelength-Specific IR Activation. *J. Phys. Chem. A* **2015**, *119* (23), 6057-6064.
5. Wang, Y.; Alhajji, E.; Rieul, B.; Berthias, F.; Maître, P., Infrared isomer-specific fragmentation for the identification of aminobutyric acid isomers separated by differential mobility spectrometry. *International Journal of Mass Spectrometry* **2019**, *443*, 16-21.
6. Isenberg, S. L.; Armistead, P. M.; Glish, G. L., Optimization of peptide separations by differential ion mobility spectrometry. *J. Am. Soc. Mass Spectrom.* **2014**, *25* (9), 1592-1599.
7. Shvartsburg, A. A., *Differential ion mobility spectrometry: nonlinear ion transport and fundamentals of FAIMS*. CRC Press: 2008.
8. Schneider, B. B.; Nazarov, E. G.; Londry, F.; Vouros, P.; Covey, T. R., Differential mobility spectrometry/mass spectrometry history, theory, design optimization, simulations, and applications. *Mass Spectrometry Reviews* **2016**, *35* (6), 687-737.
9. Campbell, J. L.; Zhu, M.; Hopkins, W. S., Ion-molecule clustering in differential mobility spectrometry: lessons learned from tetraalkylammonium cations and their isomers. *J Am Soc Mass Spectrom* **2014**, *25* (9), 1583-91.
10. Stabler, S. P.; Marcell, P. D.; Podell, E. R.; Allen, R. H.; Lindenbaum, J., ASSAY OF METHYLMALONIC ACID IN THE SERUM OF PATIENTS WITH COBALAMIN DEFICIENCY USING CAPILLARY GAS-CHROMATOGRAPHY MASS-SPECTROMETRY. *J. Clin. Invest.* **1986**, *77* (5), 1606-1612.

11. Vaidyanathan, K.; Narayanan, M. P.; Vasudevan, D. M., Organic acidurias: an updated review. *Indian J Clin Biochem* **2011**, 26 (4), 319-325.
12. Husek, P., SIMULTANEOUS PROFILE ANALYSIS OF PLASMA AMINO AND ORGANIC-ACIDS BY CAPILLARY GAS-CHROMATOGRAPHY. *J. Chromatogr. B-Biomed. Appl.* **1995**, 669 (2), 352-357.
13. Roberts, L. D.; Souza, A. L.; Gerszten, R. E.; Clish, C. B., Targeted Metabolomics. *Current Protocols in Molecular Biology* **2012**, 98 (1), 30.2.1-30.2.24.
14. Maitre, P.; Pernot, P. MS-Ana. <https://github.com/ppernot/MS-Ana/blob/master/README.rmd> (accessed 2021).
15. Alankar, S.; Vipin, B. G., Methods for the determination of limit of detection and limit of quantitation of the analytical methods. *Chronicles of Young Scientists* **2011**, 2 (1), 21-25.
16. Sanagi, M. M.; Ling, S. L.; Nasir, Z.; Hermawan, D.; Ibrahim, W. A. W.; Abu Naim, A., Comparison of Signal-to-Noise, Blank Determination, and Linear Regression Methods for the Estimation of Detection and Quantification Limits for Volatile Organic Compounds by Gas Chromatography. *J. AOAC Int.* **2009**, 92 (6), 1833-1838.
17. Thompson, M.; Ellison, S. L. R.; Wood, R., Harmonized guidelines for single-laboratory validation of methods of analysis - (IUPAC technical report). *Pure Appl. Chem.* **2002**, 74 (5), 835-855.
18. Analytical Methods Comm, A., The edge of reason: reporting and inference near the detection limit. *Anal. Methods* **2020**, 12 (3), 401-403.

Chapitre III - Lessons learned from DMS-MS analysis of organic acids

This chapter supplies a lot of relevant information on the methodology applied for analysis of organic acids using our differential mobility device hyphenated to a quadrupole ion trap mass spectrometer. Lessons learned from the choice of ionization mode is first discussed. The importance of spectra derived from differential mobility spectrometry (DMS) is highlighted. DMS spectra show processes that are not explicit using only mass spectrometry, are such as in-source fragmentation. Separation of isomeric species using modifier molecules is at the core of this work. The effect of different molecules, advantages and limitations of modifier uses are discussed. Optimization of dry gas flow needed for complete evaporation of solvents is also considered. In general, these lessons are useful for better interpretation of results and for designing future experiments.

III.1. Ionization *via* metal cationization

Our choice of positive Electrospray ionization (ESI) for organic acids (OAs) is online with our objectives, but also on preliminary experiments. We were primarily interested in resolving isomeric organic acids for quantification purpose, and DMS-MS experiments using both negative and positive ESI were performed. Under negative ionization mode, deprotonated organic acids were found highly intense. Deprotonated OAs were found to behave as hard sphere upon collisions with N_2 , and DMS peaks were found at very similar positions. Positively charged OAs were however better separated under our standard DMS conditions, *i.e.* with only N_2 as carrier gas and using a DV value of 1800 V.

Positive ion mode was thus preferred because a large number of metabolites are expected to be ionized. Our ultimate objective is to be able to explore the ability of

DMS-MS for multi-class metabolite analysis in plasma. More precisely, we were targeting simultaneous quantification of organic acids and amino acids, and we choose positive ESI because the latter are usually analyzed as protonated ions.

Only protonated species are generally considered for MS-based metabolomics. Nevertheless, many different ions can be produced during ionization such as complexes.¹ Complexation with metal cations or neutral molecules is thus used to ionize molecules that cannot be easily protonated, such as organic acids. Cations often used include lithium, sodium and potassium, which can be added to solutions or can be found in biological matrices. Metal cationization allows formation of positively charged complex, $[M+X]^+$, between a metabolite (M) and alkali metal cation (X^+).

Literature data shows that this ionization strategy can greatly improve separation of metabolites using ion mobility spectrometry.² For instance, separation of saccharides was achieved with potassium cation.³ Complexes of relevant isomeric metabolites with sodium cation have exhibited significant separation relative to protonated ions using classical ion mobility instrument.⁴ Importantly, cationization leads to structural differences between isomers which can greatly improve separation. Isomeric saccharides complexed with Li^+ , Na^+ and K^+ were analyzed using DMS.⁵ Isomers cationized with Li^+ have shown identical peak positions, which is probably due to the formation of very similar complex structures. However, two well resolved peaks were observed when isomers complexed with Na^+ and K^+ . This was rationalized based on formation of different complexes with both Na^+ and K^+ allowing for distinguishing between isomers.

Formation of lithiated complexes was first explored, and for this purpose lithium chloride ($LiCl$) was added to solution. Li^+ cation was chosen for two main reasons. It is known to tightly bind to oxygen atoms of organic molecules.⁶ More importantly, when compounds are complexed to Li^+ , structural information on isomeric forms of

molecules can be derived from MS/MS fragmentation spectra.^{5, 7-9} Indeed, lithium cationization may allow for covalent bond dissociation, thus providing rich structural information. For our targeted organic acids, Li^+ could be bound to two both carbonyl groups. One could thus expect that cyclic structures for two isomers could be sufficiently different that isomeric ions could be separated.

When electrospraying our organic acids (M), $[\text{M}+\text{Li}]^+$ complexes were the most abundant species. This is illustrated with the mass spectrum recorded for mixture 1 on our quadrupole ion trap mass spectrometer in Figure III.1. Lithiated adducts of methylmalonic (MMA), glutaric and adipic acids correspond to m/z 125, 139 and 153, respectively. DMS was operated in the so-called transparent mode, which means that the two electrodes are grounded, thus allowing for the transfer of all ions. Based on the literature data, especially on DMS-MS related ones, one should pay attention to the formation and fragmentation of dimers, corresponding to two molecules bound to the metal cation, *i.e.* $[2\text{M}+\text{Li}]^+$, or solvated ions such as monohydrated ions $[\text{M}+\text{Li}+\text{H}_2\text{O}]^+$. More precisely, the question is whether observed $[\text{M}+\text{Li}]^+$ ions are those selected when passing through the DMS device, or are formed upon fragmentation of hydrated or other Li^+ bound dimers ?

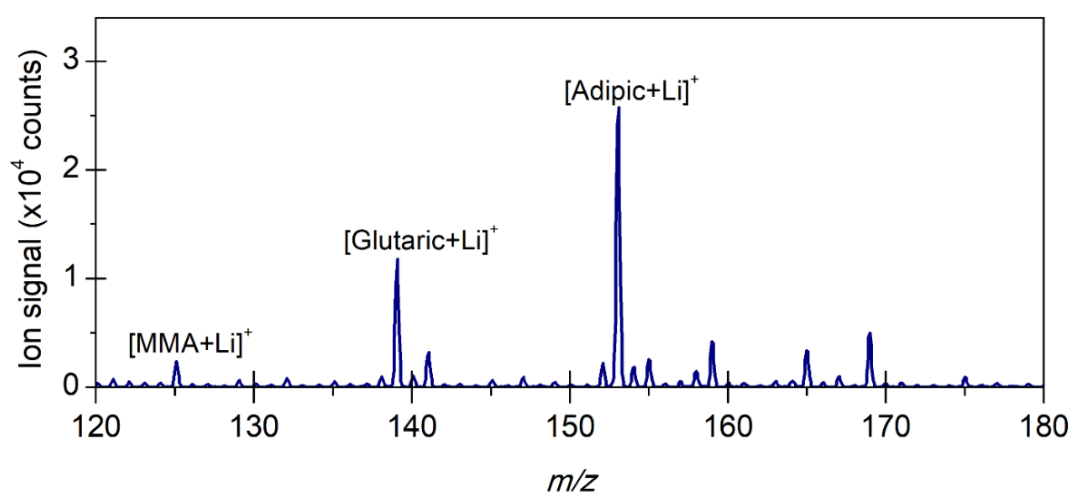


Figure III.1: Mass spectrum recorded under DMS transparent mode for methylmalonic (MMA), glutaric and adipic acids ionized as lithiated complexes.

II.2. In-source fragmentation of cation-bound dimer

It is anticipated that $[M+Li]^+$ and corresponding cation-bound dimers are transmitted at very different CV values. Indeed, they are structurally very different, and in particular charge accessibility is much better for the former than the latter. Evidence for post-DMS chemistry and fragmentation of dimers following DMS ion selection is provided by mass analysis at different CV values.

In-source fragmentation of cation-bound dimer is illustrated in Figure III.2a. DMS-selected dimer (red ions), leaving the transfer capillary, can undergo collisions with residual gas at relatively high pressure $\sim 10^{-1}$ and 10^{-2} mbar. Cation-bound dimer such as $[M+Li+H_2O]^+$ can be activated and dissociated into $[M+Li]^+$ and H_2O fragments. As a consequence, monomer $[M+Li]^+$ fragments, rather than DMS-selected dimers, are transported and detected in subsequent mass analysis. As a result, both monomer and dimer are observed at the very same CV value (CV dimer). This observation is simply related to the well-known in-source fragmentation. When DMS device is mounted, this in-source fragmentation process is also referred to as post-DMS fragmentation.

Figure III.2 also illustrates another phenomenon that leads to the formation of monohydrated dimers (Figure III.2b). DMS-selected monomers are transmitted at CV value noted CV_{monomer} towards the mass analyzer. Hydration of monomers could occur in the quadrupole ion trap due to relatively high pressure of water in helium gas line. Both monomers and dimers could thus be detected at CV_{monomer} on DMS spectra.

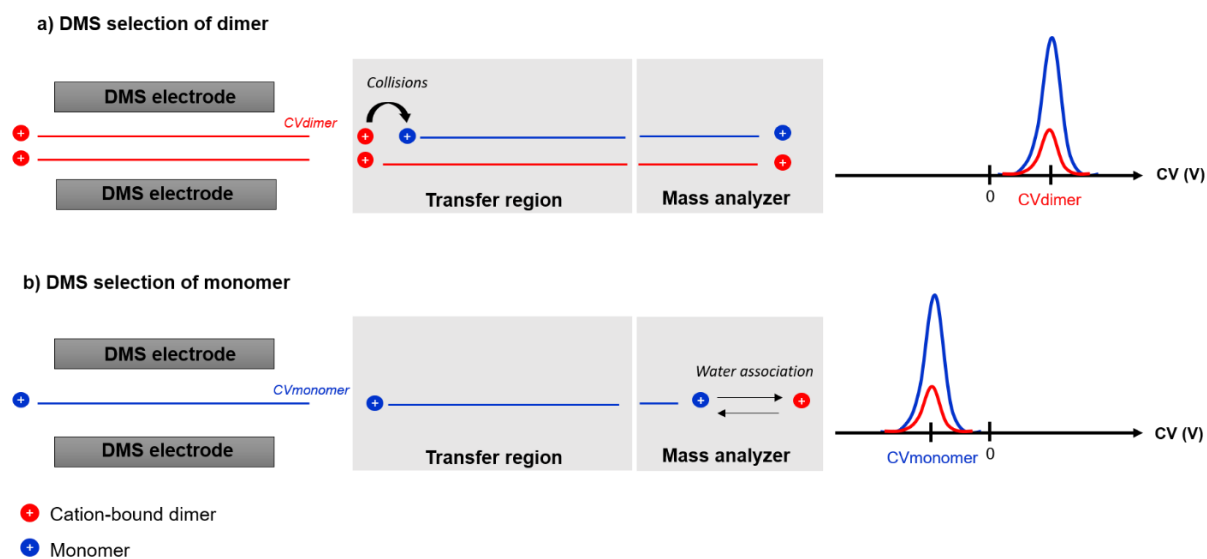


Figure III.2: Illustration of processes that can occur after DMS selection of dimer and monomer species. a) Post-DMS fragmentation of hydrated dimers of occurring in the transfer region of the mass spectrometer. b) Equilibrium between hydration of ions and fragmentation of monohydrated ions in the quadrupole ion trap due to traces of water in the helium line.

Evidence of dimer post-DMS fragmentation and there consequences on DMS spectra analysis were thoroughly discussed by G. Glush and coworkers for two isomeric sugar molecules, glucose and levoglucosan, ionized with lithium cation.¹⁰ In both cases, three different DMS peaks were found in the ionograms corresponding to m/z of $[M+Li]^+$. Such DMS spectra could thus be misinterpreted as separation of three conformers or isomers. G. Glush and coworkers have proposed a very careful analysis of these data, in particular, based on data recorded using different source conditions.¹⁰ It was found that two additional monomer peaks were derived from fragmentation of a homodimer and a heterodimer formed between each molecule and a contaminant in solution, in transfer region. It can thus be concluded that post-DMS fragmentation should be considered and assignment of DMS peaks should be made carefully.

In our cases, when abundance of $[M+Li]^+$ of each of our organic acids was plotted as a function of CV, DMS spectra were systematically displaying two peaks. An example is illustrated for adipic acid in Figure III.3, where ion intensity of $[M+Li]^+$ monomer and $[M+Li+H_2O]^+$ dimer are shown in blue and red, respectively. Two peaks corresponding

to each of these two ions are observed, and they are centered at two CV values: -2.0 V and +2.4 V. This observation by itself provides evidence of post-DMS chemistry since different mobility behaviors are expected for two structurally different ions.

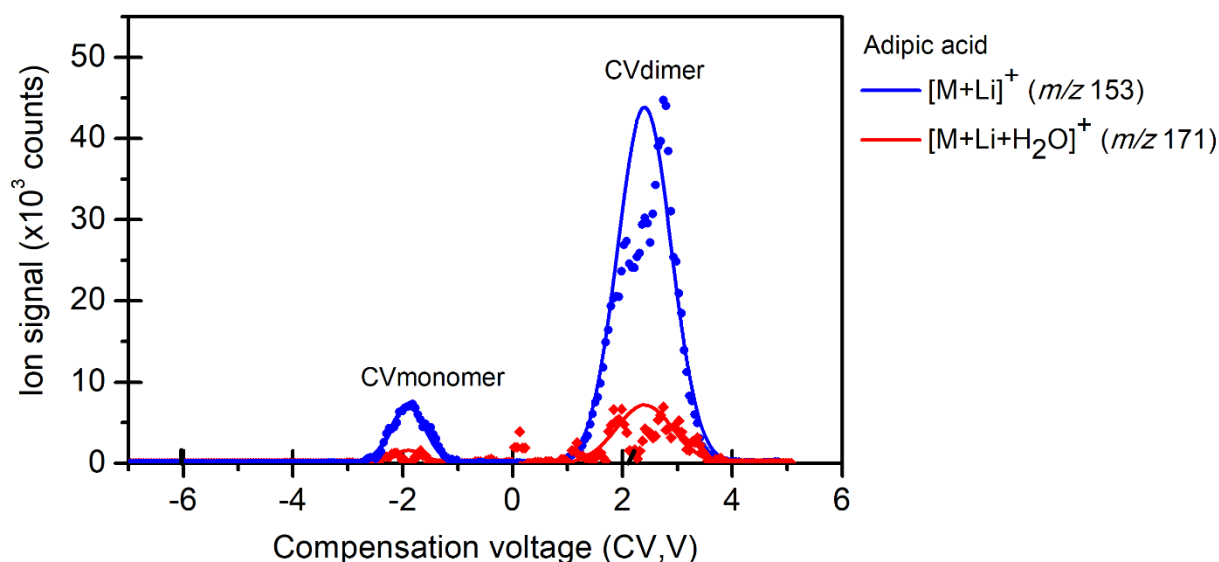


Figure III.3: DMS spectra of monomer $[M+Li]^+$ (blue) and the hydrated dimer $[M+Li+H_2O]^+$ (red) of adipic acid (M). Data are fitted and smoothed using a rolling average over two points. Peak intensity of dimer is 20-fold scaled relative to monomer peak at CVdimer.

Mass spectra extracted at both CV positions have shown abundance of monomers and very small amounts of dimers at CVdimer. Based on the literature data,¹⁰⁻¹² signal observed at positive CV values correspond to cation-bound dimers. Thus, in the present case, peaks observed at -2.0 V and +2.4 V correspond to CVmonomer and CVdimer, respectively. Identification of DMS peaks identity was discussed in the literature for ketones and organophosphorus compounds. Through mass analysis, protonated monomers were found to be dominant at negative CV value (CVmonomer), whereas ions were assigned for proton bound dimer, such as $[2M+H]^+$ or $[2M+H_2O]^+$, at positive CV value (CVdimer). These results were confirmed using on dispersion plots recorded for monomers and proton-bound dimers. Negative CV shift is observed for the first when increasing the electric field, while positive CV shift is observed for the

latter. These study shows the importance of identification of targeted ions (monomers) at the expected CV position when many DMS peaks appear on spectra.

As can be seen in Figure III.3, ion signal at CVdimer is much larger than at CVmonomer. Cation-bound dimer formation is obviously at the expense of targeted monomers, which can become a major analytical issue for DMS analysis and even more MS/MS analysis of DMS-selected ions. This issue was controlled *via* optimization of settings in the ESI source (*e.g.* dry gas flow and temperature, ion optics voltage). DMS spectrum obtained for adipic acid is shown in Figure III.4.

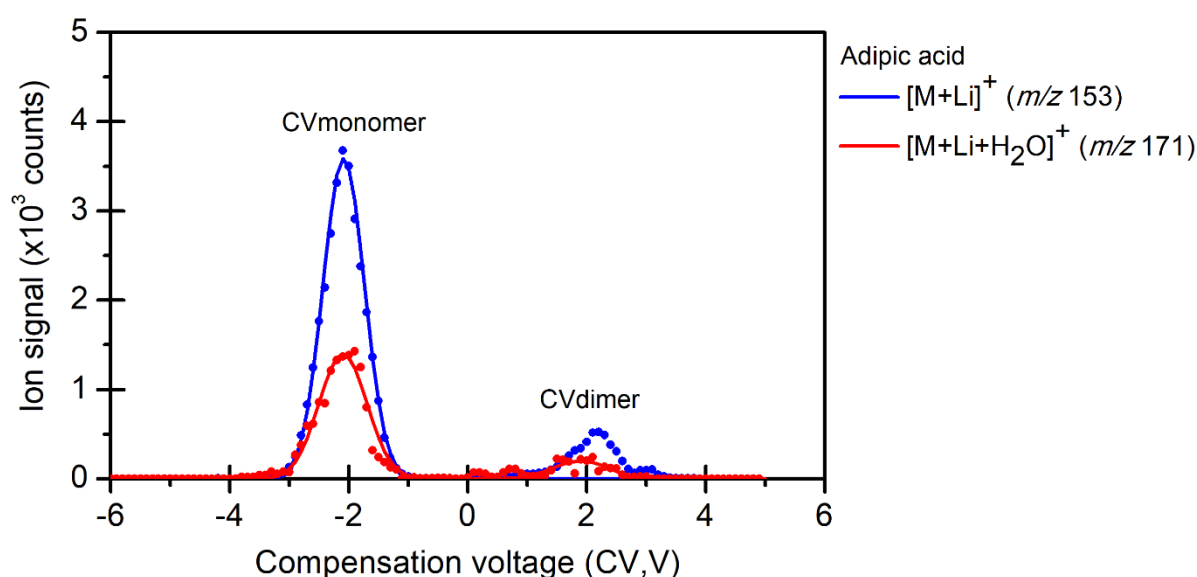


Figure III.4: DMS spectrum recorded for adipic acid complexes with lithium after optimizing post-DMS fragmentation settings in transfer region. Data are fitted and smoothed using a rolling average over two points.

Peaks at CVdimer have greatly decreased relative to monomer peak at -2.0 V. Dimer peak is also observed at this position. In fact, DMS-selected monomers are transmitted towards ion trap where formation of hydrated dimer occur due to relatively high pressure of water in helium (Figure III.2b). However, one must be careful when interpreting DMS spectra to avoid erroneous conclusions about targeted peaks when dimers are present. A positive aspect of this work illustrates the ability of DMS to

provide insight about the ions produced from the ion source that mass analysis alone is unable to provide.

III.3. Effect of dispersion voltage on DMS separation

DMS separation capability increases with dispersion or separation voltage, DV or SV respectively. This can be illustrated using dispersion plots which corresponds to the evolution of CV as a function of DV. Using our instrument, DV is typically tuned in the 1000-2000 V range with a trade-off between ion transmission and DMS resolution. Up to 600 V, no significant CV shift is observed. Using a gap of 0.7 mm, the maximum DV value is typically 2000 V, which corresponds to an electric field value of 2857.1 V/mm. Above this value, electric arcing occurs, in addition to ion losses. Our standard DV conditions were found at 1800 V, which allows for stable and reproducible results.

Dispersion plots of isomeric organic acids complexed with Li^+ are reported in Figure III.5. N_2 dry gas flow and temperature were fixed at $6.5 \text{ L}\cdot\text{min}^{-1}$ and $220 \text{ }^\circ\text{C}$, respectively. Three types of ions (Type A, B and C) can be distinguished on a dispersion plot, as discussed in Chapter I. As shown in Figure III.5, isomers of lithiated organic acids all display Type B behavior. For Type B, the CV initially decreases with increasing DV, reaches a minimum and then increases at higher DV values.

Increasing DV value can enhance CV spread or peak capacity (PC) and peak-to-peak resolution (Rpp).¹³ Rpp helps to evaluate DMS separation of two peaks. Peaks are baseline resolved when Rpp value is greater than 1.5. PC and Rpp are defined in Equations (1) and (2), where CVmin (CVmax) are the minimum (maximum) values of CV position and w is the FWHM of DMS peaks.

$$PC = 2 \times \frac{(CV_{\max} - CV_{\min})}{w_{\max} + w_{\min}} \quad (1)$$

$$Rpp = 1.178 \times \frac{(CV_1 - CV_2)}{(w_1 + w_2)} \quad (2)$$

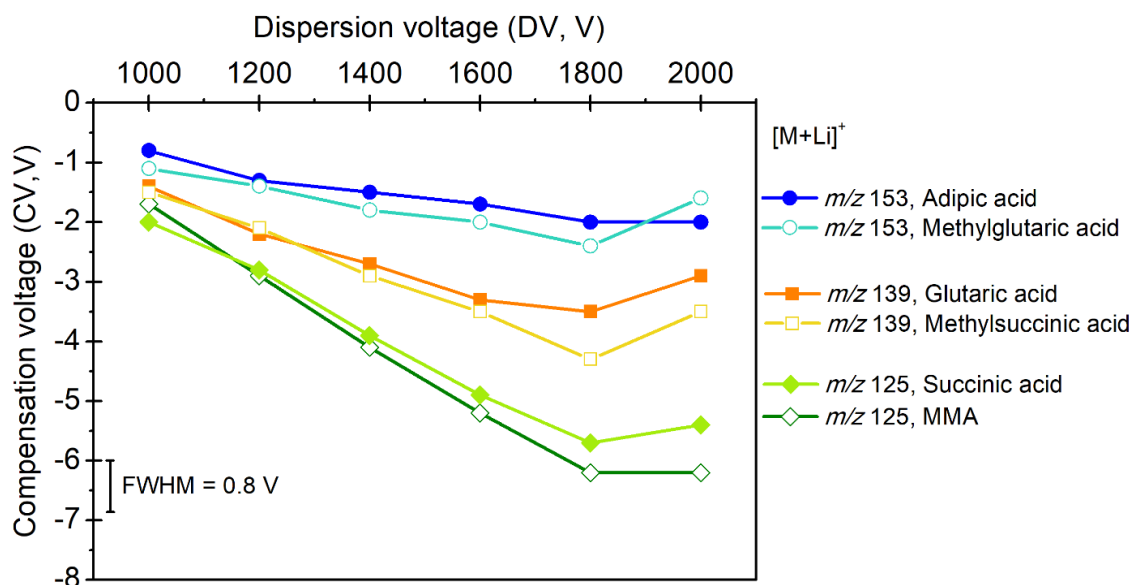


Figure III.5: Dispersion plots of isomeric organic acids complexed with lithium cation: methylmalonic acid (MMA, dark green diamonds), succinic acid (light green diamonds), glutaric acid (orange squares), methylsuccinic acid (yellow squares), adipic acid (dark blue circles) and methylglutaric acid (light blue circles). N_2 dry gas flow is fixed at $6.5 \text{ L}\cdot\text{min}^{-1}$ and its temperature is set at $220 \text{ }^\circ\text{C}$.

As generally observed, PC is found to increase when increasing DV values. In the present case, it goes from 1.2 at 1000 V to 5.8 at 2000 V. CV values of the different isomers are shifted towards negative values. Peaks width, however, remain similar and close to 0.8 V. No significant improvement of separation of isomers is observed when increasing DV value from 1000 and 1600 V. Adipic and its isomer are not separated even at 1800 and 2000 V ($R_{pp} \sim 0.3$). However, resolution of m/z 139 isomers is slightly enhanced, and R_{pp} value is close to 0.5 for a CV value of 1800 V. Similarly, MMA and succinic acid are better resolved at the highest DV values, particularly at 2000 V ($R_{pp} \sim 0.6$). Nevertheless, PC and isomer resolution are enhanced at the cost of ion signal when increasing DV values. For instance, ion signal is typically reduced by a factor of 3 at 2000 V relative to that at 1000 V. Nevertheless, since the three pairs of isomers are only (partially) resolved at high DV values, experiments were performed using a DV value of 1800 V.

III.4. Effect of polar modifiers on DMS separation

III.4.1. Modifier effect on DMS separation of organic acids

Isopropanol modifier was one of the first choices. It has been shown that isopropanol modifier can drastically improve DMS separation of isomeric species,¹⁴ as discussed in Chapter I. The settings for the flow and temperature of the drying gas flow, with or without modifier, were fixed at 5 L.min⁻¹ and 200 °C, respectively. Liquid flow rate of isopropanol is set to 2 μL.min⁻¹, which corresponds to a molar percentage on the order of 0.01%.

Dispersion plots were recorded for glutaric, methylsuccinic, adipic and methylglutaric acids (Figure III.6), using N₂ only and also with isopropanol seeded in N₂ as carrier gas. It should also be stressed that methylmalonic and its isomer were found at very small ion signal counts leading to poor DMS peak shape at these conditions used in our preliminary experiments. As such, this isomer pair is not presented in the following results.

As can be seen in Figure III.6, CV values are found to decrease with increasing DV for both carrier gas composition. CV values decrease from 0 V (at 1000 V) to -3 V (at 2000V) with N₂ only. As expected, isopropanol induces larger negative CV shift than N₂ as a function of DV. CV values range between -1 V to -10 V from 1000 to 2000 V, respectively. As already mentioned, peak width, however, is unaffected (~ 0.8 V). The four studied isomers have identical type A behavior, but it gets more pronounced with isopropanol, which reveals stronger ion-molecule interaction.

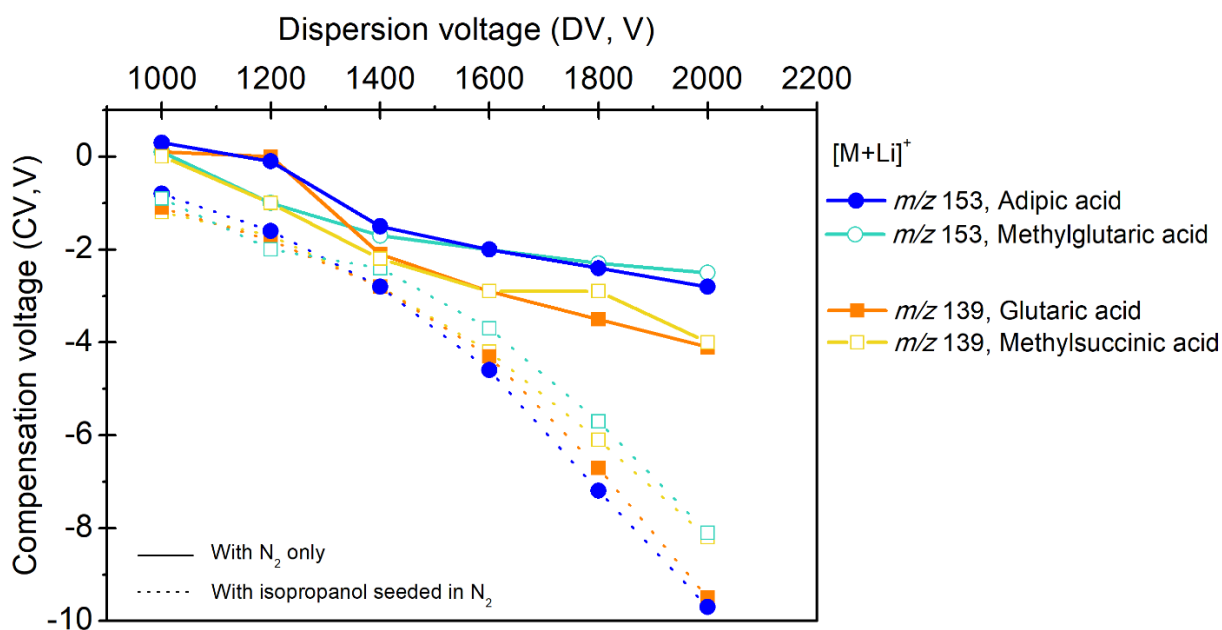


Figure III.6: Dispersion plot of isomeric lithiated organic acids for m/z 139 and m/z 153 recorded using only N_2 carrier gas (solid line) and isopropanol added as modifier at $2 \mu L \cdot min^{-1}$ (dotted line). Organic acids are glutaric acid (orange squares), methylsuccinic acid (yellow squares), adipic acid (dark blue circles) and methylglutaric acid (light blue circles). Dry gas flow and temperature are set at $5 L \cdot min^{-1}$ and $200^\circ C$, respectively.

As expected, isomer separation is also improved with isopropanol relative to dinitrogen for both isomeric pairs starting from 1600 V. Dispersion plots of isomers are parallel at 1800 V and 2000 V which reflects a significant resolution. Peak-to-peak resolution (R_{pp}) of adipic and methylglutaric acids isomers is increased from 0.2 (with N_2) to 1.2 (with isopropanol) at $DV = 1800 V$, and remains the same at 2000 V. Similarly, glutaric and methylsuccinic acids are completely resolved with isopropanol. Full resolution of corresponding DMS peaks of both isomer pair is shown in Figure III.7a at 1800 V.

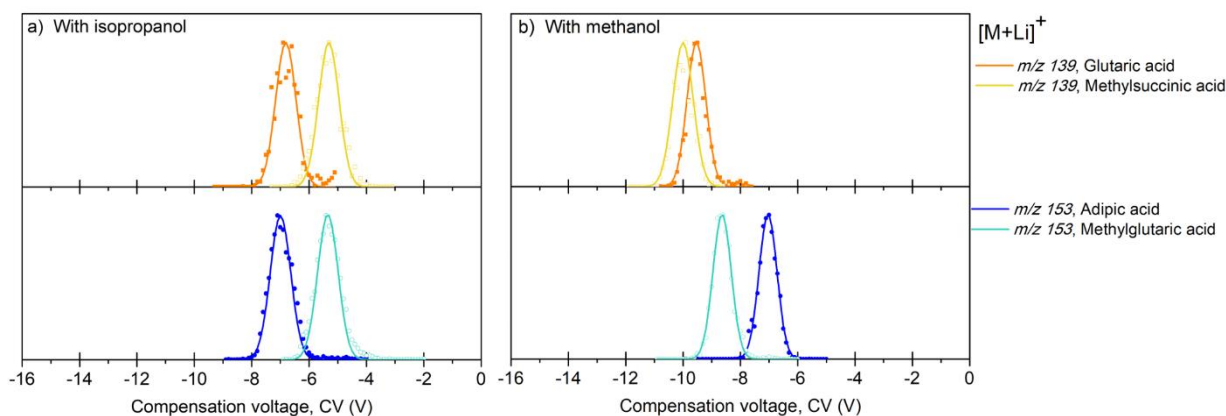


Figure III.7: DMS spectra of isomeric lithiated organic acids for m/z 139 and m/z 153 recorded upon addition of modifiers added at $2 \mu\text{L}\cdot\text{min}^{-1}$ in N_2 carrier gas. a) With isopropanol. b) With methanol. Dry gas flow and temperature are set at $5 \text{ L}\cdot\text{min}^{-1}$ and $200 \text{ }^\circ\text{C}$, respectively. Organic acids are glutaric acid (orange squares), methylsuccinic acid (yellow squares), adipic acid (dark blue circles) and methylglutaric acid (light blue circles). Data are fitted and smoothed using a rolling average over two points. All individual spectra are normalized to the maximum.

On the other hand, the effect of other modifiers has been evaluated. Baseline resolution achieved with methanol as modifier was already reported for isomeric amino acids and related compounds.^{15, 16} A liquid flow of $2 \mu\text{L}\cdot\text{min}^{-1}$ of methanol was added to N_2 dry gas fixed at $5 \text{ L}\cdot\text{min}^{-1}$. The molar percentage of methanol vapor corresponds to 0.02%. This value is on the same order of that obtained with isopropanol added at the same flow. DMS spectra were recorded for both m/z 139 and m/z 153 isomer pairs at DV value of 1800 V using methanol (Figure III.7b).

Upon methanol addition, CV range is found between -6 V and -11 V . CV is shifted towards more negative values than with isopropanol, which reflects a stronger ion-methanol interaction than ion-isopropanol interaction. Adipic and methylglutaric acids (m/z 153) are also separated with methanol, while no separation is observed for m/z 139 isomer pair. However, isopropanol seems more selective for both isomer pairs than methanol.

It is reasonable to expect differences in DMS separation when using modifiers. As discussed in Chapter I, modifiers induce the strongest clustering process which

increases isomer resolution in comparison with N₂ only. As a result, CV spread and isomer resolution are increased with modifiers. At the same time, modifier effect on DMS separation is selective. Isopropanol is found to be selective for separation of m/z 153 and 139 isomers, whereas methanol is selective for only m/z 153 isomers. It has been demonstrated that ion separation is changed in specific manner using different modifier molecules.¹⁷ This DMS selectivity is related to the strength of ion-modifier interaction that strongly depends on individual properties of modifier molecules and ions.

Modifiers can provide orthogonal DMS separations. In other words, isopropanol and methanol are orthogonal, *i.e.* if targeted isomer pair is not resolved with methanol, isopropanol would be selected to achieve separation. In the context of DMS selectivity, assessment of orthogonality between modifiers has been proposed by Schneider *et al.*¹⁸ They compared isopropanol to ethyl acetate and acetonitrile that provide high degree of orthogonality for separation of 140 different analytes. Nonetheless, acetonitrile and acetone have allowed for similar effect on DMS separation, as was shown further with tetraalkylammonium.¹⁴ Overall, each modifier separation provides a new orthogonal dimension to the analytical technique.

III.4.2. Practical limitations

Some practical limitations of using a modifier should be mentioned. Modifier choice is an important step in method development. The choice is usually based on trial and error experiments. Several studies have proposed guidance towards modifier selection.^{14, 18, 19} Findings allow for intuitive understanding of modifier effect on DMS behavior of ion, based on nature and chemical properties of both ion and modifier molecule. Systematic study is still needed to choose a modifier for best DMS separation, since DMS behavior of ions is not well understood under high electric field.

The choice of optimum flow of isopropanol, and more generally modifiers, is also critical. Optimum modifier flow must enable relatively high ion signal and 'correct' CV shift. The trend of CV position as a function of isopropanol flow added to N₂ carrier gas can be visualized in Figure III.8. Using 1 $\mu\text{L}\cdot\text{min}^{-1}$ flow rate of isopropanol, CV values remain unchanged or shift towards positive values relative to those with only N₂ (isopropanol flow = 0). Similar results were also observed with methanol added at 0.5 $\mu\text{L}\cdot\text{min}^{-1}$. This CV shift is obviously not consistent with modifier effect. We found that this is due to technical limitation in our equipment of modifiers. The syringe was not adapted for adding low modifier liquid flow $\leq 1 \mu\text{L}\cdot\text{min}^{-1}$.

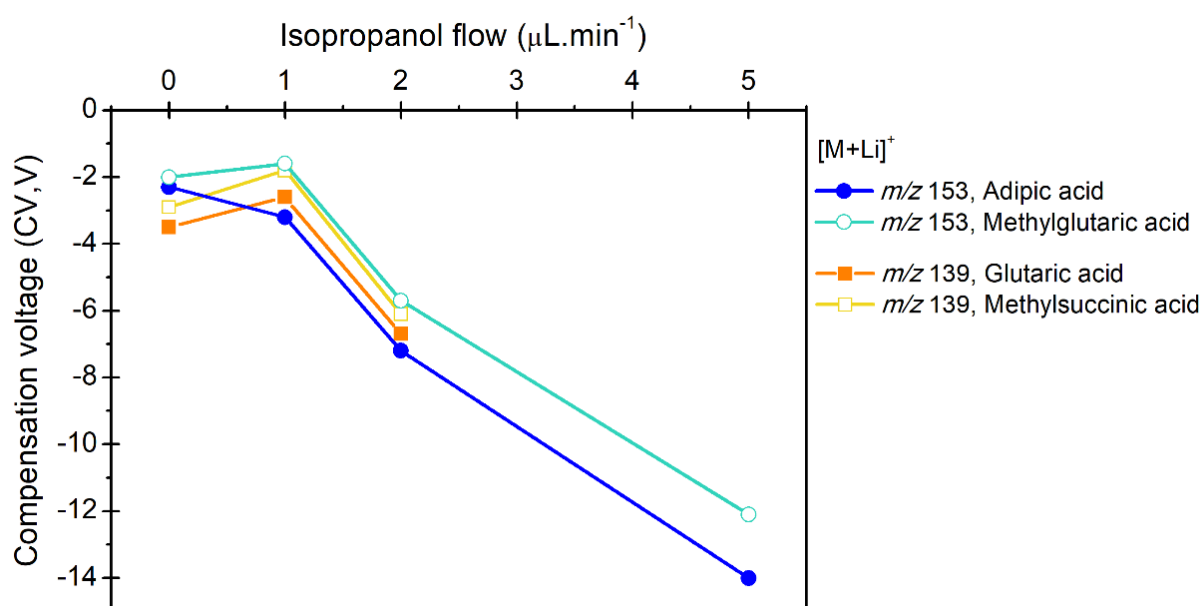


Figure III.8: Effect of isopropanol flow added in N₂ carrier gas on CV position of isomeric lithiated organic acids for m/z 139 and m/z 153: glutaric (orange squares), methylsuccinic (yellow squares), adipic (dark blue circles) and methylglutaric (light blue circles). Dry gas flow and temperature were set at 5 $\text{L}\cdot\text{min}^{-1}$ and 200 °C, respectively.

Ion signal can be sensitive to modifier nature and flow. Ion signal is found to be lower by one order of magnitude with 2 $\mu\text{L}\cdot\text{min}^{-1}$ of isopropanol compared to N₂ only. Figure III.8 shows that two ions (glutaric and methylsuccinic acids) were not detected at 5 $\mu\text{L}\cdot\text{min}^{-1}$. When isopropanol flow was increased gradually from 5 to 10 $\mu\text{L}\cdot\text{min}^{-1}$, no

ions were observed. This indicates that optimal isopropanol flow ranges between 2 and 5 $\mu\text{L}\cdot\text{min}^{-1}$ for optimal detection of ions.

Another issue is related to the nature of modifier, particularly that exhibit high cation affinity leading to ion suppression. This phenomenon was observed with acetone and ethylacetate used as modifiers for separation of lithium and also sodium complexes. In Figure III.9, mass spectra were recorded upon addition of both modifiers for methylmalonic, glutaric and adipic acids complexed with sodium cation. Only adipic acid was observed at very low intensity. Complexes corresponding to $[\text{modifier}+\text{Na}]^+$ were thus found to be highly intense on recorded mass spectra. Cation could thus be transferred to acetone and ethyl acetate that have higher affinity to cation than organic acids.

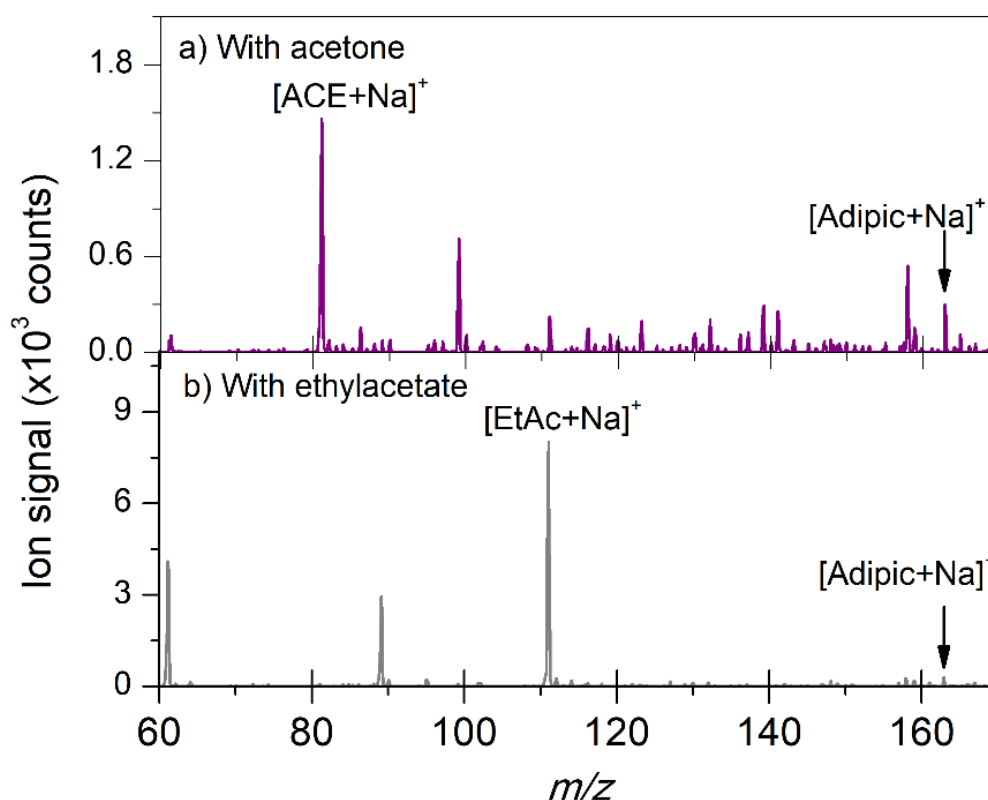


Figure III.9: Mass spectra recorded for a mixture of organic acids complexed with sodium cation upon addition of modifiers at 2 $\mu\text{L}\cdot\text{min}^{-1}$ in N_2 carrier gas fixed at 5 $\text{L}\cdot\text{min}^{-1}$. a) With acetone. b) With ethylacetate.

III.5. Lessons from unwanted modifiers

The issue of the unwanted modifiers in the carrier gas with ESI solvent was recently discussed in the literature.²⁰ First the effect of addition of different modifiers on CV position was evaluated for protonated quinoline molecules. Three modifier molecules were added individually, and it was found that the CV shifts were the largest with acetonitrile, then with isopropanol, and finally CV shifts were found to be very small using water. Second, binary mixtures of molecules were used as modifiers. Dispersion plots were recorded, and it was found that DMS behavior using a binary mixture is essentially that observed with the molecule corresponding to the largest negative CV shift.

The example of water and isopropanol effect on ion behavior is discussed (Figure III.10). Ions are generated from solutions prepared in isopropanol solvent. Dispersion plots recorded upon addition of isopropanol and water as modifiers at the same flow (flow 1) are schematized in Figure III.10. Ions behavior was associated to Type B with water (dark blue curve), and to Type A with isopropanol (red curve). This shows that stronger clustering occurs with isopropanol than with water. When a mixture of both isopropanol and water was added as modifier in the carrier gas, CV are shifted towards values obtained with only isopropanol as modifier. In addition, another experiment was performed using isopropanol added at the same flow (flow 2) as that in the mixture. The resulting trend is nearly identical to the dispersion plot recorded upon addition of modifiers mixture. This suggests that ions preferentially bind to isopropanol in modifier mixture, that is found to be a strongly binding modifier gas.

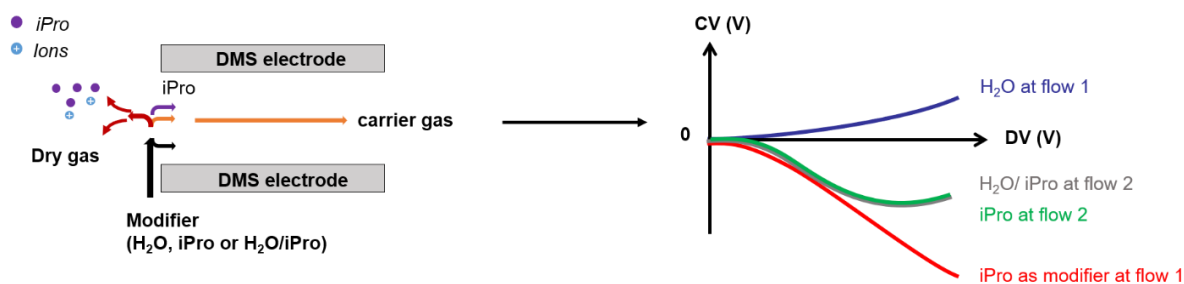


Figure III.10: Illustration of ion desolvation effect on DMS behavior based on Hopkins paper.²⁰ Abbreviation: iPro (isopropanol)

To evaluate the potential contamination of the carrier gas with ESI solvents, residual isopropanol solvent (purple arrow) could enter DMS cell and play the role of modifier. When water is added as modifier, CV shift would be influenced by isopropanol with which ions have the strongest interaction. Based on Hopkins group findings,²⁰ one can conclude that ESI solvents are completely evaporated before entering the DMS cell.

In our case, contamination of dry gas with ESI solvents was demonstrated when addition of helium gas was attempted. Addition of He to N₂ carrier gas is known to have a positive effect on DMS resolution.²¹⁻²³ Ion-helium interaction is weak, and as a result, hard sphere collision regime is expected, and positive CV shifts are observed. According to the literature, the key factor with helium addition is that narrower peaks relative to N₂ only used as a carrier gas are observed.¹³ Effect of He on organic acid isomers separation was thus investigated.

DMS spectra were recorded with only N₂ (N₂/He 100:0) and N₂/He (92:8) mixture. The percentage ratio of N₂/He mixture was found at 92:8 providing a compromise between ion signal and DMS separation. N₂ flow corresponds to 2.4 L.min⁻¹. Table III.1 lists the CV values and full width at half maximum (FWHM) of peaks obtained under these conditions for the three pairs of organic acid isomers cationized with Li⁺.

Table III.1: CV and FWHM values observed for organic acids as lithiated complexes. Data were recorded using a mixture of N₂/He gases (92:8) and N₂ only as carrier gas (100:0) fixed at 2.4 L.min⁻¹.

		N ₂ /He (100:0)		N ₂ /He (92/8)	
[M+Li] ⁺	m/z	CV (V)	FWHM (V)	CV (V)	FWHM (V)
Methylmalonic	125	-7.6	1.2	-7.2	1.1
Succinic		-9.0	1.4	-8.2	1.3
Glutaric	139	-7.5	1.3	-6.9	0.9
Methylsuccinic		-7.4	1.5	-6.7	1.0
Adipic	153	-5.7	1.2	-5.1	1.0
Methylglutaric		-6.2	1.5	-5.5	1.1

When helium is mixed into the N₂ carrier gas, CV values are shifted towards more positive values than those with N₂ only. As expected, upon addition of He, peak width is found smaller, particularly for glutaric, methylsuccinic and methylglutaric acids whose FWHM is found to be reduced by ~0.5 V (Table III.1). Nevertheless, addition of He does not significantly improve isomer resolution. The best R_{pp} values is found for MMA and SA which corresponds to ~0.7 and ~0.5 with N₂ only and N₂/He, respectively.

CV values of our target pairs of isomers using N₂ at a 2.4 L.min⁻¹ flow rate called our attention. While CV value should not depend on the gas flow rate, a negative shift was observed going from 5 to 2.4 L.min⁻¹ using N₂ only. As discussed above, such negative CV shift trend is typically observed when a polar modifier is added into the carrier gas. We thus wondered whether the carrier gas was made of 'N₂ only' when the N₂ flow rate was restricted to 2.4 L.min⁻¹?

As discussed in Chapter II, the default DMS carrier gas is N₂, which is provided by the commercially available desolvating N₂ gas line. An advantage is that both flow rate and temperature can be easily controlled using the Bruker software. As under simple ESI conditions, part of this N₂ gas flow escapes through the hole of the spray shield

and allows for ion desolvation. Under the influence of pumping system, however, part of this N₂ gas is pumped through the glass capillary transfer. This corresponding gas flow acts as DMS carrier gas.

Position of the ESI needle with respect to the entrance of DMS device was carefully optimized when our home-built source chamber was first installed. When the needle was too close, negative CV shifts were observed. These could be simply interpreted as resulting from ESI solvents mixing with N₂ in the DMS carrier gas. Similarly, when the N₂ flow rate is too low, *i.e.* 2.4 L.min⁻¹, it can be assumed that ESI solvents mix into the DMS carrier gas. This hypothesis was challenged using an increase amount of ESI solvents as modifier added into N₂ as carrier gas. In practice, since negative CV shifts are larger using methanol than water,¹⁴ only methanol was used as modifier. DMS spectra for methylmalonic and adipic acids recorded using different carrier gas flow and composition are shown in Figure III.11.

In this figure, three DMS spectra are reported. Two using "only N₂" as carrier gas, at flow rates of 5 and 2.4 L.min⁻¹, in panel (a) and (b), respectively. In panel (c), DMS spectra recorded when adding methanol at a liquid flow rate of 2 μL.min⁻¹ into the N₂ gas line at a flow rate of 5 L.min⁻¹ is given. As expected, a negative CV shift is observed upon addition of methanol in the DMS carrier gas, as can be seen in panels (a) and (c). Interestingly, peak positions observed upon addition of methanol are quite similar to those observed with a low flow rate, 2.4 L.min⁻¹, using "N₂ only". These observations thus support the hypothesis that part of the ESI solvent (methanol:water) mixes into the carrier gas when the N₂ gas flow is too low. As a matter of fact, when increasing the drying gas flow, it was found that a flow rate value of 6.5 L.min⁻¹ was required to reach the asymptotic CV value using "N₂ only".

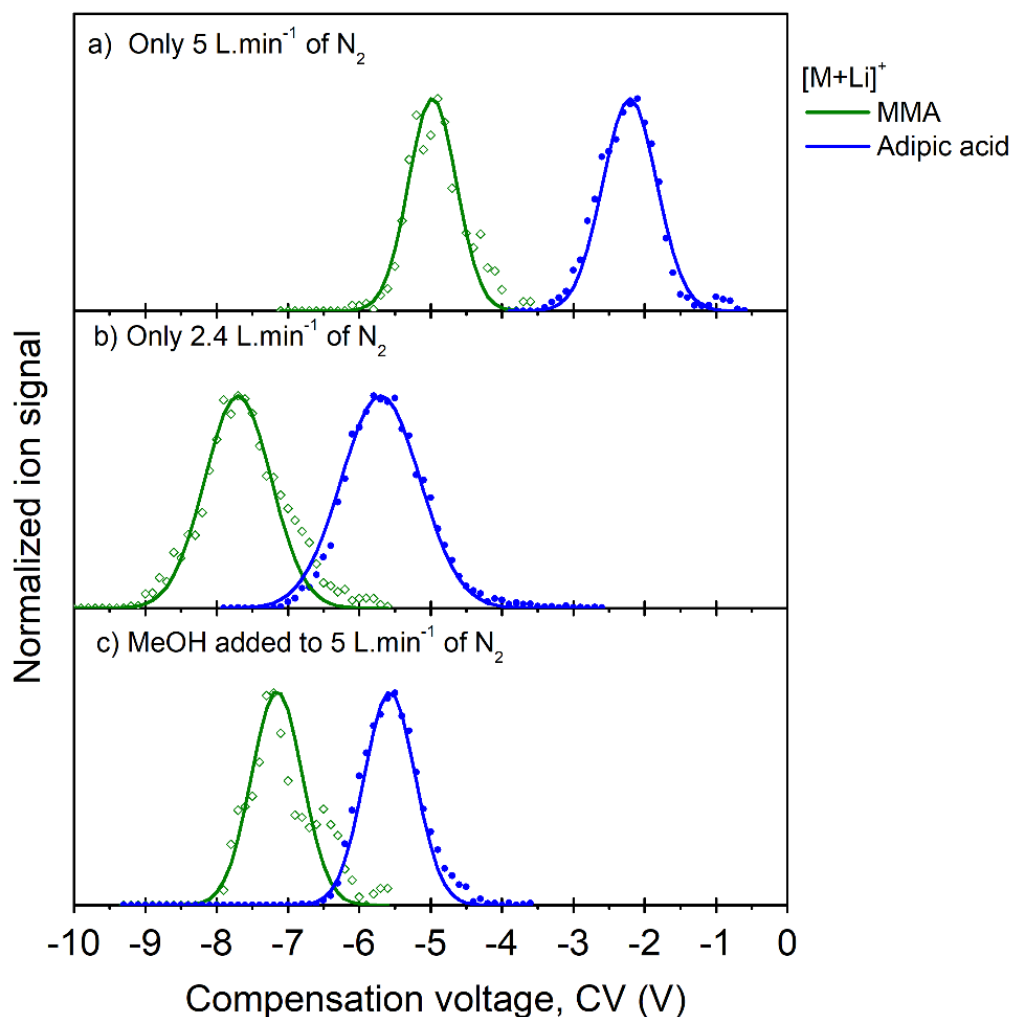


Figure III.11: DMS spectra recorded for methylmalonic acid (MMA, dark green diamonds) and adipic acid (dark blue circles) using different carrier composition. a) With only N_2 at 5 L.min^{-1} . b) With only N_2 at 2.4 L.min^{-1} . c) With $2 \mu\text{L.min}^{-1}$ of methanol seeded in 5 L.min^{-1} of N_2 carrier gas. Data are fitted and smoothed using a rolling average over two points. All individual spectra are normalized to the maximum.

III.6. Cationization of organic acids in plasma

Cationization of organic acids was successfully achieved with lithium cation added to methanol:water solutions using 1:10 ratio (OA:Li⁺). Li⁺ was added to plasma samples spiked with MMA, glutaric and adipic acids at the same OA:Li⁺ ratio. Mass spectra are shown in Figure III.12. Lithiated complexes of glutaric and adipic acids were found at very low ion signal counts but MMA complex was not detected (Figure III.12a). The

most abundant species are observed for m/z 141, 155 and 169 that corresponds to sodium complexes of the three organic acids, MMA, glutaric and adipic acids, respectively.

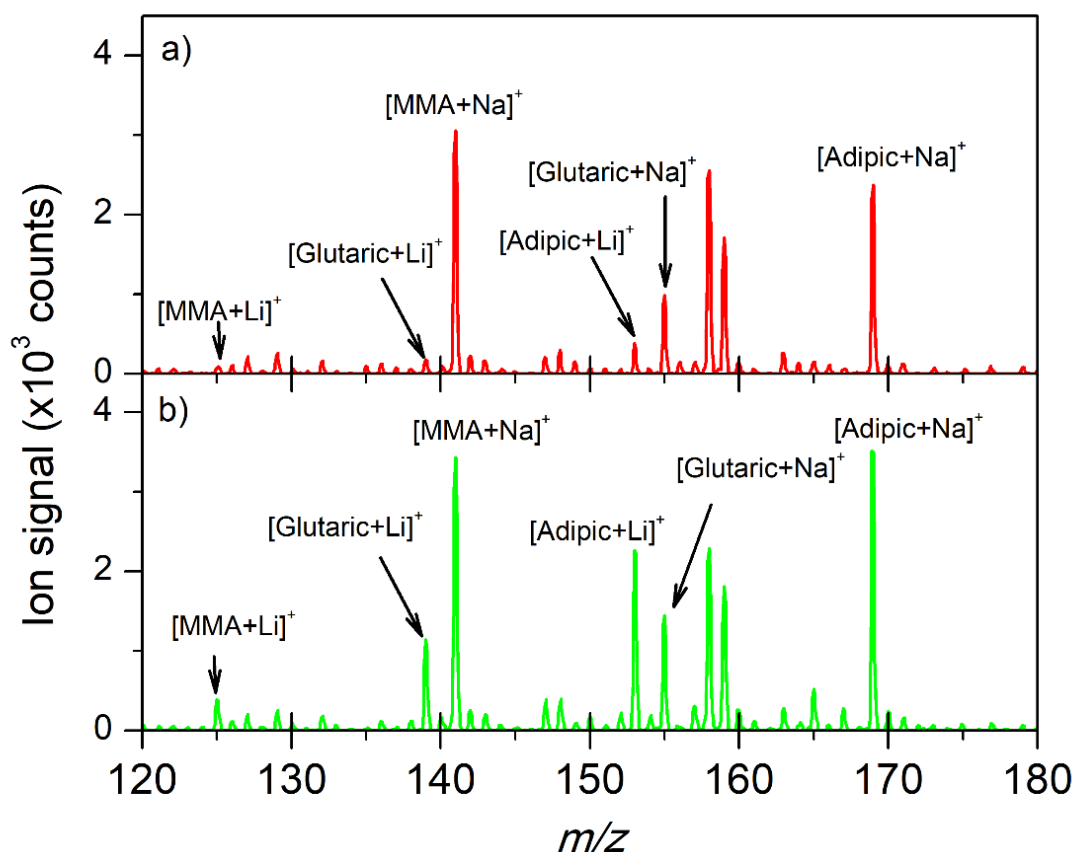


Figure III.12: Mass spectrum recorded for lithiated methylmalonic (MMA), glutaric and adipic acids in plasma diluted by: a) 1/50 and b) 1/100 dilution factor.

In fact, plasma is naturally rich in sodium cation at high physiological concentration $\sim 142 \text{ mmol.L}^{-1}$. In Figure III.12a, plasma was 50-fold diluted so as concentration of sodium is found ~ 3 -fold higher than that of Li^+ cation, which could explain the abundance of sodiated OAs. However, plasma was 100-fold diluted leading to Na^+ concentration on the order of Li^+ concentration. Even though, sodiated complexes remain the most abundant species on mass spectra (Figure III.12b).

Hence, sodium cation present in plasma could be useful for two purposes. Cationization of OAs with sodium occurs without sacrificing time for salt addition during sample preparation. It is important to stress that one issue of the use of lithium is that DMS and/or the capillary had to be cleaned regularly (and often!). Cationization with sodium could also provide better mobility resolution of isomeric metabolites than that of lithium cation.⁵ As found in literature, the best DMS separation was obtained with sodium cation for isomeric saccharides cationized with Li^+ , Na^+ and K^+ .

III.7. Summary

In summary, a careful optimization is required before DMS-MS analysis. Cationization of organic acids is used as a means to generate positively charged ions. The effect of modifiers on DMS selectivity is detailed. Isopropanol greatly improves separation of isomeric organic acids. Modifier properties such as high cation affinity can lead to ion suppression. Two crucial issues are discussed in this chapter: post-DMS fragmentation of dimers and potential contamination of DMS carrier gas by ESI solvent molecules. Such issues should be taken with great care when using DMS coupled to MS. Both ion signal intensity and peak position can be significantly influenced so that optimization allows to avoid misinterpretation of peaks on DMS spectra.

References

1. Werner, E.; Heilier, J. F.; Ducruix, C.; Ezan, E.; Junot, C.; Tabet, J. C., Mass spectrometry for the identification of the discriminating signals from metabolomics: Current status and future trends. *Journal of Chromatography B-Analytical Technologies in the Biomedical and Life Sciences* **2008**, *871* (2), 143-163.
2. Chouinard, C. D.; Wei, M. S.; Beekman, C. R.; Kemperman, R. H. J.; Yost, R. A., Ion Mobility in Clinical Analysis: Current Progress and Future Perspectives. *Clinical Chemistry* **2016**, *62* (1), 124-133.
3. Huang, Y.; Dodds, E. D., Ion Mobility Studies of Carbohydrates as Group I Adducts: Isomer Specific Collisional Cross Section Dependence on Metal Ion Radius. *Anal. Chem.* **2013**, *85* (20), 9728-9735.
4. Kaszycki, J. L.; La Rotta, A.; Colsch, B.; Fenaille, F.; Dauly, C.; Kamleh, A.; Wu, C., Separation of biologically relevant isomers on an Orbitrap mass spectrometer using high-resolution drift tube ion mobility and varied drift gas mixtures. *Rapid Communications in Mass Spectrometry* **2019**, *33*, 3-10.
5. Hernandez, O.; Isenberg, S.; Steinmetz, V.; Glish, G. L.; Maitre, P., Probing Mobility-Selected Saccharide Isomers: Selective Ion-Molecule Reactions and Wavelength-Specific IR Activation. *J. Phys. Chem. A* **2015**, *119* (23), 6057-6064.
6. Rodgers, M. T.; Armentrout, P. B., A critical evaluation of the experimental and theoretical determination of lithium cation affinities. *International Journal of Mass Spectrometry* **2007**, *267* (1-3), 167-182.
7. Hofmeister, G. E.; Zhou, Z.; Leary, J. A., LINKAGE POSITION DETERMINATION IN LITHIUM-CATIONIZED DISACCHARIDES - TANDEM MASS-SPECTROMETRY AND SEMIEMPIRICAL CALCULATIONS. *Journal of the American Chemical Society* **1991**, *113* (16), 5964-5970.
8. Lattimer, R. P., Tandem mass spectrometry of lithium-attachment ions from polyglycols. *J Am Soc Mass Spectrom* **1992**, *3* (3), 225-34.
9. Olsher, U.; Izatt, R. M.; Bradshaw, J. S.; Dalley, N. K., Coordination chemistry of lithium ion: a crystal and molecular structure review. *Chem. Rev.* **1991**, *91* (2), 137-164.
10. Campbell, M. T.; Glish, G. L., Fragmentation in the ion transfer optics after differential ion mobility spectrometry produces multiple artifact monomer peaks. *International Journal of Mass Spectrometry* **2018**, *425*, 47-54.

11. Krylov, E.; Nazarov, E. G.; Miller, R. A.; Tadjikov, B.; Eiceman, G. A., Field Dependence of Mobilities for Gas-Phase-Protonated Monomers and Proton-Bound Dimers of Ketones by Planar Field Asymmetric Waveform Ion Mobility Spectrometer (PFAIMS). *The Journal of Physical Chemistry A* **2002**, *106* (22), 5437-5444.
12. Krylova, N.; Krylov, E.; Eiceman, G. A.; Stone, J. A., Effect of moisture on the field dependence of mobility for gas-phase ions of organophosphorus compounds at atmospheric pressure with field asymmetric ion mobility spectrometry. *J Phys Chem A* **2003**, *107* (19), 3648-54.
13. Schneider, B. B.; Covey, T. R.; Coy, S. L.; Krylov, E. V.; Nazarov, E. G., Chemical effects in the separation process of a differential mobility/mass spectrometer system. *Anal. Chem.* **2010**, *82* (5), 1867-1880.
14. Campbell, J. L.; Zhu, M.; Hopkins, W. S., Ion-molecule clustering in differential mobility spectrometry: lessons learned from tetraalkylammonium cations and their isomers. *J Am Soc Mass Spectrom* **2014**, *25* (9), 1583-91.
15. Berthias, F.; Maatoug, B.; Glish, G.; Moussa, F.; Maitre, P., Resolution and Assignment of Differential Ion Mobility Spectra of Sarcosine and Isomers. *J. Am. Soc. Mass Spectrom.* **2018**, *29* (4), 752-760.
16. Wang, Y.; Alhajji, E.; Rieul, B.; Berthias, F.; Maître, P., Infrared isomer-specific fragmentation for the identification of aminobutyric acid isomers separated by differential mobility spectrometry. *International Journal of Mass Spectrometry* **2019**, *443*, 16-21.
17. Schneider, B. B.; Nazarov, E. G.; Covey, T. R., Peak capacity in differential mobility spectrometry: effects of transport gas and gas modifiers. *International Journal for Ion Mobility Spectrometry* **2012**, *15* (3), 141-150.
18. Schneider, B.; Covey, T.; Nazarov, E., DMS-MS separations with different transport gas modifiers. *International Journal for Ion Mobility Spectrometry* **2013**, *16* (3), 207-216.
19. Ruskic, D.; Hopfgartner, G., Modifier Selectivity Effect on Differential Ion Mobility Resolution of Isomeric Drugs and Multidimensional Liquid Chromatography Ion Mobility Analysis. *Anal. Chem.* **2019**, *91* (18), 11670-11677.
20. Coughlan, N. J. A.; Liu, C.; Lecours, M. J.; Campbell, J. L.; Hopkins, W. S., Preferential Ion Microsolvation in Mixed-Modifier Environments Observed Using Differential Mobility Spectrometry. *J. Am. Soc. Mass Spectrom.* **2019**, *30* (11), 2222-2227.

21. Isenberg, S. L.; Armistead, P. M.; Glish, G. L., Optimization of Peptide Separations by Differential Ion Mobility Spectrometry. *J. Am. Soc. Mass Spectrom.* **2014**, *25* (9), 1592-1599.
22. Shvartsburg, A. A.; Creese, A. J.; Smith, R. D.; Cooper, H. J., Separation of a Set of Peptide Sequence Isomers Using Differential Ion Mobility Spectrometry. *Anal. Chem.* **2011**, *83* (18), 6918-6923.
23. Shvartsburg, A. A.; Danielson, W. F.; Smith, R. D., High-Resolution Differential Ion Mobility Separations Using Helium-Rich Gases. *Anal. Chem.* **2010**, *82* (6), 2456-2462.

Chapitre IV - Separation, identification and quantification of organic acids in plasma

Our ultimate goal is to provide a proof of concept for a simple and fast analysis of organic acids (OAs) in plasma using a new differential mobility spectrometry-mass spectrometry (DMS-MS) approach. In this perspective, we first focused on quantification of MMA, a specific biomarker of methylmalonic acidemia. This chapter discusses DMS-MS analysis from fundamental understanding of DMS behavior of OA isomers to developing a robust method for separation, identification and quantification of targeted biomarker. DMS-MS performance is evaluated using methanol:water solution and plasma samples. Based on high reproducibility and stability of DMS measurements, calibration results are presented for selected OAs. Finally, evaluation of a multi-class analysis of endogenous OAs and amino acids (AAs) as found in a pool of plasma is also presented. Amino and organic acids are connected within a network of metabolic pathways. Multi-class DMS-MS analysis could thus be of interest as a fast approach for providing a global view of the clinical status of patients.

IV.1. Lessons learned from DMS behavior of isomeric organic acids

IV.1.1. Organic acids isomers as sodium complexes

Isomeric organic acids complexed with sodium cation are our analytical targets. Three isomeric pairs of organic acids are studied (Table IV.1): succinic and methylmalonic acids (MMA) (Pair 1), glutaric and methylsuccinic acids (Pair 2) and adipic and methylglutaric acids (Pair 3). Structural information is reported in Table IV.1. Each pair is made of a linear and a branched dicarboxylic acid with carbon number of 4, 5 or 6, respectively. Each OA isomer pair is characterized by its corresponding m/z value of

$[M+Na]^+$ complex: m/z 141 for succinic and methylmalonic acids, m/z 155 for glutaric and methylsuccinic acids and m/z 169 for adipic and methylglutaric acids.

Table IV.1: Structural properties related of organic acids complexed with sodium cation.

Pair	OA	Carbon chain	OA carbon number	$[M+Na]^+$ (m/z)	Na ⁺ ring size
1	Succinic	Linear	4	141	7
	MMA	Branched			6
2	Glutaric	Linear	5	155	8
	Methylsuccinic	Branched			7
3	Adipic	Linear	6	169	9
	Methylglutaric	Branched			8

Structure of sodium complexes formed with small molecules such as dicarboxylic acids has been the subject of numerous studies.^{1, 2} Sodium cation is likely bound to the two atoms of oxygen of carbonyl groups, through electrostatic and charge transfer interactions. This would lead to the formation of a six-membered ring with MMA and seven-membered ring with succinic and methylsuccinic acids. Eight-membered rings are formed with glutaric and methylglutaric acids, while the largest cycle of 9 members would be formed with adipic acid. Assuming that all ions preferentially adopt such a ring structure, we initially thought that it could be a key parameter for understanding CV shift effect. Ring size is thus given in Table IV.1

IV.1.2. Effect of structural properties on DMS behavior

DMS behavior of isomeric organic acids reveals the influence of structural properties of ions to potential interactions with carrier gas molecules. DMS spectra of isomers complexed with sodium cation in methanol:water solution are recorded using N₂ as carrier gas and a DV value of 1800 V, *i.e.* our standard conditions. Values of dry gas flow and temperature were fixed at 6.5 L.min⁻¹ and 220 °C, respectively, which were

found to be our optimal conditions as mentioned in the previous chapter. DMS spectra are represented in Figure IV.1. Panels (a), (b), and (c) show DMS peaks of sodiated complexes with m/z 144, 155 and 169, respectively.

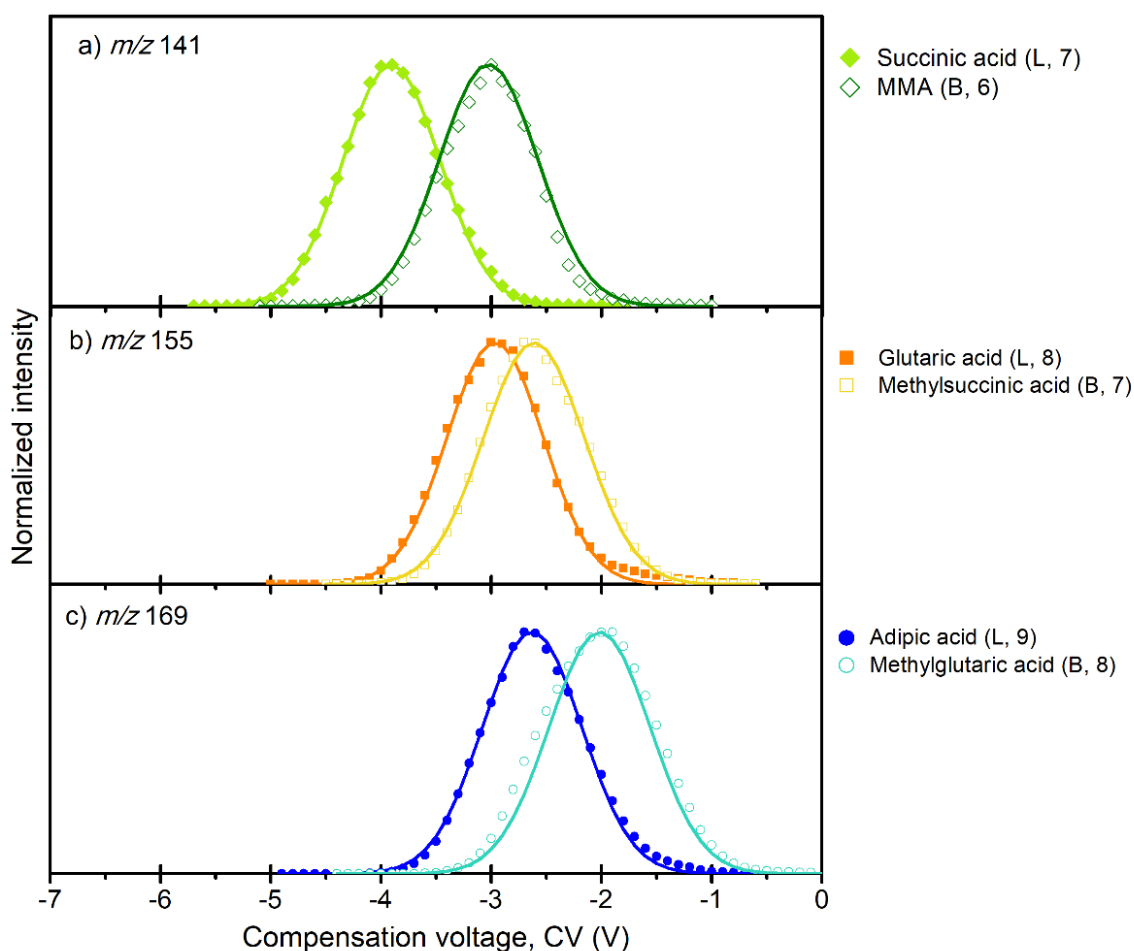


Figure IV.1: DMS spectra recorded for sodiated organic acids (OAs) using N_2 as carrier gas. a) m/z 141 isomers of succinic and methylmalonic (MMA) acids. b) m/z 155 isomers of glutaric and methylsuccinic acids. c) m/z 169 isomers of adipic and methylglutaric acids. Carbon chain structure of OAs (linear or branched) and number of atoms in sodiated ring are noted in brackets. Experiments were performed using methanol:water solution and dispersion voltage value of 1800 V. To facilitate visualization, all individual spectra are fitted and normalized to the maximum. Abbreviations: L (linear), B (branched).

As can be seen in this Figure, a single peak is observed for each combination of cation and OA, suggesting that a single conformation is formed. The conformation of heavier ions may be difficult to predict. In the case of the ions associated with MMA and its

isomer, this observation could be, however, consistent with the formation of a cyclic isomer alone.

Each pair of isomers is partially resolved under our standard DMS conditions. The best separation is observed for the lightest isomers at m/z 141. The second general observation is that CV values get more positive when the m/z ratio increases from 141 to 169. Experimental data shows that differential mobility coefficient is influenced by mass and charge of ions.^{3, 4} Heavy ions exhibit weak interactions with carrier gas molecules so that they are transmitted at more positive CV values than ions with low mass.

A clear structural trend can be observed in DMS spectra (Figure IV.1). Sodiated complex formed with linear OAs (succinic, glutaric and adipic) are transmitted at more negative CV value than its corresponding isomer formed with branched OAs (MMA, methylsuccinic and methylglutaric). It could be argued that the methyl moiety of branched OAs could lead to charge shielding in the branched complex, preventing from strong ion-molecule interaction. Systematic studies have explored the relationship between DMS behavior and structural properties of ions.^{3, 5} Steric effect was found to play a critical role on ion-molecule interaction, as demonstrated with tetraalkylammonium cations and quinoline derivatives described in Chapter I. Assuming a ring size conformation, and considering the remote position of the methyl substituent group with respect to the electric charge, however, such direct steric effect seems unlikely.

We initially thought that ion-molecule interaction, and thus CV values, would be intimately correlated with the size of rings. More specifically, as observed in organic chemistry, 5- or 6-membered rings are the most favorable because they are associated with the strongest intra cyclic bonds. If the two intra cyclic bonds formed between Na^+ and the carbonyl groups are strong, it can be expected that the binding of an

additional (polar) molecule used as a modifier would be small. This effect is likely to decrease with cycle size.

This reasoning seems consistent with the observed evolution of isomer separation as a function of m/z value. The best resolution is observed for MMA and its isomer, while nearly no separation is observed for heavier isomers. Assuming a ring structure with Na^+ bound to the two carbonyl oxygen atoms, the most favorable $[\text{MMA}+\text{Na}]^+$ structure is six-membered ring, while a less favorable seven-membered ring structure would be formed for succinic isomer. It can thus be expected that bonding of Na^+ with carrier gas molecules is weaker for the former than for the latter, which is consistent with the relative position of their DMS peaks.

Always in the hypothesis of a cyclic structure, ion with the largest m/z value corresponding to a branched OA, is found at the most positive CV value. For example, both succinic and methylsuccinic acids form seven-membered ring with Na^+ . The former m/z 141 ion is found at -3.9 V and the latter (m/z 155) at -2.6 V. A similar positive CV shift is observed for eight-membered ring structures from glutaric acid (CV = -3.0 V) to methylglutaric acid (CV = -1.9 V). Thus, steric effect of methyl moiety can also modulate DMS behavior of cycles formed between OA and Na^+ .

IV.2. DMS separation: attempts for improvement

IV.2.1. Effect of dispersion voltage

In order to probe dispersion voltage (DV) effect on DMS separation of isomers, DMS spectra were recorded at DV values ranging from 1200 V to 2000 V for organic acids diluted in methanol:water solution. Dry gas flow and temperature were fixed at 6.5 $\text{L}\cdot\text{min}^{-1}$ and 220 °C, respectively. Dispersion plots corresponding to the evolution of CV as a function of DV for each sodiated complex, are reported in Figure IV.2.

As expected, CV values are shifted towards negative values when increasing DV value. Full width at half-maximum (FWHM) of DMS peaks does not vary with DV, and was found to be 1.1 V. As mentioned in Chapter III, increasing DV value can, however, enhance peak capacity (PC) and peak-to-peak resolution (R_{pp}). PC increases linearly ($R^2 = 0.990$) with DV from PC = 0.8 at 1200 V to PC = 2.2 at 2000 V. The evolution of PC as a function of DV is represented in Figure IV.S1 in the Annex.

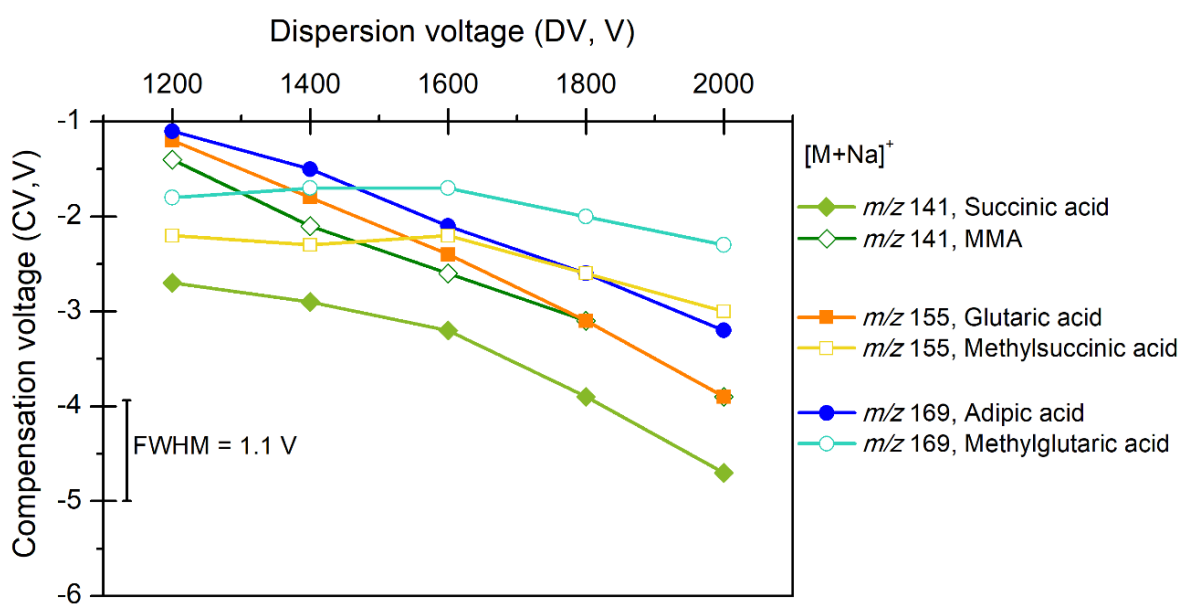


Figure IV.2: Dispersion plot recorded for sodiated organic acids using N_2 carrier gas: m/z 141 isomers of succinic and methylmalonic (MMA) acids (green diamonds), m/z 155 isomers of glutaric and methylsuccinic acids (orange squares), m/z 169 isomers of adipic and methylglutaric acids (blue circles). Experiments were performed using methanol:water solution. Dry gas flow and temperature were set at $6.5 \text{ L}\cdot\text{min}^{-1}$ and $220 \text{ }^\circ\text{C}$.

As can be seen in Figure IV.2, dispersion plots of two isomers can be different, thus giving hopes for improving R_{pp}. For both m/z 155 and m/z 169 cases, the two isomer pairs are partially separated at 1200 V. R_{pp} is 0.5 for the former and 0.4 V for the latter. Isomers are found at similar CV values between 1400V and 1600 V. Then, at the highest DV values, 1800 V and 2000 V, CV values become different which results in increased isomer resolution, and R_{pp} becomes similar to that observed at 1200 V. In the case of

m/z 141 isomers, the two dispersion plots are essentially parallel, and no significant Rpp change is observed.

The best DMS performance is, however, observed at DV = 2000 V, the maximum value that can be reached with our setup. One might keep in mind that PC and isomer resolution are enhanced at DV value of 2000 V at the cost of ion signal. As mentioned in the previous chapter, a DV value of 1800 V was found to provide a good compromise between ion transmission, DMS separation and CV spread. This DV value is applied for DMS-MS experiments throughout this chapter.

The use of sodium cation leads to a good DMS separation of isomeric organic acids. A comparison between dispersion plots recorded for sodiated and lithiated complexes of organic acids allows for three observations. First, dispersion plots reveal different ion behaviors. Sodiated complexes behave as Type A (*i.e.*, decreasing CV with DV), which is associated to clustering/declustering cycles. In contrast, lithiated complexes were found to behave as Type B. These observations can be simply interpreted considering the availability of the alkali charge center for bond formation with dinitrogen. Based on literature data,^{2,6} bonding of a carbonyl oxygen is much stronger to Li⁺ (55.0 kJ.mol⁻¹) than to Na⁺ (31.8 kJ.mol⁻¹). As a result, assuming a ring structure upon formation of two M⁺-carbonyl bonds, Li⁺ would be less available to clustering with carrier gas molecules than Na⁺.

Second, dispersion plots also show that CV spread of lithium complexes is larger than that observed with sodium cation. For instance, PC with Li⁺ was 4.7 at a DV value of 1800 V, whereas PC with Na⁺ was found to be 1.8. Finally, isomer resolution is improved with sodium cation. Isomers are separated with sodium even at low DV values, as observed at 1200 V. Adipic and methylglutaric acids are unresolved with Li⁺, but

become separated with Na⁺. Sodium cation thus seems an appropriate alternative to lithium cation for separation of isomeric organic acids.

IV.2.2. Effect of polar modifier

Modifier addition such as methanol was investigated in order to improve isomer separation. Methanol was added at a flow rate of 2 $\mu\text{L}\cdot\text{min}^{-1}$, which corresponds to $\sim 0.02\%$ of methanol vapor added to N₂ dry gas fixed at 6.5 $\text{L}\cdot\text{min}^{-1}$. CV values of isomers obtained are given in Table IV.2. Comparison between CV values observed with and without methanol clearly shows that CV values of isomers are nearly the same.

Methanol was introduced at different flow rates ranging from 1 to 5 $\mu\text{L}\cdot\text{min}^{-1}$. Increasing modifier flow rate can improve resolution at the expense of ion signal. This was found to be particularly true for MMA and its isomer, *i.e.* the lightest isomers. For such light ions, it is conceivable that ion trajectories are the most sensitive to ion-molecule collisions leading to ion loss. Addition of other modifier such as isopropanol was attempted and similar results were observed (see Figure IV.S2 in Annex). Considering these findings, the best DMS performance of was achieved using only N₂ as carrier gas and a DV value of 1800 V.

Table IV.2: CV values obtained from DMS spectra recorded with and without methanol used as modifier gas in N₂ dry gas. N₂ dry gas flow was set at 6.5 $\text{L}\cdot\text{min}^{-1}$ and methanol flow was fixed at 2 $\mu\text{L}\cdot\text{min}^{-1}$ which corresponds to $\sim 0.02\%$ molar percentage.

N ₂ dry gas flow at 6.5 $\text{L}\cdot\text{min}^{-1}$		Without methanol	With methanol
OA	[M+Na] ⁺ (m/z)	CV (V)	CV (V)
Succinic	141	-3.8	-7.0
MMA		-2.9	-7.0
Glutaric	155	-2.8	-5.3
Methylsuccinic		-2.4	-5.5
Adipic	169	-2.4	-4.5
Methylglutaric		-1.8	-4.1

IV.3. Fast identification of organic acids in plasma

IV.3.1. Determination of CV values in plasma

Our targeted DMS-MS method for rapid quantification would rely on the fact that a biomarker could be characterized by its CV value, and thus at its non-dependency on matrix composition. CV values of OAs were thus first determined for sodiated complexes in methanol:water and plasma samples. Experiments were performed for organic acids added at the same concentration (100 μ M) to both matrices. DMS spectra were recorded at DV value of 1800 V using N₂ as carrier gas, and DMS data are given in Table IV.3. CV and FWHM values of sodiated OAs found in methanol:water solution are reproducible in plasma, resulting in very similar Rpp value for each isomer pair.

Table IV.3: Comparison between DMS data recorded in methanol:water and plasma solutions for sodiated organic acids.

OA	[M+Na] ⁺ (m/z)	Methanol:water			Plasma		
		CV (V)	FWHM (V)	Rpp	CV (V)	FWHM (V)	Rpp
Succinic	141	-3.7	1.0	0.4	-3.7	1.0	0.5
MMA		-2.9	1.0		-2.9	1.1	
Glutaric	155	-2.8	1.1	0.3	-2.9	1.0	0.3
Methylsuccinic		-2.3	1.0		-2.3	1.1	
Adipic	169	-2.2	1.1	0.3	-2.2	1.1	0.3
Methylglutaric		-1.8	1.1		-1.8	1.0	

Importantly, our biomarker of interest, MMA, can be distinguished from its isomer, succinic acid based on 0.8 V difference in CV values. The corresponding Rpp value (0.5) can be sufficient for achieving reliable quantification of MMA. Indeed, similar

difference in retention time was obtained for underivatized MMA and succinic in other biological matrices using LC-MS/MS method.^{7, 8}

IV.3.2. Robustness of CV measurement

Robustness of DMS method in terms of peak position is important in the perspective of biomarker identification using its specific CV value for maximum transmission. The mean CV value associated to standard deviation (SD) of DMS peak position of sodiated organic acids obtained over 4 months are given in Table IV.4.

Multiple CV measurements were carried out in different conditions. Eight plasma samples collected from different control patients were used for preparation of working solutions for optimization, so that plasma composition was not constant. Plasma samples were also diluted at either 1/100 or 1/50 final dilution factor. Potential effects of both nature and concentration of the biological matrix are found to be negligible based on SD values small or equal to 0.1 V over these experiments.

Table IV.4: CV values recorded for organic acid added to methanol:water solution and plasma sample over a period of 4 months.

[M+Na] ⁺	Methanol:water		Plasma	
	CV (V)	SD (V)	CV (V)	SD (V)
Succinic	-3.7	0.1	-3.7	0.1
MMA	-3.0	0.1	-3.0	0.1
Glutaric	-2.9	0.1	-2.9	0.1
Methylsuccinic	-2.3	0.1	-2.4	0.1
Adipic	-2.3	0.2	-2.5	0.2
Methylglutaric	-1.7	0.2	-1.8	0.1

Influence of analytes concentration on CV values could also be expected. OAs were spiked into plasma at different concentrations ranging from 5 to 250 μ M. DMS peak shape was characterized even at very low concentration at the expected CV position.

Note that peak width was found not to be correlated with concentration value examined and FWHM variations were smaller than 0.1 V. There is also an excellent agreement between CV values of the two sets of values given in Table IV.4, and hence there is no evidence of concentration effects.

These experiments were carried out over a period of 4 months, during which DMS device had to be mounted and unmounted several times. Stability of CV values of sodiated OAs over time demonstrates that no instrumental bias affects CV measurements. The mean SD values are all found to be smaller than 0.1 V, which corresponds to the CV increment value fixed at 0.1 V for all our experiments. Higher SD was observed for adipic and methylglutaric acids (SD = 0.2 V). Overall, CV value does not depend on matrix nor on analyte concentration.

A pilot study based on the same DMS-MS experiments was conducted with a set of amino acids and related compounds in plasma samples in our group.⁹ Effect of matrix and concentration of analytes were found to be negligible. Variations of CV positions were also on the order of 0.1 V over a large period of time (6 months). Therefore, CV value is a robust and stable parameter that could be a means for reliable identification of metabolites in biological matrices using a DMS-MS approach.

IV.4. Quantification of MMA in plasma samples

Quantification of MMA in plasma allows for both diagnosis and follow-up of methylmalonic acidemia. In the case of a patient with methylmalonic acidemia, MMA is usually found at concentration higher than 50 μM in plasma.^{10, 11} MMA concentration can even reach values of 2000 μM in severe cases. We thus primarily focus our attention on fast quantification of MMA in this high concentration range (*i.e.* 50-2000 μM) in plasma. Our protocol for quantification was simultaneously applied to MMA, glutaric and adipic acids for purpose of method validation.

As mentioned in Chapter II, glutaric and adipic acids are chosen because both can be found in plasma and can be involved in diagnosis of organic acidemias. Glutaric acid is a biomarker of glutaric acidemia Type I when present at a concentration higher than 12 μM in plasma.¹² Adipic acid is a specific biomarker of a mitochondrial fatty acid β -oxidation deficiency,¹³ even though its concentration in plasma greatly depends on nutritional state of subjects. Adipic and also glutaric acids are both produced during a long period of fasting leading to high levels in plasma.

Quantification of MMA, glutaric and adipic acids in plasma using our DMS-MS approach was achieved using a single stable internal standard (IS, MMA- d_3). That is, MMA- d_3 is the common IS for the three organic acids. Calibration samples were prepared with samples collected from healthy control patients, so as OAs are present at physiological concentration. Typically, concentrations of MMA, glutaric and adipic acids lower than 0.5 μM are expected. Plasma was diluted by 1/50 in calibration samples. This dilution factor was found to provide the best ion signal.

Five calibration levels in the 5-50 μM range, corresponding to 250-2500 μM in plasma, were chosen. Calibration curves were obtained from six independent experiments performed over six days. Limit of detection (LOD) and quantification (LOQ) are determined, and precision of our method in terms of quantification is assessed. Finally, matrix effect on concentration of analytes is evaluated. Determination of these detection and quantification limits is based on guidelines of IUPAC^{14, 15} as implemented in our RStudio-written code.¹⁶

IV.4.1. Determination of linear range, LOD and LOQ

Calibration curves of MMA, glutaric and adipic acid are represented in Figure IV.3. The ratio of DMS peak area of standard organic acid and IS is plotted against spiked concentration of OAs in calibration sample. Linearity is defined in the working range

from 5 to 50 μM for the three organic acids. Mean, standard deviation (SD) and relative SD (RSD) values of slope and intercept are given in Table IV.5. Results are stable and reproducible for both slope and intercept. Linear correlation coefficients are found to be greater than 0.99.

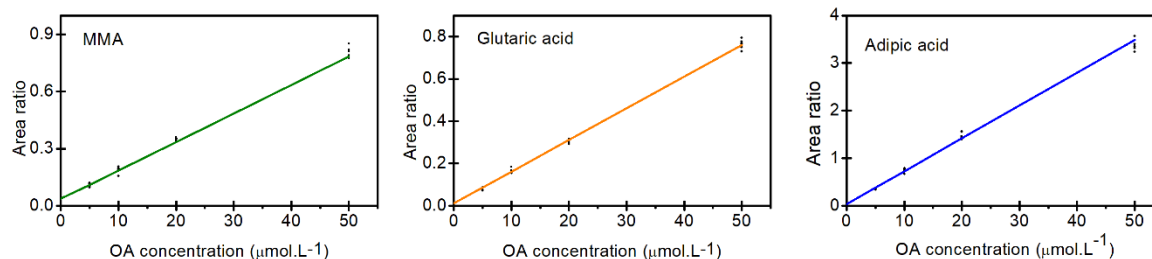


Figure IV.3: Calibration curves of MMA, glutaric and adipic acids spiked in healthy plasma samples. Area ratio organic acid (OA)/internal standard is plotted against OA concentration after dilution. Calibration curves were obtained from experiments performed in duplicate over 6 independent experiments.

Table IV.5: Slope, intercept and R^2 values associated with linear regression equation for MMA, glutaric and adipic acids averaged for experiments performed over 6 independent experiments.

Analyte	Slope		Intercept		R^2 value
	Mean (SD)	RSD (%)	Mean (SD)	RSD (%)	
MMA	0.015(<0.001)	1.34	0.038 (0.002)	6.14	0.99
Glutaric	0.015 (<0.001)	1.37	0.011 (0.002)	2.41	0.99
Adipic	0.069 (0.002)	3.58	0.037 (0.012)	30.76	0.99

Linearity was then assessed at lower concentrations. Calibration samples were prepared with plasma spiked with organic acids within 0.1-2 μM concentration range, considering the plasma dilution factor (1/50). This range is equivalent to 5-100 μM in plasma. Calibration curves show linear profile ($R^2 > 0.99$) are represented in Figure IV.S3 in Annex.

LOD and LOQ are two key parameters for our protocol of quantification. LOD and LOQ values of each analyte are derived from linear regression method mentioned in Chapter II. Based on calibration curves obtained in 5-100 μM range in plasma, LOD

value for our three organic acids is found in the 3-8 μM range in plasma (Table IV.6). The detection limit is very similar to that obtained for amino acids, *i.e.* on the order of 1 μM in the analyzed plasma sample, using our quadrupole ion trap.⁹

LOQ values were estimated at 10.0, 20.2, and 23.8 μM for MMA, glutaric and adipic acids, respectively. Based on MMA linear range and LOQ value, methylmalonic acidemia situations can be covered with our method. Plasma samples containing higher than 2500 μM of MMA are thus simply diluted to a concentration in the calibration range. LOD value found for glutaric acid is 6.7 μM , which is slightly higher than physiological levels (0-1.8 μM).¹⁷ Adipic is as well detected at 8.0 μM which is in the same order of magnitude of other organic acids. High concentration of adipic acid may depend on nutritional state of patients.

Table IV.6: Mean values of limit of detection (LOD) and quantification (LOQ) in μM derived using linear regression method for analytes.¹⁸

Analyte	LOD	LOQ
	Mean	Mean
MMA	3.4	10.0
Glutaric	6.7	20.1
Adipic	8.0	23.8

On the other hand, OAs should be ideally quantified at physiological levels. Preliminary experiments were carried out using samples spiked with OAs at concentrations below 5 μM in plasma. Organic acids were however not sufficiently detected due to intrinsic limitation of our instrument in terms of sensitivity and linear dynamic range.

As a final note, relatively good linearity was also found when concentration range was expanded from 2.5 to 5000 and also 50000 μM in preliminary assays, although with larger SD values at high concentrations. This low precision could be instrument dependent. Using QIT, a high concentration of analytes causes space charge effects

and thus saturation of the ion trap. A more careful for saturation option is thus required.

IV.4.2. Assessment of intra- and inter-day precision

Intra- and inter-day precisions of our protocol of quantification are investigated at two calibration levels, 20 and 50 μM after plasma dilution, which corresponds to 1000 and 2500 μM in plasma. Control solutions were prepared in two different plasma samples noted P1 and P6. Good intra-day and inter-day precision are observed when relative standard deviation values are lower than 4% and 8%, respectively.

Intra-day or intra-assay precision was evaluated for 6 replicates of each sample analyzed on one day ($n = 6$ in Table IV.7). Results are given in Table IV.7 for control samples prepared in P1. Satisfactory results are found for all analytes spiked at both concentration levels (Table IV.7). RSD values range from 1.5% to 3.4%. Intra-day precision is also found acceptable in P6 (Table IV.S1, see Annex), even though variability is systematically higher than 5% at 20 μM .

Table IV.7: Intra-day precision data associated with concentration measurement of MMA, glutaric and adipic acids. Control samples are prepared from one plasma sample (P1) by spiking a mixture of three OAs at 20 and 50 μM after dilution. Mean concentration, standard deviation (SD) and relative SD (RSD) are calculated for each concentration using 6 replicates ($n = 6$) analyzed on one day.

Analyte	Plasma P1, n = 6					
	Nominal concentration = 20 μM			Nominal concentration = 50 μM		
	Mean	SD	RSD (%)	Mean	SD	RSD (%)
MMA	21.4	0.7	3.3	54.9	1.2	2.2
Glutaric	20.6	0.5	2.2	56.9	0.8	1.5
Adipic	20.8	0.7	3.4	57.8	1.4	2.4

Inter-day precision is also found acceptable (Table IV.8). RSD values range between 5 and 8% for MMA, glutaric and adipic at low and high calibration levels, regardless of

which plasma sample was used. In Table IV.8, inter-day precision was evaluated for the same control sample analyzed over n different days. Sample prepared in P6 spiked with 20 μM is analyzed in duplicate on 4 days ($n = 4$), while plasma P1 spiked at 50 μM is analyzed over 11-day period ($n = 11$). RSD values determined at each concentration are, however, found comparable. The difference in terms of number of days thus seems to weakly influence inter-day precision for measurement of low concentration of OAs.

Table IV.8: Inter-day precision of concentration measurement of MMA, glutaric and adipic acids spiked at 20 or 50 μM into two different plasma, P6 and P1, after dilution. Control sample in P6 and P1 are analyzed over 4 days ($n = 4$), and 11 days ($n = 11$), respectively. Mean concentration, standard deviation (SD) and relative SD (RSD) are calculated for each concentration.

Analyte	Plasma P6, n = 4			Plasma P1, n = 11		
	Nominal concentration = 20 μM			Nominal concentration = 50 μM		
	Mean	SD	RSD (%)	Mean	SD	RSD (%)
MMA	20.7	1.1	5.3	51.9	4.2	8.2
Glutaric	21.5	0.8	3.8	53.7	3.8	7.1
Adipic	21.2	1.4	6.4	51.3	3.3	6.4

It could have been expected that using non-specific internal standard for glutaric and adipic acids would result in high variance of their concentration. However, good reproducibility was obtained for adipic and glutaric acids when MMA- d_3 is used as reference compound. In order to improve reproducibility, specific internal standards could be used for glutaric and adipic acids in further experiments. Overall, the coefficient of variation (RSD) met requirements for repeatable and reproducible analysis.

IV.4.3. Assessment of matrix effect on analyte concentration

Six plasma (P1-P6) samples collected from different controls were used to evaluate matrix effect on concentration of OAs at 20 and 50 μM in calibration samples. Recovery and RSD are listed in Table IV.9. Recovery values of MMA are homogenous at both

concentrations, ranging from 99.8% (in P3) to 111.2 % (in P4). The mean value of recovery is found at 105.4%. Similarly, results are satisfactory for glutaric and adipic acids in plasma samples, except in P3 where recovery exceeds 120% at both concentrations. However, recovery values are also acceptable in the expected range 85-115%: mean values are 111.0% and 107.1% for glutaric and adipic respectively. It can be concluded that matrix effect will not exert significant influence on the analyte response and in turn on quantification of the three OAs.

Table IV.9: Matrix effect on MMA, glutaric and adipic acid concentration. Analytes are spiked at 20 and 50 μ M in calibration sample in six different plasma samples (P1-P6). Corresponding recovery and relative standard deviation (RSD) are calculated for each concentration.

Plasma sample	Nominal concentration (μ M)	MMA		Glutaric		Adipic	
		Recovery (%)	RSD (%)	Recovery (%)	RSD (%)	Recovery (%)	RSD (%)
P1	20	104.1	0.9	104.7	2.7	105.4	3.4
	50	111.2	3.3	114	3.3	116.9	3.1
P2	20	105.6	5.6	111.5	0.8	105.5	2.8
	50	105.9	1.2	101.7	1.1	98.0	2.7
P3	20	108.7	2.7	131.4	1.0	121.8	1.0
	50	99.8	2.0	134.7	2.8	120.2	2.5
P4	20	111.2	4.7	100.4	0.6	106.0	0.7
	50	106.1	0.1	104.3	1.8	93.5	0.9
P5	20	100.7	3.1	93.7	1.4	100.3	0.5
	50	101.5	3.9	112.7	2.6	109.5	0.7
P6	20	101.6	3.1	112.4	2.6	113.7	5.1
	50	108.1	1.6	110.6	2.1	94.9	2.6
Average		105.4		111.0		107.1	

Three interpretations of overestimated concentrations of glutaric and adipic acids in sample P3 can be proposed. First, it is assumed that MMA concentration is below 0.5

μM in collected plasmas. Since samples are analyzed anonymously, we do not have information about patient status prior to blood sample nor plasma composition. As a result, concentration of glutaric and adipic acids in one sample could be higher than regular endogenous MMA concentration in samples. Second, high endogenous amounts of both organic acids can result from long fasting period.¹⁹ Fasting induces beta-oxidation of fatty acids to produce energy, leading to increased levels of adipic and glutaric acids in plasma. In such situation, MMA level is not affected.

Relative standard deviation (RSD) values were also calculated for each sample analyzed in duplicate. As can be seen in Table IV.9, RSD values of the three OAs are acceptable. The maximum RSD values are 5.6% and 5.1% for MMA in P2 and adipic acid in P6, respectively. These findings suggest that one replicate can provide sufficient results for quantification of organic acids in plasma.

IV.4.4. Added value of DMS-MS for MMA quantification

From the above discussion it can be concluded that quantification of MMA can be successfully achieved using DMS-MS protocol for diagnosis of methylmalonic acidemia (MMA $>100 \mu\text{M}$ in plasma). The key advantage is that our proposed protocol is simple and fast. These are important assets in the context of clinical diagnosis and therapeutic follow-up. MMA analysis is routinely achieved using conventional methods based on GC- or LC- coupled to a triple quadrupole mass spectrometer. A comparison between protocols is presented in this section.

Starting with sample preparation, our protocol requires a single step for deproteinization of plasma sample with sulfosalicylic acid. Our simple sample preparation helps to minimize errors and loss of analytes. The use of sulfosalicylic acid can provide good robustness of ion separation together and minimal matrix effect, as found using LC-MS for quantification of amino acids in plasma.²⁰ Since sodium is

already present in plasma, addition of salt or other ionizing agents is not needed. Hence, our sample preparation is easy and fast which is clearly the benefit.

Conventional methods require complicated and time-consuming procedure.²¹⁻²³ Several steps of extraction (liquid-liquid or solid-phase) and subsequent derivatization reaction need around 2 hours prior to chromatographic separation. Pretreatment is also custom-made in laboratories. Different protocols are proposed using different materials for extraction^{21, 23} and different reagents for derivatization^{24, 25} such as silylation and butylation. Thus, the quality of MMA analysis may be affected in terms recovery and limit of detection. Instead, one protocol based on DMS-MS is suitable for MMA analysis and other organic acids without extraction and derivatization.

The overall time required for DMS-MS analysis based on a full-scan is less than 3 min. Analysis time can be significantly shortened to ~seconds in selective mode, *i.e* when DMS-MS is only performed at a fixed CV value corresponding to maximum transmission of biomarkers. The above discussion suggests that the stability of CV value associated to MMA should be sufficient for this purpose. Subsequent quantification of these biomarkers can be achieved by recording mass spectra of DMS-selected ions only at identified CV values. DMS analysis becomes indeed faster than GC (30-60 min) and also LC separation that can take ~1 min.²² Hence, DMS-MS allows for fast targeted quantification.

Performance characteristics of our quantification approach differs from conventional methods. Linear range of our method is found between 5 and 2500 μM in plasma, and linearity near physiological levels is still required. Intra- and inter-day precision are however found satisfactory for measurement of high concentrations in plasma. Sensitivity of both methods is not comparable. LOD value obtained with our method, in particular for MMA, is higher than that found in literature.^{22, 23} The lack of sensitivity found with our method can be likely due to intrinsic limitations of our mass

instrument. The lowest limit of detection found with our instrument is 0.1 μM in calibration sample, *i.e.* 5 μM in plasma. Quantification of OAs at physiological levels in plasma (MMA < 0.4 μM) was demonstrated using a triple quadrupole mass spectrometer.^{22, 23} Although, it has been demonstrated that both ion trap and triple quadrupole instruments have been effectively used for qualitative and quantitative analyses of small molecules.^{27, 28} For target compound identification, a triple quadrupole is often the ideal choice for sensitive measurement.²⁶

On the other hand, DMS-QIT quantification of underivatized species seems not sensitive as for derivatized MMA, and OAs in general, using conventional methods. LOD value lower than 0.4 μM was obtained for derivatized MMA using a triple quadrupole mass spectrometer. Derivatization is typically used to improve sensitivity and detection using conventional methods.^{29, 30} Sample preparation could thus be a crucial factor on the basis of sensitivity differences between our method and conventional ones. Using solid-phase extraction in order to increase OA concentration in biological samples could be also investigated, which should lower LOD values. Since our objective is simple and fast sample preparation, additional steps would increase the time needed for sample preparation.

It will be thus useful to improve our sample treatment without adding steps to our protocol. For instance, protein precipitation reagent such as methanol may help to reduce matrix effect more than sulfosalicylic acid. Note that trials have been carried out to improve sensitivity of underivatized OAs with our method. As such, increasing dilution factor of plasma and addition of sodium using physiological serum to improve ionization of OAs. However, LOD values were not significantly enhance (14-21 μM). Quantification of underivatized MMA with DMS hyphenated to a triple quadrupole mass spectrometer is a part of our future work.

It is also important to consider other factors that could affect sensitivity of MS instrument. Sensitivity strongly depends on ionization mode.³¹ Without derivatization, organic acids are generally analyzed in negative ion mode using LC-MS/MS,^{7, 32, 33} since organic acids are easily deprotonated. High ion signal is expected to be obtained for deprotonated ions, leading to higher limit of detection in negative than in positive ion mode. Nevertheless, detection is found more sensitive in positive mode relative to negative mode with electrospray source, using a triple quadrupole in clinical field.³⁴ Quantification of organic acids in negative ionization mode using our QIT is one of the perspectives of this project.

It should also be added that deprotonated OAs were found to behave as hard sphere upon collisions with N₂. Upon modifier addition, no significant trend towards isomer resolution was expected in preliminary assays. Positive ionization was thus preferred for DMS-MS analysis of OAs, which is also the ionization mode used for amino acids, thus opening the way towards a single multi-class analysis of OAs and AAs.

As discussed in Chapter III, high dispersion voltage value applied for DMS analysis is generally at the expense of ion signal of analytes. The effect of DV on sensitivity was discussed in the literature. Significant decrease in sensitivity was observed at high DV values.^{35, 36} DMS-MS experiments performed at low DV value such as 1200 V can improve ion signal of MMA without affecting its separation from its isomer, succinic acid. Our optimized DV value is, however, set at 1800 V leading to ion signal in the order of magnitude as that observed at 1200 V. High DV value is also important to spread ions over wide range of CV values, which is required for multi-class metabolites analysis.

IV.5. Multi-class calibration in plasma samples

The idea of multi-class calibration consists of simultaneous analysis of organic acids and amino acids within a plasma sample in a single run. In the present case, DMS-MS conditions optimized for OAs were used. A representative set of amino acids (AAs) was selected for multi-class calibration including alanine (Ala), valine (Val), leucine (Leu), methionine (Met), phenylalanine (Phe) and arginine (Arg).

Organic acids were spiked into plasma at 10-50 μM concentration range. Considering plasma dilution factor, this range covers MMA pathological concentrations (500-2500 μM). Amino acids were added at four concentrations (1.7, 3.3, 6.7 μM) in a way to detect physiological (or pathological) concentrations. As mentioned in Chapter II, corresponding standards and internal standards of each compound were added in the same calibration sample. It is important to note that samples were diluted in acidified methanol:water solvent mixture (0.5% formic acid, HCOOH) so as AAs are essentially ionized as protonated ions. Preliminary results of multi-class calibration experiments performed over one day are discussed in this section.

IV.5.1. Influence of amino acids on organic acids ionization and calibration

Simultaneous detection of OAs and AAs in plasma using DMS-MS is illustrated in Figure IV.4. DMS spectra is recorded at DV value of 1800 V using N_2 as carrier gas. N_2 dry gas flow and temperature are fixed at $6.5 \text{ L}\cdot\text{min}^{-1}$ and $220 \text{ }^\circ\text{C}$, respectively. Sodiated organic acids are observed at expected CV values of -3.0 V, -3.0 V and -2.4 V for MMA, glutaric and adipic acids, respectively. Protonated AAs are transmitted at CV positions ranging between -8.1 and +0.3 V, as already reported with the same instrument and experimental conditions.⁹ As can be seen in Figure IV.4, CV value is found to increase with m/z value. For a similar m/z value, CV values of an OA is very similar to that of an AA.

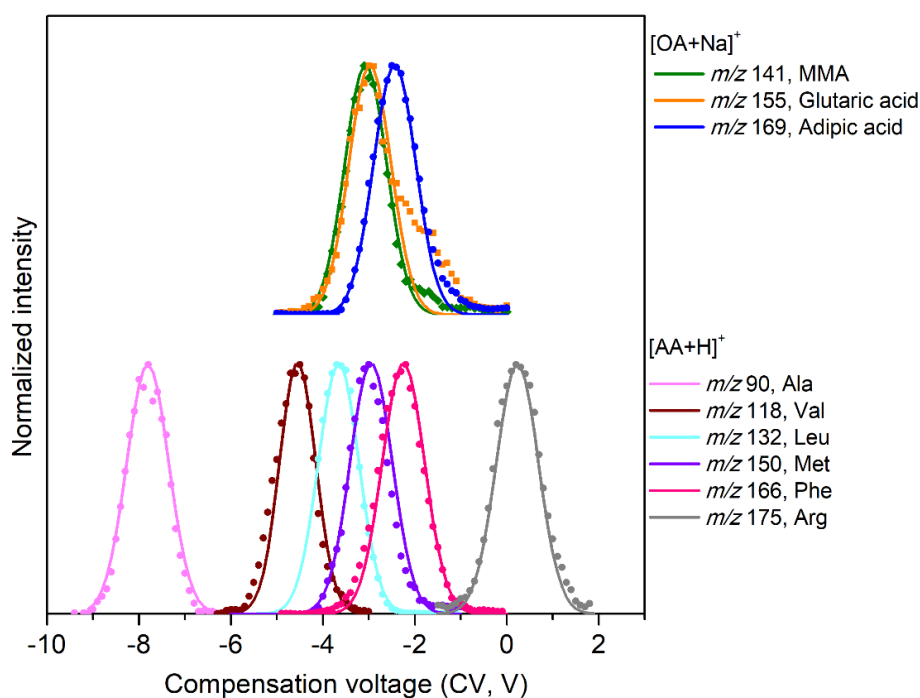


Figure IV.4: DMS spectra illustrating simultaneous detection of organic acids and amino acids spiked in plasma. Organic acids are detected as sodiated ions: methylmalonic (MMA), glutaric and adipic acids. Amino acids are detected as protonated ions: alanine (Ala), valine (Val), leucine (Leu), methionine (Met), phenylalanine (Phe) and arginine (Arg). Data are recorded using a DV value of 1800 V, and dry N₂ flow set at 6.5 L.min⁻¹. All individual spectra are normalized to the maximum and smoothed using a rolling average over two points.

It was found that the presence of amino acids and formic acid does not strongly interfere with ionization and detection of organic acids. In particular, formic acid has no significant effect on ionization of OAs. As mentioned above, DMS-MS conditions were those optimized for OAs. Regarding sample preparation, formic acids was added to water:methanol solvent mixture in the present case. As illustrated in mass spectra in Figure IV.5, similar [OA+Na]⁺ ion counts are found with and without formic acid.

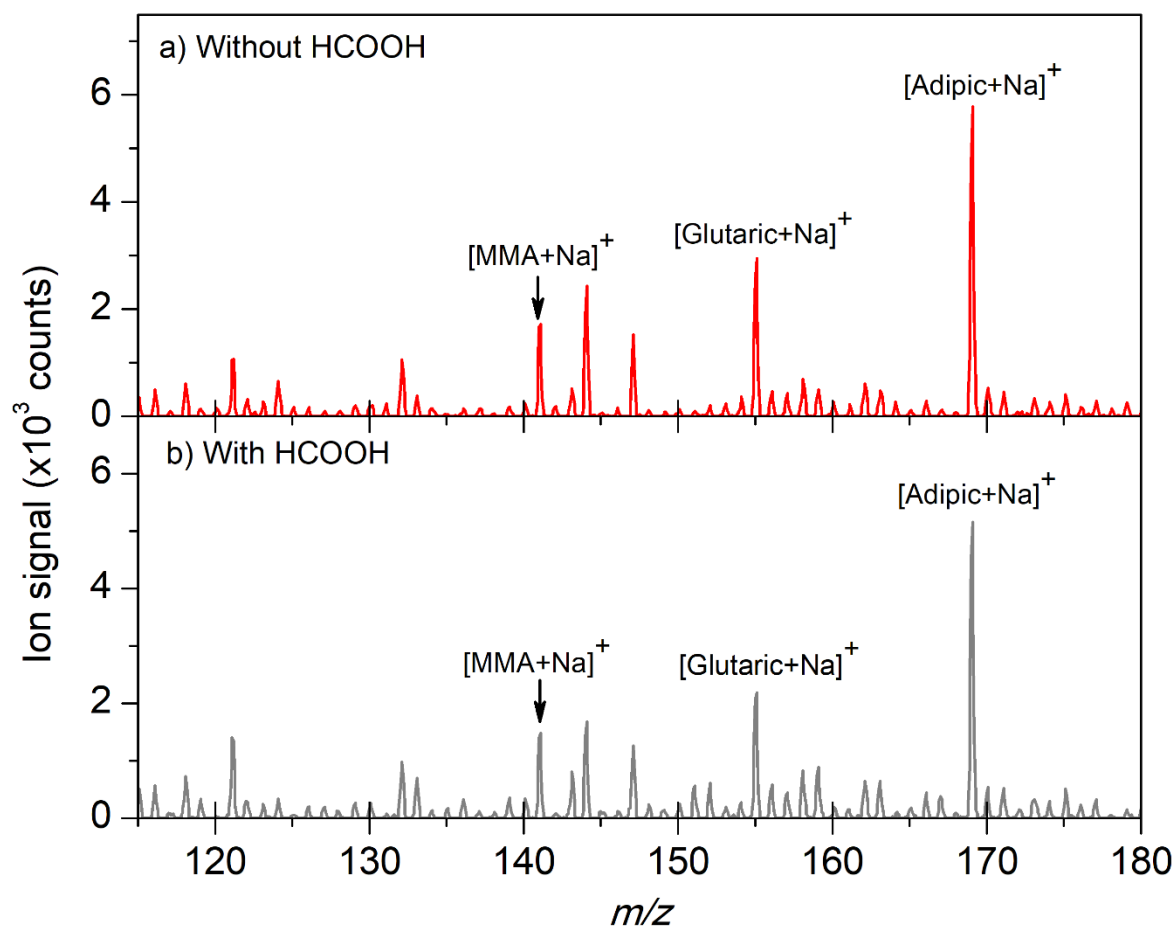


Figure IV.5: MS spectra recorded for MMA, glutaric and adipic spiked in plasma. a) without HCOOH. b) with HCOOH.

Calibration of OAs in presence of AAs in plasma are consistent with those obtained for OAs only (Table IV.10). It is important to note that different plasma samples were used: plasma noted P0 was used for OA calibration and plasma P6 was used for multi-class calibration. Slope and intercept values derived from linear regression in the two cases are very similar.

This can be illustrated by deriving OAs concentration from one or the other equation using a hypothetical area ratio. For instance, concentration of MMA for a hypothetical area ratio of 0.5 is 30.8 μM from OAs calibration and 30.1 μM from multi-class

calibration. This strongly suggests that the presence of AAs and formic acid does not significantly influence quantification of organic acids in plasma.

Table IV.10: Linearity parameters derived from measurements on organic acids (OAs) and multi-class calibration.

Analyte	OAs calibration	Multi-class calibration
	Slope	Slope
MMA	0.015	0.016
Glutaric	0.015	0.014
Adipic	0.069	0.061

IV.5.2. Quantification of endogenous concentration of amino acids

Linear regression curves of selected AAs are represented in Figure IV.6. Concentration of AAs ranges from 1.7 to 6.7 μM . The response becomes non-linear when increasing AA concentration to 20 μM , which reflects saturation of the ion trap. Further experiments are planned in order to avoid saturation at high concentration.

Mean and standard deviation values of slope and intercept are given in Table IV.11. Calibration curves obtained were fitted to a linear equation ($R^2 \geq 0.9$). In the case of alanine, a similar linear profile has already been obtained in our group for quantification of amino acids at pathological levels.⁹ Quantification of the lightest amino acids, such as glycine and alanine, was difficult due to low DMS transmission and low MS sensitivity, at the same time, thus leading to poor DMS peak shape definition.

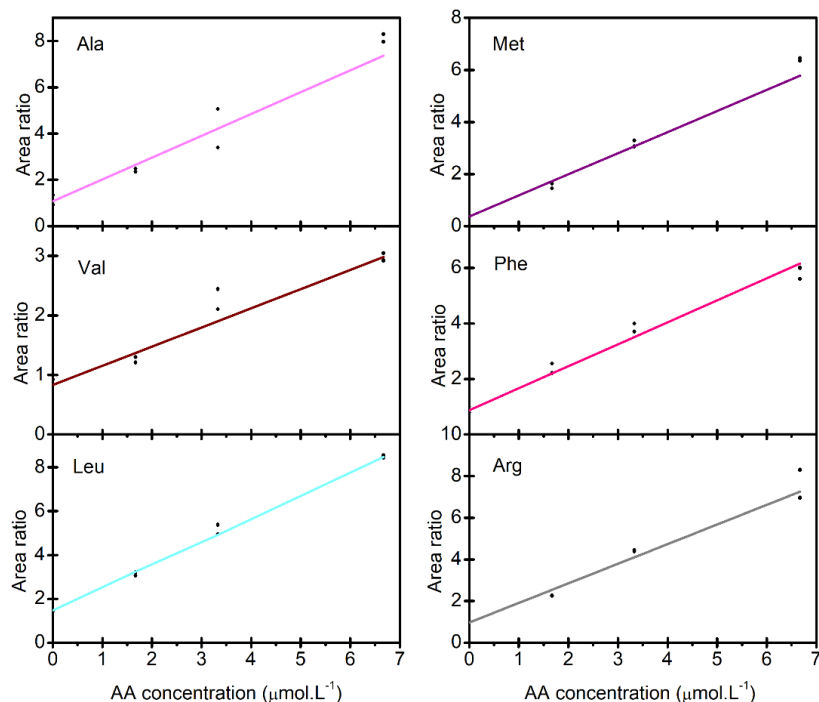


Figure IV.6: Calibration curves of amino acids (AAs) derived from multi-class calibration: alanine (Ala), valine (Val), leucine (Leu), methionine (Met), phenylalanine (Phe) and arginine (Arg).

Table IV.11: Slope, intercept and R^2 values associated with linear regression equation of amino acids.

AA	Multi-class calibration		
	Slope	Intercept	R^2
Ala	0.943	1.08	0.94
Val	0.32	0.83	0.93
Leu	1.05	1.47	0.99
Met	0.81	0.37	0.98
Phe	0.79	0.88	0.98
Arg	0.94	0.97	0.97

Multi-class calibration aims to quantify endogenous concentration of AAs in plasma at physiological levels. Concentrations given in Table IV.12 are measured using calibration curves discussed above. Measured concentrations are consistent with physiological reference levels. Preliminary findings suggest that DMS-MS can be

applied for multi-class calibration. Simultaneous quantification of OAs and AAs can also be carried out. Experiments will be performed to reproduce results with six calibration concentrations of calibration and over different independent experiments to improve linearity and validate the method.

Table IV.12: Endogenous concentration measured for amino acids in plasma compared to typical reference concentration range.

Analyte	Measured concentration (μM)	Reference concentration (μM)
Val-AA	129.7	110-340
Leu-AA	70.0	60-90
Met-AA	22.8	18-42
Phe-AA	55.7	35-90
Arg-AA	51.6	40-120

IV.5.3. DMS-MS: towards a multi-class metabolites analysis method

DMS-MS could be a promising multi-class metabolite analysis method. Based on our results, the critical advantage of DMS is that organic and amino acids found in a plasma sample can be simultaneously detected using the same DMS device and under identical experimental conditions. The subject of multi-class analysis using DMS-MS has been addressed in a recent work.³⁷ It has been demonstrated that a broad metabolite coverage is achieved, but quantification was not performed. CV values were determined for a set of 529 metabolite standards related to 10 different classes in pure solutions, under the same DMS-MS conditions, in both positive and negative ionization modes.

Current developments are still directed towards metabolite-multiclass methods for analyzing a larger number of compounds in a biological sample in order to answer the need of emergency diagnosis. Since metabolites are connected in a complex network, simultaneous quantification allows for better understanding of clinical status of

patients. In literature, different multi-class protocols have been proposed for simultaneous quantification of organic acids and amino acids. More than 20 AAs and 30 OAs found in plasma were first analyzed using capillary GC method.³⁸ GC-MS based protocols were later developed for combined measurement of OAs and AAs in plasma and urine to improve diagnosis of metabolic disorders.³⁹⁻⁴¹ However, all GC-based protocols require tedious and time-consuming analytical workflow. DMS-MS based protocol is simple and fast which is suitable for clinical practice, as demonstrated in the present study and previous ones.^{9, 35}

In clinical field, multi-class analysis is also a challenging task. Countless in-house protocols are currently applied in laboratories of diagnosis and multiple techniques are needed to characterize different classes of metabolites.^{42, 43} For instance, for diagnosis of one sample in emergency, GC-MS is applied for analysis of OAs in urine, whereas LC-MS/MS is used for analysis of AAs and few OAs (e.g. MMA) in plasma. Each technique has a protocol for preparation and treatment, depending on biological sample and metabolites. The overall analysis is tedious and time-consuming ~5 hours per sample. Imagine the time needed for at least 3 samples per day! DMS-MS protocol can thus be a valuable alternative for fast analysis of both classes of metabolites found one sample in a single analytical run.

Future studies will focus on extending metabolite classes, such as acylcarnitine that can also be found in plasma and many compounds are considered biomarkers of metabolic disorders. Multi-class analysis will also be explored in urine, where different classes of metabolites including organic acids can be used for diagnosis of interest.

IV.6. Summary

To the best of our knowledge, this is the first report of a simple and fast analysis of organic acids in plasma using DMS-QIT for diagnosis of organic acidemias, particularly,

methylmalonic acidemia. A DMS-MS protocol is developed for more practical clinical procedure. Sodium complexation of organic acids occurs directly in plasma with no need for derivatization. DMS isomer separation is achieved under our standard conditions, using only N₂ as a carrier gas, and DV value fixed at 1800 V. Full resolution of isomeric organic acids is still required.

In particular, CV values are determined for each metabolite in plasma. CV is found to be reproducible over a large period of time (4 months), and thus fast identification of metabolites/biomarkers can thus be achieved in plasma. It can thus be concluded that CV value can be used as an additional parameter in the context of metabolite identification.

Analysis time can be significantly reduced with DMS compared to conventional methods based on chromatography coupled to mass spectrometry. A full CV scan can be performed within ~3 minutes. Furthermore, a full CV scan is no longer needed once the CV values are known for metabolites. CV can be tuned for maximum transmission of a target, and subsequently a single MS acquisition is achieved. For instance, a metabolite of interest, such as MMA, can be selected using DMS set at a specific CV value of -2.9 V. This fixed CV value allows for fast identification on the order of seconds.

Under optimal conditions, robust and reliable data are obtained for quantification of organic acids at pathological levels. Experiments for assessment of linearity, precision and matrix effect at physiological levels of OAs will be carried out to provide valuable input for OAs quantification. Multi-class analysis is also performed with our DMS-MS instrument. Our proposed protocol is used for quantification of amino acids present together with organic acids in plasma. Measured concentration of AAs are found in good agreement with reference values at physiological levels. It could be concluded that DMS-MS is a powerful alternative to chromatographic techniques for separation, identification and quantification of organic acids, as well as other classes of

metabolites found in the same plasma sample. Multi-class experiments are performed in one analytical run, under identical conditions, opening the way for emergency diagnosis application.

References

1. McMahon, T. B.; Ohanessian, G., An experimental and ab initio study of the nature of the binding in gas-phase complexes of sodium ions. *Chem.-Eur. J.* **2000**, *6* (16), 2931-2941.
2. Armentrout, P. B.; Rodgers, M. T., An absolute sodium cation affinity scale: Threshold collision-induced dissociation experiments and ab initio theory. *J. Phys. Chem. A* **2000**, *104* (11), 2238-2247.
3. Campbell, J. L.; Zhu, M.; Hopkins, W. S., Ion-molecule clustering in differential mobility spectrometry: lessons learned from tetraalkylammonium cations and their isomers. *J Am Soc Mass Spectrom* **2014**, *25* (9), 1583-91.
4. Schneider, B. B.; Covey, T. R.; Coy, S. L.; Krylov, E. V.; Nazarov, E. G., Chemical effects in the separation process of a differential mobility/mass spectrometer system. *Anal. Chem.* **2010**, *82* (5), 1867-1880.
5. Liu, C.; Le Blanc, J. C. Y.; Shields, J.; Janiszewski, J. S.; Ieritano, C.; Ye, G. F.; Hawes, G. F.; Hopkins, W. S.; Campbell, J. L., Using differential mobility spectrometry to measure ion solvation: an examination of the roles of solvents and ionic structures in separating quinoline-based drugs. *Analyst* **2015**, *140* (20), 6897-6903.
6. Rodgers, M. T.; Armentrout, P. B., A critical evaluation of the experimental and theoretical determination of lithium cation affinities. *International Journal of Mass Spectrometry* **2007**, *267* (1-3), 167-182.
7. Monostori, P.; Klinke, G.; Richter, S.; Barath, A.; Fingerhut, R.; Baumgartner, M. R.; Kolker, S.; Hoffmann, G. F.; Gramer, G.; Okun, J. G., Simultaneous determination of 3-hydroxypropionic acid, methylmalonic acid and methylcitric acid in dried blood spots: Second-tier LC-MS/MS assay for newborn screening of propionic acidemia, methylmalonic acidemias and combined remethylation disorders. *Plos One* **2017**, *12* (9), 16.
8. Körver-Keularts, I.; Wang, P.; Waterval, H.; Kluijtmans, L. A. J.; Wevers, R. A.; Langhans, C. D.; Scott, C.; Habets, D. D. J.; Bierau, J., Fast and accurate quantitative organic acid analysis with LC-QTOF/MS facilitates screening of patients for inborn errors of metabolism. *J Inherit Metab Dis* **2018**, *41* (3), 415-424.
9. Berthias, F.; Wang, Y. L.; Alhajji, E.; Rieul, B.; Moussa, F.; Benoist, J. F.; Maitre, P., Identification and quantification of amino acids and related compounds based on Differential Mobility Spectrometry. *Analyst* **2020**, *145* (14), 4889-4900.

10. Stabler, S. P.; Marcell, P. D.; Podell, E. R.; Allen, R. H.; Lindenbaum, J., Assay of methylmalonic acid in the serum of patients with cobalamin deficiency using capillary gas-chromatography mass-spectrometry. *J. Clin. Invest.* **1986**, 77 (5), 1606-1612.
11. Fenton, W. A.; Gravel, R. A.; Rosenblatt, D. S., Disorders of Propionate and Methylmalonate Metabolism. In *The Online Metabolic and Molecular Bases of Inherited Disease*, Valle, D. L.; Antonarakis, S.; Ballabio, A.; Beaudet, A. L.; Mitchell, G. A., Eds. McGraw-Hill Education: New York, NY, 2019.
12. Poge, A. P.; Autschbach, F.; Korall, H.; Trefz, F. K.; Mayatepek, E., Early clinical manifestation of glutaric aciduria type I and nephrotic syndrome during the first months of life. *Acta Paediatr.* **1997**, 86 (10), 1144-1147.
13. Bennett, M. J., The laboratory diagnosis of inborn-errors of mitochondrial fatty-acid oxidation. *Ann. Clin. Biochem.* **1990**, 27, 519-531.
14. Thompson, M.; Ellison, S. L. R.; Wood, R., Harmonized guidelines for single-laboratory validation of methods of analysis - (IUPAC technical report). *Pure Appl. Chem.* **2002**, 74 (5), 835-855.
15. Currie, L. A., Nomenclature in evaluation of analytical methods including detection and quantification capabilities (IUPAC RECOMMENDATIONS 1995). *Pure Appl. Chem.* **1995**, 67 (10), 1699-1723.
16. Maitre, P.; Pernot, P. MS-Ana. <https://github.com/ppernot/MS-Ana/blob/master/README.rmd> (accessed 2021).
17. Hoffmann, G. F.; Meieraugenstein, W.; Stockler, S.; Surtees, R.; Rating, D.; Nyhan, W. L., Physiology and pathophysiology of organic-acids in cerebrospinal-fluid. *J. Inherit. Metab. Dis.* **1993**, 16 (4), 648-669.
18. Analytical Methods Comm, A., The edge of reason: reporting and inference near the detection limit. *Anal. Methods* **2020**, 12 (3), 401-403.
19. Zhang, Y.; Ashok, S.; Seol, E.; Ainala, S. K.; Lee, S. G.; Madan, B.; Xu, J. H.; Park, S., NADH-dependent lactate dehydrogenase from *Alcaligenes eutrophus* H16 reduces 2-oxoadipate to 2-hydroxyadipate. *Biotechnol. Bioprocess Eng.* **2014**, 19 (6), 1048-1057.
20. Desmons, A.; Thioulouse, E.; Hautem, J.-Y.; Saintier, A.; Baudin, B.; Lamazière, A.; Netter, C.; Moussa, F., Direct liquid chromatography tandem mass spectrometry analysis of amino acids in human plasma. *Journal of Chromatography A* **2020**, 1622, 461135.

21. Magera, M. J.; Helgeson, J. K.; Matern, D.; Rinaldo, P., Methylmalonic acid measured in plasma and urine by stable-isotope dilution and electrospray tandem mass spectrometry. *Clinical Chemistry* **2000**, *46* (11), 1804-1810.
22. Kushnir, M.; Komaromy-Hiller, G.; Shushan, B.; Urry, F. M.; Roberts, W., Analysis of dicarboxylic acids by tandem mass spectrometry. High-throughput quantitative measurement of methylmalonic acid in serum, plasma, and urine. *Clinical chemistry* **2001**, *47* 11, 1993-2002.
23. Schmedes, A.; Brandslund, I., Analysis of Methylmalonic Acid in Plasma by Liquid Chromatography–Tandem Mass Spectrometry. *Clinical Chemistry* **2006**, *52* (4), 754-757.
24. Norman, E. J.; Berry, H. K.; Denton, M. D., Identification and quantitation of urinary dicarboxylic acids as their dicyclohexyl esters in disease states by gas chromatography mass spectrometry. *Biomed Mass Spectrom* **1979**, *6* (12), 546-53.
25. Marquis, B. J.; Louks, H. P.; Bose, C.; Wolfe, R. R.; Singh, S. P., A New Derivatization Reagent for HPLC-MS Analysis of Biological Organic Acids. *Chromatographia* **2017**, *80* (12), 1723-1732.
26. Roberts, L. D.; Souza, A. L.; Gerszten, R. E.; Clish, C. B., Targeted Metabolomics. *Current Protocols in Molecular Biology* **2012**, *98* (1), 30.2.1-30.2.24.
27. Krahmer, M.; Fox, K.; Fox, A., Comparison of ion trap and triple quadrupole gas chromatography-tandem mass spectrometry in the quantitative and qualitative trace analysis of muramic acid in complex matrices. *International Journal of Mass Spectrometry* **1999**, *191*, 321-329.
28. Fitzgerald, R. L.; Oneal, C. L.; Hart, B. J.; Poklis, A.; Herold, D. A., Comparison of an ion-trap and a quadrupole mass spectrometer using diazepam as a model compound. *J. Anal. Toxicol.* **1997**, *21* (6), 445-450.
29. Higashi, T.; Ogawa, S., Chemical derivatization for enhancing sensitivity during LC/ESI-MS/MS quantification of steroids in biological samples: a review. *J Steroid Biochem Mol Biol* **2016**, *162*, 57-69.
30. Xu, F. G.; Zou, L.; Liu, Y.; Zhang, Z. J.; Ong, C. N., Enhancement of the capabilities of liquid chromatography-mass spectrometry with derivatization: general principles and applications. *Mass Spectrometry Reviews* **2011**, *30* (6), 1143-1172.

31. Cech, N. B.; Enke, C. G., Practical implications of some recent studies in electrospray ionization fundamentals. *Mass Spectrometry Reviews* **2001**, *20* (6), 362-387.
32. Fasching, C.; Singh, J., Quantitation of Methylmalonic Acid in Plasma Using Liquid Chromatography - Tandem Mass Spectrometry. In *Clinical Applications of Mass Spectrometry: Methods and Protocols*, Garg, U.; HammettStabler, C. A., Eds. Humana Press Inc: Totowa, 2010; Vol. 603, pp 371-378.
33. Lakso, H. A.; Appelblad, P.; Schneede, J., Quantification of Methylmalonic Acid in Human Plasma with Hydrophilic Interaction Liquid Chromatography Separation and Mass Spectrometric Detection. *Clinical Chemistry* **2008**, *54* (12), 2028-2035.
34. Tebani, A.; Schlemmer, D.; Imbard, A.; Rigal, O.; Porquet, D.; Benoist, J. F., Measurement of free and total sialic acid by isotopic dilution liquid chromatography tandem mass spectrometry method. *Journal of Chromatography B-Analytical Technologies in the Biomedical and Life Sciences* **2011**, *879* (31), 3694-3699.
35. Chen, P.-S.; Chen, S.-H.; Chen, J.-H.; Haung, W.-Y.; Liu, H.-T.; Kong, P.-H.; Yang, O. H.-Y., Modifier-assisted differential mobility–tandem mass spectrometry method for detection and quantification of amphetamine-type stimulants in urine. *Analytica Chimica Acta* **2016**, *946*, 1-8.
36. Beach, D. G.; Kerrin, E. S.; Giddings, S. D.; Quilliam, M. A.; McCarron, P., Differential Mobility-Mass Spectrometry Double Spike Isotope Dilution Study of Release of β -Methylaminoalanine and Proteinogenic Amino Acids during Biological Sample Hydrolysis. *Scientific Reports* **2018**, *8* (1), 117.
37. Wernisch, S.; Afshinnia, F.; Rajendiran, T.; Pennathur, S., Probing the application range and selectivity of a differential mobility spectrometry–mass spectrometry platform for metabolomics. *Analytical and Bioanalytical Chemistry* **2018**, *410* (12), 2865-2877.
38. Husek, P., Simultaneous profile analysis of plasma amino and organic-acids by capillary gas-chromatography. *J. Chromatogr. B-Biomed. Appl.* **1995**, *669* (2), 352-357.
39. Windelberg, A.; Arseth, O.; Kvalheim, G.; Ueland, P. M., Automated assay for the determination of methylmalonic acid, total homocysteine, and related amino acids in human serum or plasma by means of methylchloroformate derivatization and gas chromatography-mass spectrometry. *Clinical Chemistry* **2005**, *51* (11), 2103-2109.
40. Paik, M. J.; Lee, H. J.; Kim, K. R., Simultaneous retention index analysis of urinary amino acids and carboxylic acids for graphic recognition of abnormal state. *Journal of*

Chromatography B-Analytical Technologies in the Biomedical and Life Sciences **2005**, 821 (1), 94-104.

41. Kvitvang, H. F. N.; Andreassen, T.; Adam, T.; Villas-Boas, S. G.; Bruheim, P., Highly Sensitive GC/MS/MS Method for Quantitation of Amino and Nonamino Organic Acids. *Anal. Chem.* **2011**, 83 (7), 2705-2711.

42. Wootner, M.; Goodman, S. I., Chromatographic analysis of amino and organic acids in physiological fluids to detect inborn errors of metabolism. *Curr Protoc Hum Genet* **2006**, Chapter 17, Unit 17.2.

43. la Marca, G.; Rizzo, C., Analysis of organic acids and acylglycines for the diagnosis of related inborn errors of metabolism by GC- and HPLC-MS. *Methods Mol Biol* **2011**, 708, 73-98.

Annex

Figure IV.S1: Relationship between peak capacity and dispersion voltage values

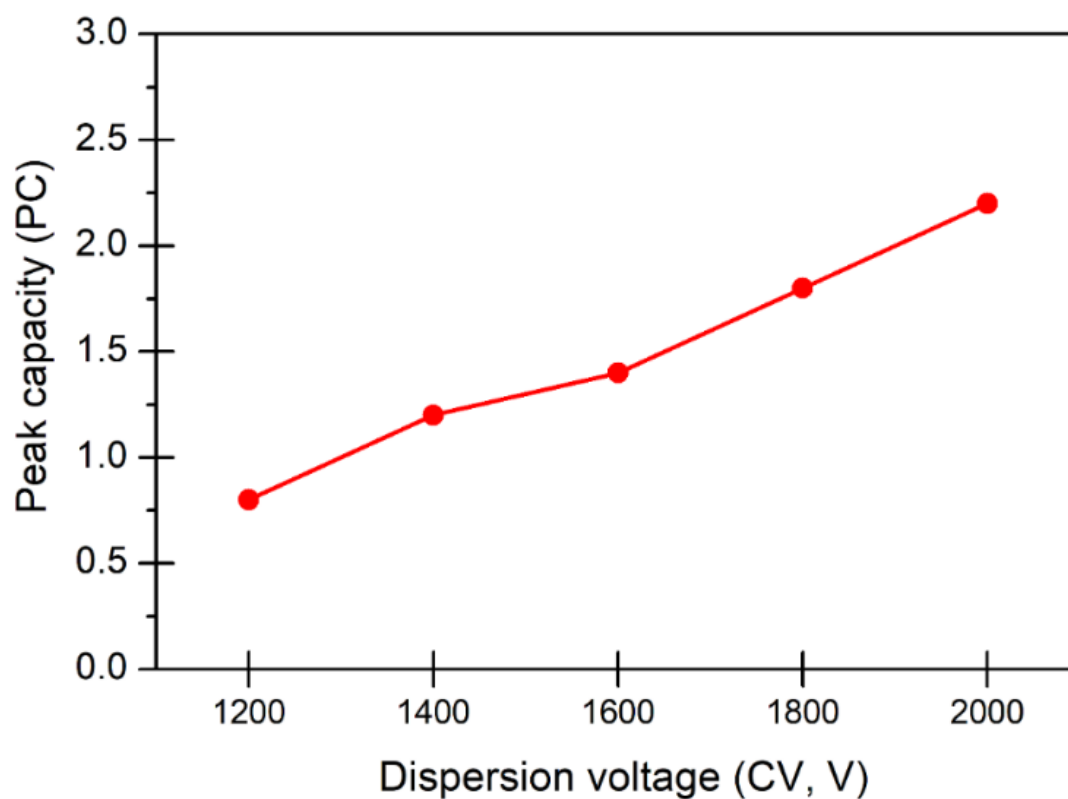
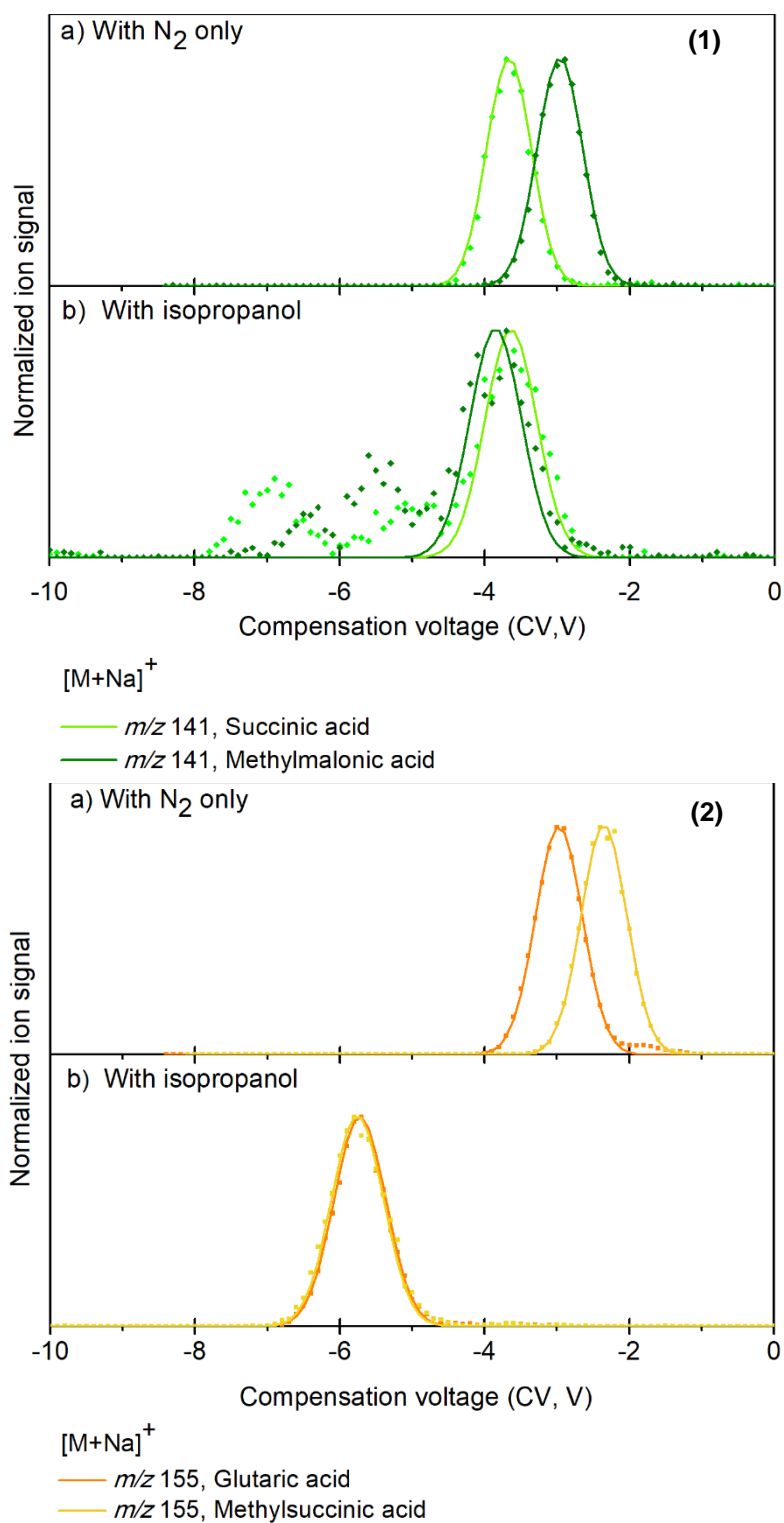


Figure IV.S1: Peak capacity as a function of the dispersion voltage (DV). Dispersion plots were recorded for sodiated organic acids in methanol:water solution using N_2 only as carrier gas.

Figure IV.S2: Effect of isopropanol on DMS separation of sodiated organic acids



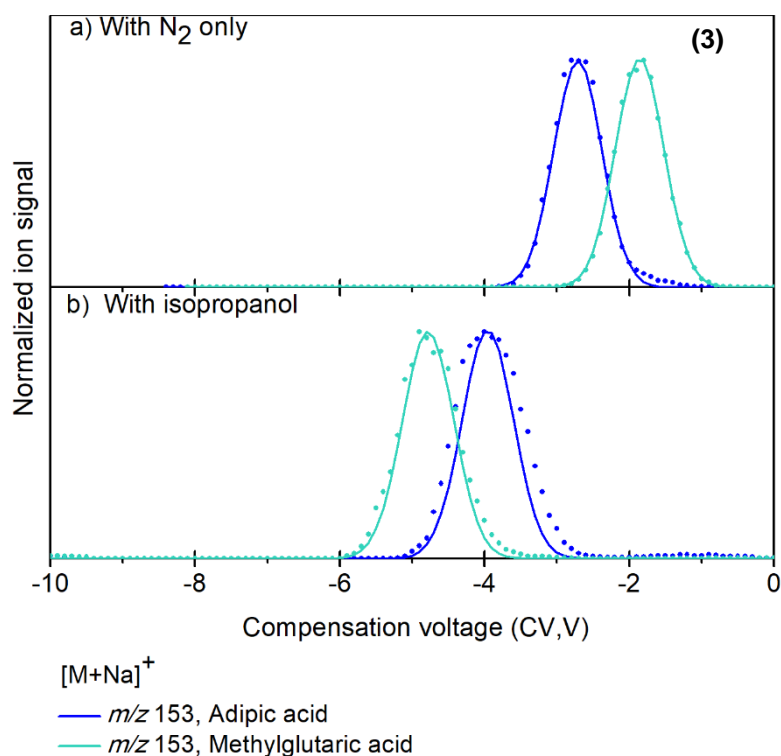


Figure IV.S2: DMS spectra recorded for sodiated organic acids: m/z 141 isomers of succinic and methylmalonic acids (panel 1, green diamonds), m/z 155 isomers of glutaric and methylsuccinic acids (panel 2, orange squares), and m/z 169 isomers of adipic and methylglutaric acids (panel 3, blue circles). a) with N₂ as carrier gas only fixed at 6.5 L.min⁻¹. b) with isopropanol added in N₂ as carrier gas. N₂ flow and temperature are fixed at 6.5 L.min⁻¹ and 220 °C, respectively. Isopropanol flow was set at 2 μL.min⁻¹. Experiments were performed using methanol:water solution and using a dispersion voltage value of 1800 V. To facilitate visualization, all individual spectra are fitted and normalized to the maximum.

Figure IV.S3: Calibration curves of organic acids spiked at low concentrations in plasma

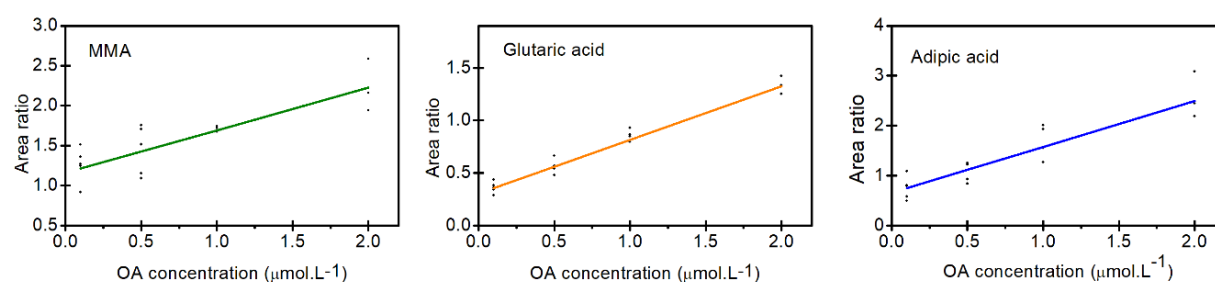


Figure IV.S3: Calibration curves of MMA, glutaric and adipic acids spiked in healthy plasma samples. Concentration of organic acids (OAs) in calibration samples varies within 0.1-2 μM range, corresponding to 5-100 μM in plasma. Area ratio organic acid/internal standard is plotted against OA concentration after dilution.

Table IV.S1: Intra-day precision of concentration measurement obtained from control samples prepared in plasma noted P6

Table IV.S1: Intra-day precision of concentration measurement of MMA, glutaric and adipic acids. Analytes are spiked in plasma sample P6 at 20 and 50 μM after plasma dilution. Mean concentration, standard deviation (SD) and relative SD (RSD) are calculated for each concentration using 6 replicates ($n = 6$) analyzed on one day.

Analyte	Plasma P6, n = 6					
	Nominal concentration = 20 μM			Nominal concentration = 50 μM		
	Mean	SD	RSD (%)	Mean	SD	RSD (%)
MMA	21.8	0.7	7.6	50.2	1.5	2.9
Glutaric	21.3	1.1	5.3	54.7	1.5	2.7
Adipic	21.3	1.3	5.9	48.2	1.0	2.1

Chapitre V - Conclusions and perspectives

This section aims to address conclusions on the use of differential mobility spectrometry hyphenated to mass spectrometry (DMS-MS) in the frame of targeted metabolomics for clinical purpose, and also to summarize practical issues associated with DMS-MS as well as fundamental questions still to be answered.

DMS-MS would be a useful alternative or complementary method for clinical diagnosis. In the frame of my PhD, diagnosis of organic acidemias has been targeted, but conclusions hold true for other metabolic disorders with specific biomarker. A comprehensive DMS-MS protocol has been developed for simple, fast and accurate analysis of specific biomarkers in biological fluids. This translational research project meets the need for time and cost-reduction in clinical laboratories. Considering the spread of ion mobility spectrometry for biochemical analysis, one could expect that a practical outcome of our work would be a technological transfer from our research to clinical chemistry. From a fundamental point of view, experimental and theoretical methods are needed for the issue of DMS peak assignment.

Separation based on DMS would be indeed well-suited for clinical practice. First, it could be installed at very low cost on current diagnostic platforms. A technical advantage is that DMS does not require complicated vacuum nor drift tube equipment. It is a small device which can be easily implemented in the ion source of a mass spectrometer and DMS operation is also simple. Another important asset of DMS is that a single device used with standard settings (N_2 gas as a carrier gas, maximum DV voltage) is adapted for all classes of metabolites, which can be analyzed under negative and positive ionization mode. Finally, as demonstrated in recent literature,¹ DMS can also be coupled to LC-MS/MS for separation of co-eluted isomers in a single run, and would not affect analysis time.

Second, DMS enables fast and accurate identification of metabolites. More precisely, DMS allows to target the specific biomarker of a metabolic disorder, *i.e.* methylmalonic acid for methylmalonic academia. Data acquisition can be significantly, and thus storage and analysis can be significantly simplified compared to current methods. Used in specific cases such as methylmalonic academia, DMS could avoid the use of complementary second tier analysis, as it is often the case for routine diagnosis. More precisely, as shown in this thesis, the reduction of data acquisition relies on the fact that compensation voltage (CV) values of organic acids were found to be very stable over a large period of time. CV can thus be fixed to the specific value and DMS can be used as an ion-filter. As a result, only mass spectra associated with CV values specific of targeted biomarkers are recorded.

Importantly, if the same DMS device is hyphenated to our FT-ICR or QIT mass spectrometers, the very same CV values specific of targeted biomarkers were observed. The same device will be soon coupled to a triple quadrupole mass spectrometer in our laboratory. The consistency of the results obtained with DMS coupled with different MS/MS instruments should increase confidence in this new method, and contribute to CV values being considered as an identifier. These results are particularly interesting in the perspective of high throughput analysis of a large set of samples for clinical analysis of a set of targeted metabolites.

Finally, multiple metabolites found in a biological sample can be analyzed in a single run using the same DMS device and under the same experimental conditions (*i.e.* dry gas flow and temperature, DV value....). Preliminary results on simultaneous quantification of few organic acids and amino acids present in plasma are provided. Future work will aim to cover a larger panel of pertinent metabolites found in plasma and urine. As such, a single

run of 40 to 80 metabolites featuring different physicochemical natures can be performed. If successful, this would open the route for emergency DMS-MS diagnosis of treatable metabolic disorders. Rather than using specific liquid chromatographic conditions for each class of metabolite, a single DMS-MS instrument and protocol could be used.

Further gains in terms of performance, and particularly for isomer separation and quantification, are expected, and multiple practical aspects associated with our DMS-MS system should be improved. In the present study, cationization using sodium cation is found valuable for isomer separation of organic acids. Since sodium is naturally occurring in plasma, it facilitates sample preparation without salt addition. Isomer separation was found optimal using our standard DMS conditions (N_2 only as carrier gas and DV value of 1800 V). Nevertheless, addition of modifier to the carrier gas is undoubtedly the approach of choice for improving isomer resolution. Full resolution of isomeric organic acids was not achieved using isopropanol nor methanol. Further experiments should be able to contribute to lift technical barriers for investigating separation and quantification of different molecules using various modifiers at various flows.

The other side of the coin is that one might be careful with unwanted modifiers since DMS is very sensitive to the composition of carrier gas. In Chapter 4, it was illustrated that ESI solvents can pass through DMS and play the role of modifiers. Dry gas flow should be high enough, and ESI needle position should be optimized to avoid contamination of carrier gas with solvents. We also experienced difficulties with our dinitrogen generator, for example, and CV shifts observed were found to be the signature of impurities, may be also water vapors, contained in the N_2 line. A planned maintenance can effectively mitigate against these unwanted effects.

It is important to note that a very small volume of modifiers can considerably improve DMS separation. This is an important asset of DMS-MS/MS compared to LC-MS/MS, which requires handling of large volume of solvents, often toxic and difficult to recycle.

On the other hand, prediction of modifier effect is very difficult. The CV peak ordering of two ions can change from using methanol to isopropanol, for example. As a result, an *a priori* assignment of DMS peaks is a key challenge. CV value and/or CV shifts cannot be quantitatively correlated to ion structure, due to a lack of knowledge about ion mobility under high electric fields. Recently, literature report suggests that collision cross section can be measured from DMS data using a machine learning-based calibration.² Peak identification is still, however, required.

In the course of this PhD, only DMS-MS experiments were performed, but our two set-ups can be used for DMS-MS/MS. In particular, collision induced dissociation (CID) or infrared multiple photon dissociation (IRMPD) can be used to improve identification in general. The use of IRMPD for DMS peak assignment has been demonstrated in the frame of studies of separation of isomeric metabolites such as sarcosine and its alanine isomers, and also aminobutyric acids.^{3, 4} When two isomeric metabolites present similar fragmentation patterns, they can in principle be distinguished using IRMPD at specific laser wavelengths which will be absorbed by one isomer and not the others.

Combined experimental and theoretical results are usually presented in literature^{5, 6} to provide a better understanding of ion-molecule clusters in DMS environments. Computational methods can help to identify structures of complexes involved in ion-molecule clustering. Calculated modifier-ion binding energies were found to be consistent with trends observed for dispersion plots of series of isomeric molecules.

Recent ion mobility instruments based on structures for lossless ion manipulations ion mobility (SLIM)^{7,8} open the door to very high resolution and high sensitivity. SLIM method allows for a significant improvement isomer resolution by increasing the ion path length in the mobility device.^{9,10} Importantly, SLIM separation is based on lossless fashion since ions are not neutralized on the electrodes. SLIM thus seems attractive for a sensitive detection and quantification of metabolites in biological fluids.

References

1. Varesio, E.; Le Blanc, J. C. Y.; Hopfgartner, G., Real-time 2D separation by LC × differential ion mobility hyphenated to mass spectrometry. *Analytical and Bioanalytical Chemistry* **2012**, 402 (8), 2555-2564.
2. Ieritano, C.; Lee, A.; Crouse, J.; Bowman, Z.; Mashmoushi, N.; Crossley, P. M.; Friebe, B. P.; Campbell, J. L.; Hopkins, W. S., Determining Collision Cross Sections from Differential Ion Mobility Spectrometry. *Anal. Chem.* **2021**, 93 (25), 8937-8944.
3. Berthias, F.; Maatoug, B.; Glish, G.; Moussa, F.; Maitre, P., Resolution and Assignment of Differential Ion Mobility Spectra of Sarcosine and Isomers. *J. Am. Soc. Mass Spectrom.* **2018**, 29 (4), 752-760.
4. Wang, Y.; Alhajji, E.; Rieul, B.; Berthias, F.; Maître, P., Infrared isomer-specific fragmentation for the identification of aminobutyric acid isomers separated by differential mobility spectrometry. *International Journal of Mass Spectrometry* **2019**, 443, 16-21.
5. Campbell, J. L.; Zhu, M.; Hopkins, W. S., Ion-molecule clustering in differential mobility spectrometry: lessons learned from tetraalkylammonium cations and their isomers. *J Am Soc Mass Spectrom* **2014**, 25 (9), 1583-91.
6. Ruskic, D.; Hopfgartner, G., Modifier Selectivity Effect on Differential Ion Mobility Resolution of Isomeric Drugs and Multidimensional Liquid Chromatography Ion Mobility Analysis. *Anal. Chem.* **2019**, 91 (18), 11670-11677.
7. Webb, I. K.; Garimella, S. V. B.; Tolmachev, A. V.; Chen, T. C.; Zhang, X. Y.; Norheim, R. V.; Prost, S. A.; LaMarche, B.; Anderson, G. A.; Ibrahim, Y. M.; Smith, R. D., Experimental Evaluation and Optimization of Structures for Loss less Ion Manipulations for Ion Mobility Spectrometry with Time-of-Flight Mass Spectrometry. *Anal. Chem.* **2014**, 86 (18), 9169-9176.
8. Ibrahim, Y. M.; Hamid, A. M.; Deng, L. L.; Garimella, S. V. B.; Webb, I. K.; Baker, E. S.; Smith, R. D., New frontiers for mass spectrometry based upon structures for lossless ion manipulations. *Analyst* **2017**, 142 (7), 1010-1021.
9. Chouinard, C. D.; Nagy, G.; Webb, I. K.; Shi, T. J.; Baker, E. S.; Prost, S. A.; Liu, T.; Ibrahim, Y. M.; Smith, R. D., Improved Sensitivity and Separations for Phosphopeptides using Online Liquid Chromatography Coupled with Structures for Lossless Ion Manipulations Ion Mobility-Mass Spectrometry. *Anal. Chem.* **2018**, 90 (18), 10889-10896.

10. Nagy, G.; Attah, I. K.; Garimella, S. V. B.; Tang, K. Q.; Ibrahim, Y. M.; Baker, E. S.; Smith, R. D., Unraveling the isomeric heterogeneity of glycans: ion mobility separations in structures for lossless ion manipulations. *Chem. Commun.* **2018**, 54 (83), 11701-11704.